

FOREWORD

This report was prepared by Battelle Memorial Institute under USAF Contract No. 33(616)-8267. The principal investigators were Mr. J. V. Baum, Project Director, and Mr. B. Goobich, Research Engineer. The contract was initiated under Project No. 6373, "Equipment for Life Support in Aerospace," and Task No. 637302, "Respiratory Support Equipment." Research was performed at the request of the 6570th Aerospace Medical Research Laboratory, Aeronautical Systems Division, with Mr. Irving H. Lantz serving as the contract monitor. This report covers research from May 1, 1961 to June 30, 1962.

The authors acknowledge the invaluable assistance of Dr. J. W. Droege, Senior Research Chemist, and Mr. A. E. Weller, Research Adviser.

Contrails

ABSTRACT

A research program was conducted to investigate the relative safety of 7500-psi gaseous oxygen systems when used as a source of breathing oxygen in aerospace vehicles. Experiments were performed to investigate the effects on the system of temperature, vibration, shock, extended storage, and contamination. Also studied were the effects of high pressure, high-velocity flow, and heating due to rapid compression. Evaluation of the results of this program indicates that 7500-psi gaseous oxygen systems can be comparatively safe if proper safety precautions are taken. Under controlled operations, the hazard of explosion because of contamination can be overcome. Stainless steel and Monel alloys were found to be acceptable materials of construction. Teflon and Kel-F compounds appear to be suitable for seals. Hydrocarbons in minute concentrations were found not to be dangerously reactive. Electrostatic charges due to high-velocity flow were small, but there was evidence that erosion could be a serious problem. Although no appreciable chemical reactions occurred during the normal experimental program, it must be realized that controlled laboratory procedures are not widely prevalent. High-pressure oxygen systems must be treated as "new" and representing dangerous, explosive possibilities. It is recommended that further detailed studies of the combustion process be performed. Spontaneous ignition temperatures for the materials and contaminants considered in this research should be investigated under both static and dynamic conditions. It is recommended that, before high-pressure gaseous oxygen systems be used extensively as are systems at lower pressures, reliability of the system and equipment used for handling the gas be increased through improved equipment design.

PUBLICATION REVIEW

This technical documentary report has been reviewed and is approved.

Wayne H. McCandless
WAYNE H. McCANDLESS
Chief, Life Support Systems
Laboratory

TABLE OF CONTENTS

	<u>Page</u>
INTRODUCTION	1
RESEARCH PROGRAM	2
Information Research	2
Technical Literature	2
Results of Other Research Programs	2
Analytical Studies	4
Energy of Chemical Reaction	4
Pressure-Temperature Relationships	9
Laboratory Investigations	9
Location and Construction of Laboratory	9
Design and Assembly of Equipment	9
High-Pressure Oxygen Generation	14
Experiments Performed	15
Experimental Methods	15
Temperature	15
Vibration	17
Shock	17
Storage	17
Flow	19
Surge	22
EVALUATION OF EXPERIMENTAL RESULTS	22
Materials Compatibility	24
Materials Investigated	24
Evaluation of Results	24
Conclusions	27
Hydrocarbon Contaminants	29
Experiments Performed	29
Evaluation of Results	31
Conclusions	31
Solid-Particle Contamination	32
Experiments Performed	32
Evaluation of Results	32
Conclusions	34
Materials of Construction	34
Materials Investigated	34
Experiments Performed	35
Evaluation of Results	36
Conclusions	44
Electrostatic Charges	48
Experiments Performed	48
Evaluation of Results	49
Conclusions	49
Adiabatic Heating	49
Experiments Performed	49
Evaluation of Results	50
Conclusions	51

TABLE OF CONTENTS
(Continued)

	<u>Page</u>
Experimental Equipment Evaluation	51
High-Pressure Regulator	51
High-Pressure Valves	52
High-Pressure Tubing Connections	55
CONCLUSIONS	57
RECOMMENDATIONS	58
REFERENCES	59
APPENDIXES	
I. BIBLIOGRAPHY	61
II. ENERGY OF CHEMICAL REACTION	63
III. PRESSURE-TEMPERATURE RELATIONSHIPS	71
IV. TABLES OF EXPERIMENTS PERFORMED	77
V. PARTIAL PRESSURE OF HYDROCARBON GAS FOR CONCENTRATION OF 10 PARTS PER MILLION.	85

LIST OF FIGURES

Figure 1. Projected Effect on Pressure and Temperature of Oxygen System Caused by the Combustion of Iron	6
Figure 2. Projected Effect on Pressure and Temperature of Oxygen System Caused by the Combustion of Copper	7
Figure 3. Projected Effect on Pressure and Temperature of Oxygen System Caused by the Combustion of $(CH_2)_x$	8
Figure 4. Plan of Laboratory Cell	10
Figure 5. Elevation of Laboratory Cell Showing the Sand Barriers	10
Figure 6. View of Safe Side of Front Protective Barrier	11
Figure 7. View of Test Area and Set-Up for Temperature Experiments	12
Figure 8. Schematic of Experimental System	13
Figure 9. System Used for Temperature-Variation Experiments	16

LIST OF FIGURES (Continued)

	<u>Page</u>
Figure 10. System Used for Shock Experiments and Typical Chart of Shock Loads Imposed	18
Figure 11. System Used to Charge Reactors With Gaseous Hydrocarbons	18
Figure 12. Reactors Assembled for 500-Hour Dynamic Storage, Experiments 126 Through 130	20
Figure 13. Schematic of Flow Experiment	21
Figure 14. Details of Orifice and Retainer	21
Figure 15. Electrostatic Voltage Recorded During Experiment 93	23
Figure 16. System Used for Surge Experiments	23
Figure 17. Teflon Orifice Disk After Exposure to 10,000-PSI Oxygen	27
Figure 18. Face and Cross-Sectional View of 0.006-Inch-Diameter Kel-F Orifice	28
Figure 19. 0.005-Inch-Diameter Brass Orifice After 13 Minutes 47 Seconds of Flow, Before and After Cleaning	33
Figure 20. Ignition Temperature of Metals as a Function of Oxygen Pressure	35
Figure 21. Test-Tube Reactor and Tensile Specimens	40
Figure 22. Surface Oxidation of Monel, Brass, and Stainless Steel Reactors Exposed for 616 Hours to 7500-PSI Oxygen	41
Figure 23. Surface Oxidation of Copper Reactors Exposed for 616 Hours to High-Pressure Oxygen	42
Figure 24. Progressive Erosion of a 0.005-Inch-Diameter Brass Orifice Exposed to High-Pressure High-Velocity Flow	45
Figure 25. Cross Section Through 0.005-Inch-Diameter Brass Orifice	46
Figure 26. Photomicrographs of 0.013-Inch-Diameter Stainless Steel Orifice After 15 Minutes of Flow	47
Figure 27. Instantaneous Rise in Pressure and Temperature Caused by Rapid Compression	50
Figure 28. Cross Section of High-Pressure Regulator	53
Figure 29. Regulator Body After Internal Combustion and Burnout	54

LIST OF FIGURES
(Continued)

	<u>Page</u>
Figure 30. Standard Valve Rated at 30,000 PSI	56
Figure 31. Mechanical Tubing Connection	56
Figure 32. Compressibility Factor for Oxygen at 298.2 K	63
Figure 33. Generalized Compressibility Chart for High-Pressure Range	73
Figure 34. Per Cent Deviation of the Compressibility Factor for Ethylene, Nitrogen, and Ammonia From Observed Measurements	75

LIST OF TABLES

Table 1. Tensile-Test Results for Teflon, Kel-F, Viton, and Neoprene O-Rings	26
Table 2. Test Conditions and Tensile-Test Results for Teflon, Kel-F, and Nylon Dumbbells	26
Table 3. Acceptable Limits of Hydrocarbon Contaminants	29
Table 4. Concentrations, Maximum Temperatures, and Mass Spectroscopic Analyses of Hydrocarbon Experiments	30
Table 5. Results of Tensile Tests of Exposed and Unexposed Stainless Steel, Monel, Brass, and Copper	38
Table 6. Vacuum-Fusion Analysis of Oxygen Concentrations in Stainless Steel, Monel, and Copper	43
Table 7. Mean Heat Capacity at Constant Volume From 300 to 5000 K.	67
Table 8. Adiabatic Temperatures and Calculated Pressures for Combustion of Iron to Form Fe_2O_3 and $Fe_{.95}O$	67
Table 9. Adiabatic Temperatures and Calculated Pressures for Combustion of Copper to Form CuO and Cu_2O	68
Table 10. Adiabatic Temperatures and Calculated Pressures for Combustion of (CH_2) in Oxygen	69
Table 11. Theoretical Pressures Generated by Evolving Liquid Oxygen Into a Gas at Equal Density	72
Table 12. Temperature-Variation Experiments	77

LIST OF TABLES
(Continued)

	<u>Page</u>
Table 13. Vibration Experiments	78
Table 14. Shock Experiments	79
Table 15. Storage Experiments	80
Table 16. Flow Experiments	81
Table 17. Surge Experiments	83

AN EVALUATION OF HIGH-PRESSURE OXYGEN SYSTEMS

by

J. V. Baum, B. Goobich, and T. M. Trainer

INTRODUCTION

The problem of supplying oxygen for breathing during aerospace flight has become increasingly significant in the last few years because of rapid progress in aerospace programs. Although liquid-oxygen converters are available and are being used, their use for flights of short duration creates difficult problems related to excessive weight and volume. The weight-volume advantage of extreme-high-pressure gaseous systems is known^{(1)*}; however, the disadvantages and hazards associated with such systems are not well understood and require evaluation. To determine the relative safety of 7500-psi gaseous oxygen systems when used for aerospace breathing, a study was conducted from May 1, 1961, to June 30, 1962, by Battelle Memorial Institute under the sponsorship of the Aeronautical Systems Division, Wright-Patterson Air Force Base, Ohio.

Specifically, the research was planned to determine the effects of the following variables on 7500-psi gaseous oxygen systems:

- (1) Temperatures from -65 to +260 F
- (2) Vibration from 0.2 to 500 cycles per second
- (3) Shock at 25 g's
- (4) Storage period
- (5) Hydrocarbon contaminants
- (6) Solid-particle contaminants
- (7) Condition of metallic surfaces
- (8) Materials compatibility
- (9) Possible material embrittlement caused by oxygen diffusion
- (10) Electrostatic charges due to oxygen flow
- (11) Orifice and valve-seat deterioration
- (12) Adiabatic heating due to rapid compression.

*Numbers in parentheses refer to references on p 59.

RESEARCH PROGRAM

The extent and usefulness of available knowledge in the open literature and the experience of researchers at Battelle and elsewhere were ascertained. Analytical studies of possible chemical reactions and analyses of the resulting stresses in pressure vessels were conducted. Both of these activities provided guide lines for (1) selecting experimental equipment, (2) designing a suitable laboratory facility, (3) conducting experimental investigations, and (4) evaluating experimental results. The following discussion is organized around the three major activities of the program:

- Information Research
- Analytical Studies
- Laboratory Investigations.

Information Research

Technical information was obtained from the Battelle library and from written and oral reports of past research at Battelle and elsewhere.

Technical Literature

During a 3-month period at the start of the program, a comprehensive library survey was conducted. Although it was found that there is much published material available on the general subject of high-pressure technology, most of it concerns research with solids, liquids, and gases other than oxygen. Only a few articles contain information directly related to high-pressure oxygen reactions. These are listed in Appendix I. Other articles which provided helpful information about general equipment, instrumentation, experimental techniques, and safety procedures are also listed in Appendix I.

Results of Other Research Programs

Other research programs surveyed included compatibility studies of titanium, Kel-F, and Teflon. Also, recent development programs resulting in operating systems were investigated.

Titanium. Battelle recently completed a program which provided significant experimental results and conclusions about the reactivity of titanium alloys in a liquid-oxygen environment. This study was conducted for the Aeronautical Systems Division, Wright-Patterson Air Force Base. (2) Although no experimental work with gaseous oxygen was performed in the study, a possible mechanism by which the titanium-oxygen reaction initiates under impact was hypothesized. It was suggested that heat generated by impact produces a pocket of gaseous oxygen in the liquid oxygen. If the trapped gas is compressed at the point of impact, the fresh surface of titanium exposed by the

Contrails

impact tends to react with the high-pressure oxygen gas. Propagation is dependent upon the balance between the amount of heat generated and the rate of heat loss from the site of the reaction.

In subsequent research⁽³⁾, experimental work with gaseous oxygen was performed to substantiate this hypothesis. It was shown that over the temperature range from -250 F to room temperature an oxygen pressure of 100 psi is all that is required for propagating the reaction. The results of an investigation completed in 1958 by Stanford Research Institute⁽⁴⁾ showed that under static conditions a pressure of 350 psi was necessary to initiate the reaction with titanium in 100 per cent oxygen, whereas a pressure of 2000 psi was required with 45 per cent oxygen by volume. With pure oxygen and dynamic conditions the reaction could be initiated at a pressure of 50 psi.

Kel-F and Teflon. In a study completed at Battelle in 1956, various Kel-F materials were tested to determine their reactivity with different metal alloys in a high-pressure gaseous oxygen atmosphere. Studies were conducted at a pressure of 2000 psi and a temperature of 300 F. Experimental results indicated general unreactivity of the metal-Kel-F-oxygen system. However, because some of the experiments were incomplete and because there was evidence of some metallic oxidation, unreserved acceptance of these fluorocarbons for use in oxygen systems was not recommended at that time.

In 1958 the National Bureau of Standards reported on the ignition of Kel-F and Teflon in high-pressure gaseous oxygen atmospheres.⁽⁵⁾ The ignitions were produced by rapidly "impacting" samples of these materials at room temperature. The samples consisted of 1/16-inch-thick, 3/16-inch-diameter disks scratched on both faces. The pressure of the gas ranged from 1640 to 2530 psi. Ignition of the samples was obtained in only a small proportion of the attempts. In the impact range of 1620 to 1790 psi, about 3 per cent of the attempts made with Kel-F resulted in chemical reaction; about 1 per cent of the attempts made with Teflon resulted in reaction. Throughout the entire pressure range of 1620 to 2530 psi, the results were 4.1 per cent ignition with Kel-F and 2.7 per cent ignition with Teflon.

Materials Compatibility. In 1958 Douglas Aircraft Company, Inc.⁽⁶⁾, published a fairly comprehensive report covering the problem of materials compatibility with liquid and gaseous oxygen. Some of the significant conclusions resulting from this study are:

- (1) Reactions and explosions with oxygen even in the liquid state are always initiated in the gaseous phase.
- (2) Combustible materials, including metals, ignite in gaseous oxygen at lower temperatures than they would in air.
- (3) Materials for ozone and oxygen service may be passivated by immersion in ozone or oxygen-rich atmospheres prior to use.
- (4) The use of high-purity oxygen is not a complete safeguard against explosion and detonation since spark ignition and adiabatic compression may trigger an explosion.

In 1958, Convair Astronautic⁽⁷⁾ recommended that "Kel-F, fluorolube, and halo-carbon" lubricants not be used with aluminum or magnesium because even in the absence of oxygen atmospheres, detonations have occurred in aluminum-fluorolube systems.

Miscellaneous Studies. Kidde Aero-Space Division of Walter Kidde & Company, Inc., and the AiResearch Manufacturing Company of the Garrett Corporation are the only two organizations that are known to have recent experience with 7500-psi gaseous oxygen systems. In both cases, the primary goal was to develop working hardware and not to investigate or evaluate the physical and chemical phenomena associated with high-pressure oxygen gas.

Kidde Aero-Space Division has worked with an 11,000-psi oxygen system. However, aerospace breathing was not the operational objective. No reports have been published but their experience and knowledge have been transmitted verbally.*

AiResearch Manufacturing Company did the development work for the environmental control system used in the Mercury capsule. Sufficient oxygen for a 28-hour flight is stored in two spherical cylinders pressurized at 7500 psi. The high-pressure gas is reduced to an appropriate pressure for breathing in a single-stage pressure reducer. It is then passed through a series of filters and is purified before being pumped into the capsule. In the course of the development work, AiResearch had occasion to investigate some of the physical phenomena of interest to the present project. Very little of this, however, is in published form. The information made available to the Battelle research staff deals mostly with materials compatibility and external environmental conditions such as shock and vibration.

Another research program of significance is one conducted by the U. S. Bureau of Mines.^(8,9) This work was performed in 1923 at a pressure of only 2000 psi. However, because there has been no subsequent experimental work uncovered which related directly to this subject, the work and conclusions must be seriously considered. These conclusions are discussed later in the report.

Analytical Studies

As already indicated, analytical studies were important for selecting the proper experimental equipment and for conducting and evaluating the research. The main considerations were the energy of chemical reaction and the pressure-temperature relationship of gaseous oxygen.

Energy of Chemical Reaction

Before a safe stress level or working pressure limit could be specified for the experimental equipment, it was necessary to know the pressures, temperatures, and levels of energy that would be expected during a chemical reaction. Therefore, the conditions which might result from chemical reaction were determined analytically.

*See pages 14, 35, 55 of this report.

Contrails

Method of Calculation. The heat energy released during a confined reaction is equivalent to the internal energy change, ΔE , in a reacting system. This value is not directly measurable but may be calculated from the tabulated values of the enthalpy change, ΔH , the heat of reaction at constant pressure. Heat capacities at constant volume were estimated for the oxides and gases of interest and these were then used to determine the adiabatic temperature. It was assumed that all the heat produced in combustion is absorbed by the unused oxygen and the combustion products.

On the basis of Van der Waals equation of state, the corresponding pressure was then calculated from the volume-temperature relationship. Since the heat capacities at extreme temperatures are not well defined, and since heat loss to the container could be appreciable under extreme conditions, side effects such as decomposition of gases and vaporization of oxides which might occur, were discounted in the calculations. Finally, an alternative assumption was made that all the heat produced is absorbed by the pressure-vessel material; the vessel's final temperature was then determined.

Results and Conclusions. Results of the calculations showing the effect on pressure and temperature of the oxygen from initial conditions of 7500 psi and 80 F caused by combustion of different materials are shown graphically in Figures 1, 2, and 3. Derivations of formulas used, sample calculations, and tabulated results are included in Appendix II. The most important conclusions derived from the results of these studies are:

- (1) For small concentrations of hydrocarbons such as 15×10^{-6} moles of methane (CH_4), the rise in pressure and temperature is negligible.
- (2) For larger concentrations such as 1×10^{-3} moles of decane ($\text{C}_{10}\text{H}_{22}$), the final pressure and temperature are 17,500 psi and 525 F when initial conditions are 7500 psi and 80 F.
- (3) If a chemical reaction, involving stoichiometric quantities, occurred in an 8-1/2-pound steel vessel containing a constant volume of oxygen gas at 7500 psi and room temperature, and if it is assumed that all the heat of reaction is distributed throughout the vessel and its contents, the following would result:
 - (a) With iron as the combustible material the final temperature is 510 F.
 - (b) With copper as the combustible material the final temperature is 370 F.
 - (c) With a hydrocarbon plastic as the combustible material the final temperature is 450 F.
 - (d) With Teflon as the combustible material, the heat produced would only be 10 per cent of that produced with a hydrocarbon plastic.

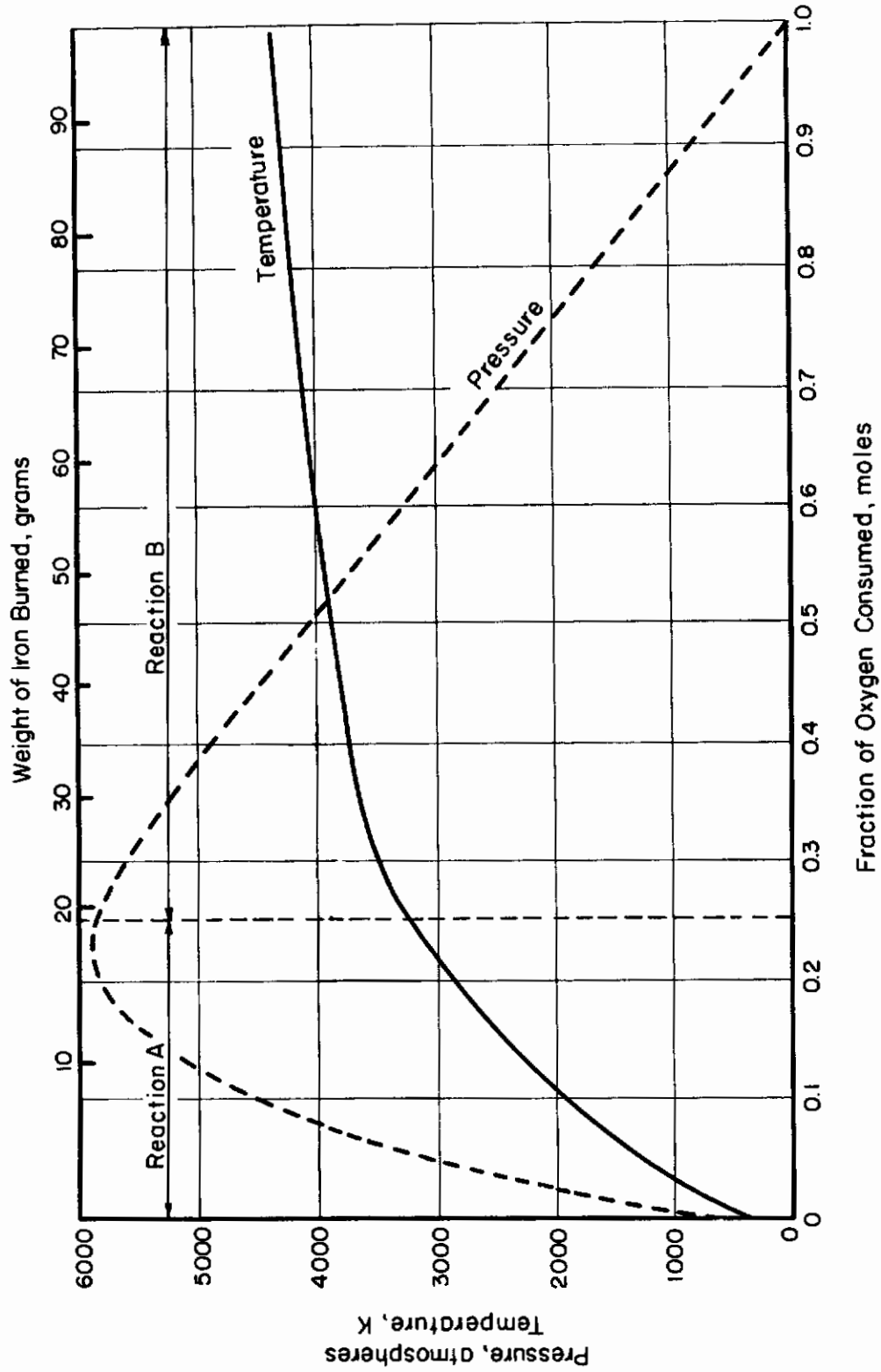


FIGURE 1. PROJECTED EFFECT ON PRESSURE AND TEMPERATURE OF OXYGEN SYSTEM CAUSED BY THE COMBUSTION OF IRON



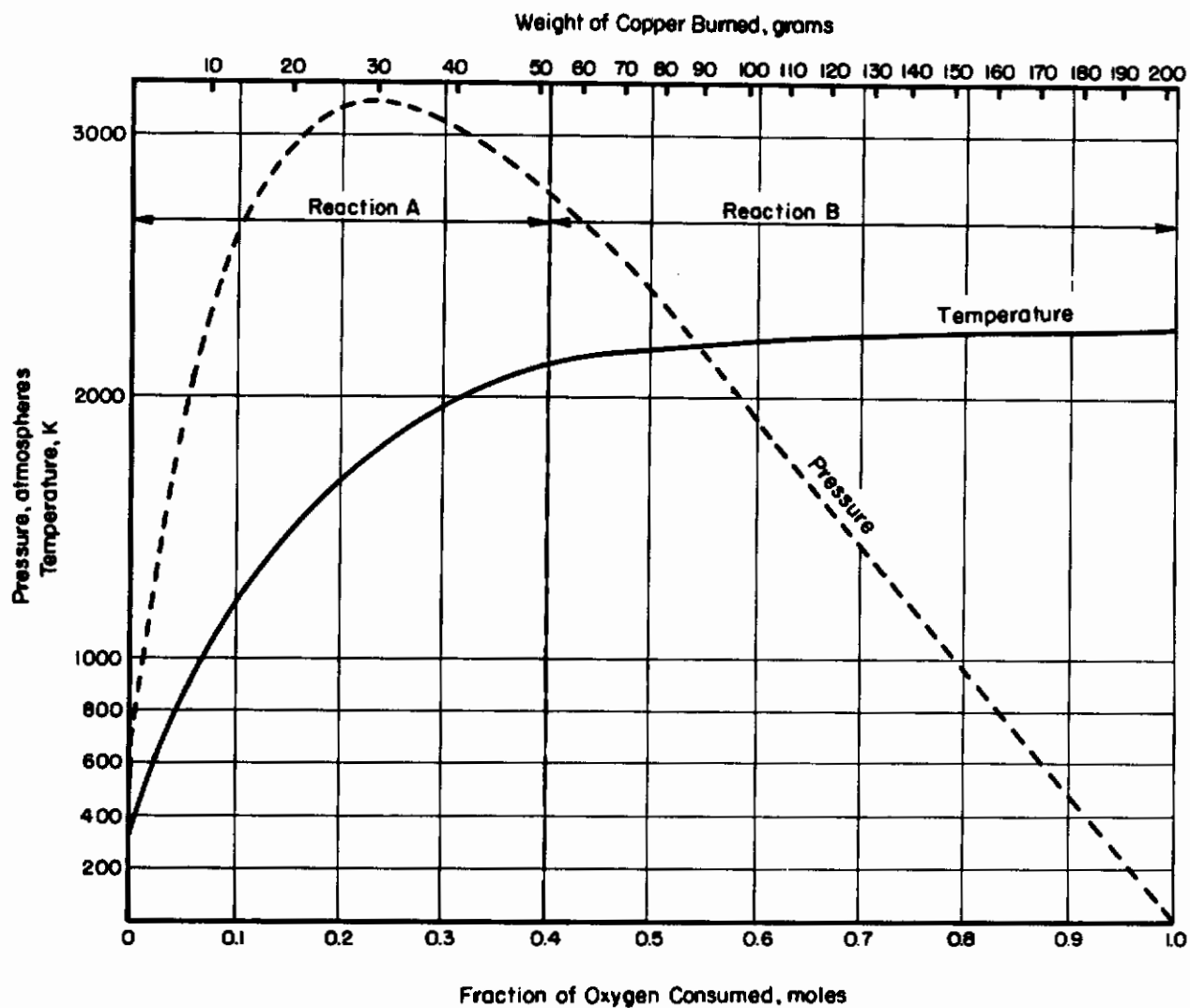


FIGURE 2. PROJECTED EFFECT ON PRESSURE AND TEMPERATURE OF OXYGEN SYSTEM CAUSED BY THE COMBUSTION OF COPPER

Based on Reaction (A) $2\text{Cu} + \text{O}_2 \rightarrow 2\text{CuO}(\text{solid})$ and
 Reaction (B) $4\text{Cu} + \text{O}_2 \rightarrow 2\text{Cu}_2\text{O}(\text{solid})$.

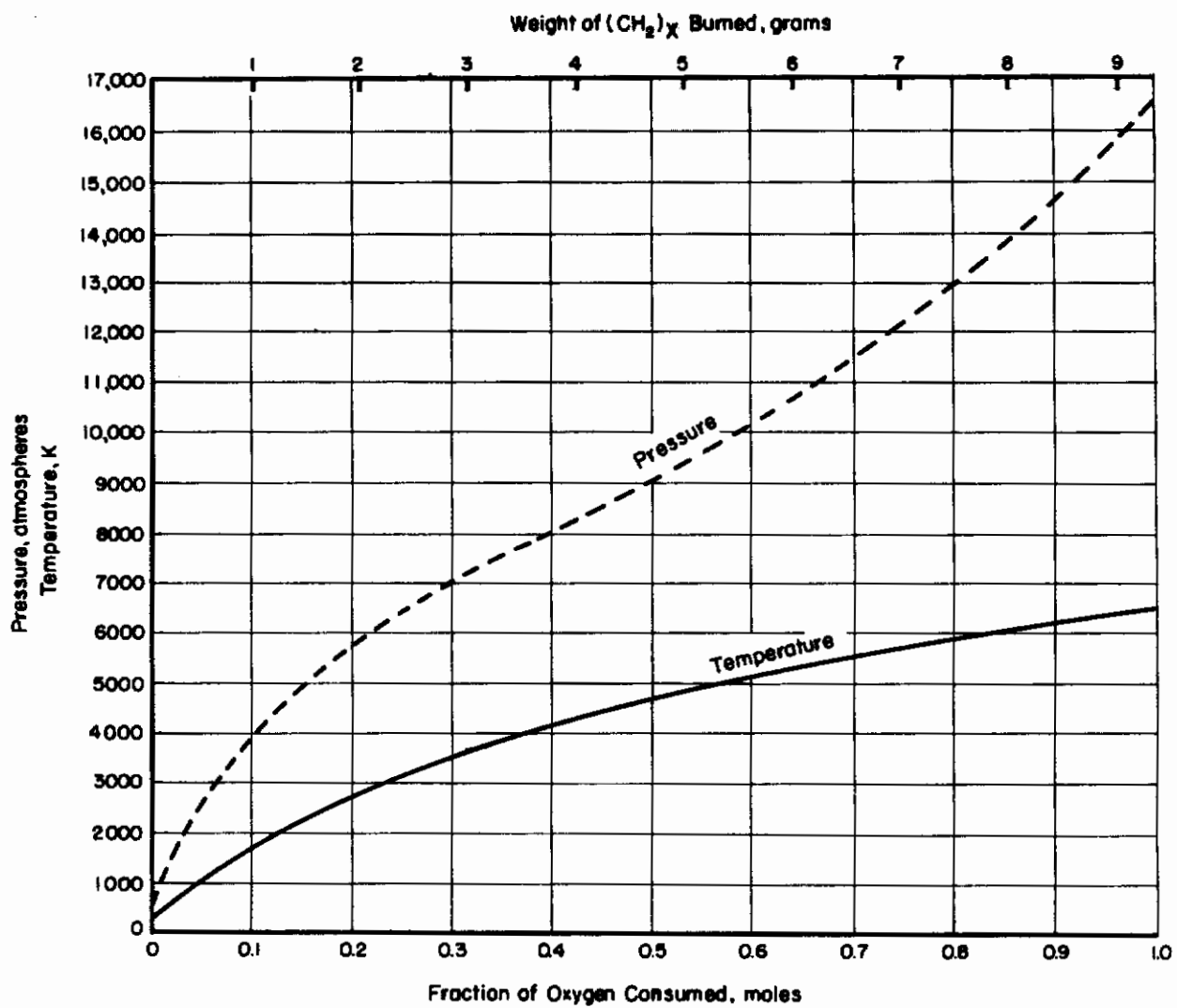


FIGURE 3. PROJECTED EFFECT ON PRESSURE AND TEMPERATURE OF OXYGEN SYSTEM CAUSED BY THE COMBUSTION OF (CH₂)_X

Based on the reaction $\frac{2}{3X} (\text{CH}_2)_X + \text{O}_2 \rightarrow \frac{2}{3} \text{CO}_2 + \frac{2}{3} \text{H}_2\text{O}(\text{gas})$.

Pressure-Temperature Relationships

To design safe experimental equipment of the proper internal volume and wall thickness, it was necessary to know the temperatures, pressures and resulting stresses, and gaseous volumes which would be produced in the process of generating high-pressure oxygen gas. Therefore, although the scope of the research program did not include a determination of the PVT relationship, some analytical determinations were necessary.

The method employed in generating the high-pressure gas was to heat a sealed container filled with liquid oxygen to room temperature. Details are given on page 14. The pressure which could be attained at different temperatures ranging from the boiling point of oxygen up to 100 F were determined by application of two different methods of calculation: (1) the theorem of corresponding states, and (2) the perfect gas law. Only the first method is comparatively accurate for the pressure range of interest. However, calculations based on the perfect gas law are also included to indicate their degree of inaccuracy. The results and sample calculations are given in Appendix III.

Laboratory Investigations

Location and Construction of Laboratory

Two factors were considered in providing the needed laboratory space: location of the building and erection of adequate barriers. The laboratory work was performed in a special building at Battelle's Columbus location. This building, although located in a populated area, is safe for operations with small explosive charges. A blowout wall made of flimsy material which permits immediate dissipation of the explosion energy faces a steep hill 15 feet high which acts as a shock buffer. Each laboratory cell in the building is equipped with an adequate, independent ventilating system and the interior walls separating the cells are made of reinforced concrete. The roof of the building, although not as flimsy as the blowout wall, is also designed to fail before major damage to the building occurs. For double assurance that the surrounding area was safe during the investigation, the protection offered by the steep hill was augmented in the form of a sandbag wall 10 feet high and 1-1/2 feet thick, erected 4 feet from the blowout wall.

Internal barriers were also erected as shown in Figures 4 and 5. As shown in Figure 4, the concrete walls were lined with sandbags to prevent ricocheting of exploding fragments. The construction of the front protective barrier is illustrated in Figure 5. Fittings, valves, and equipment were mounted on the 1/2-inch-thick steel instrument panel in the test area. The control panel was made of 1/4-inch steel plate. The wall below and above the steel panels was constructed from sandbags. While the experiments were in progress, all visual observations were made remotely by means of mirrors. Actual appearance of the cell barriers is shown in Figures 6 and 7.

Design and Assembly of Equipment

Figure 8 is a schematic of the basic system designed for the experimental program. Shown to the left of the dotted line is high-pressure oxygen-generating Subsystem A. Subsystem B, to the right, was used for thermal, vibration, and shock

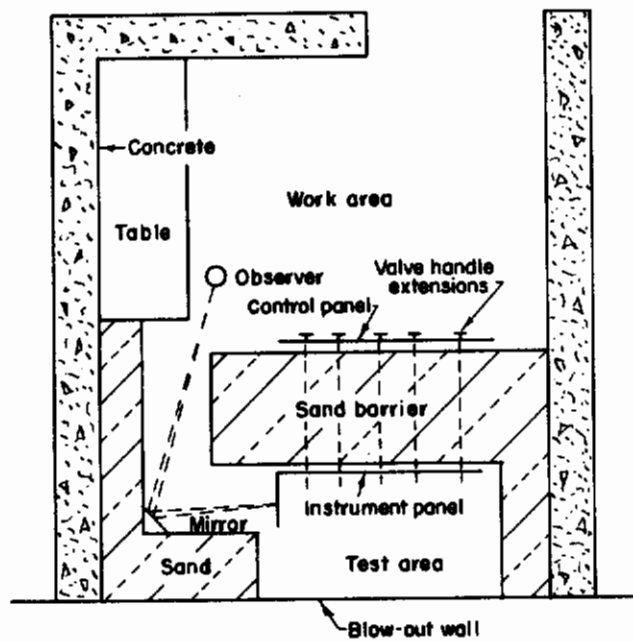


FIGURE 4. PLAN OF LABORATORY CELL

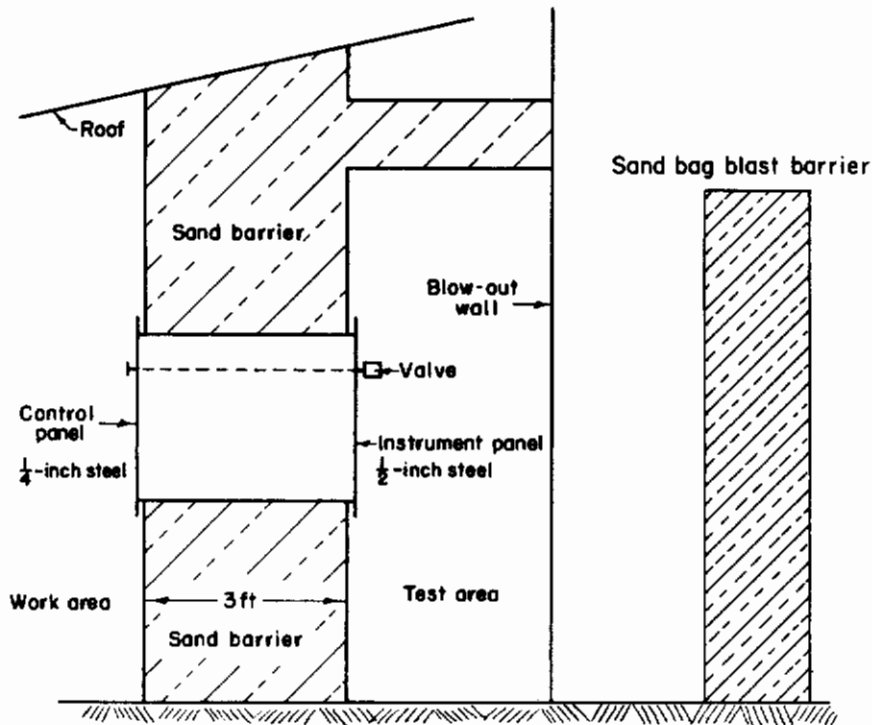


FIGURE 5. ELEVATION OF LABORATORY CELL SHOWING THE SAND BARRIERS

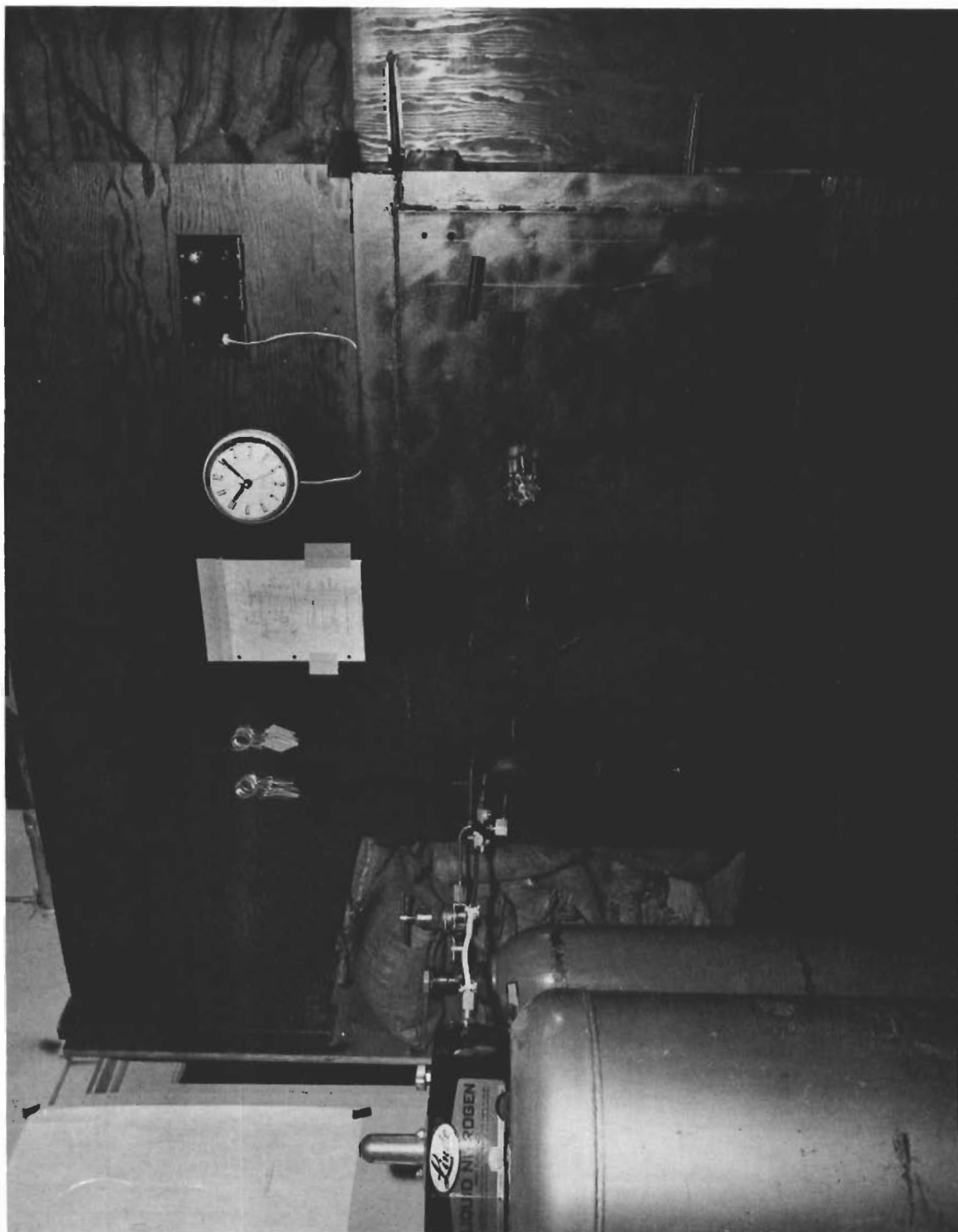


FIGURE 6. VIEW OF SAFE SIDE OF FRONT PROTECTIVE BARRIER

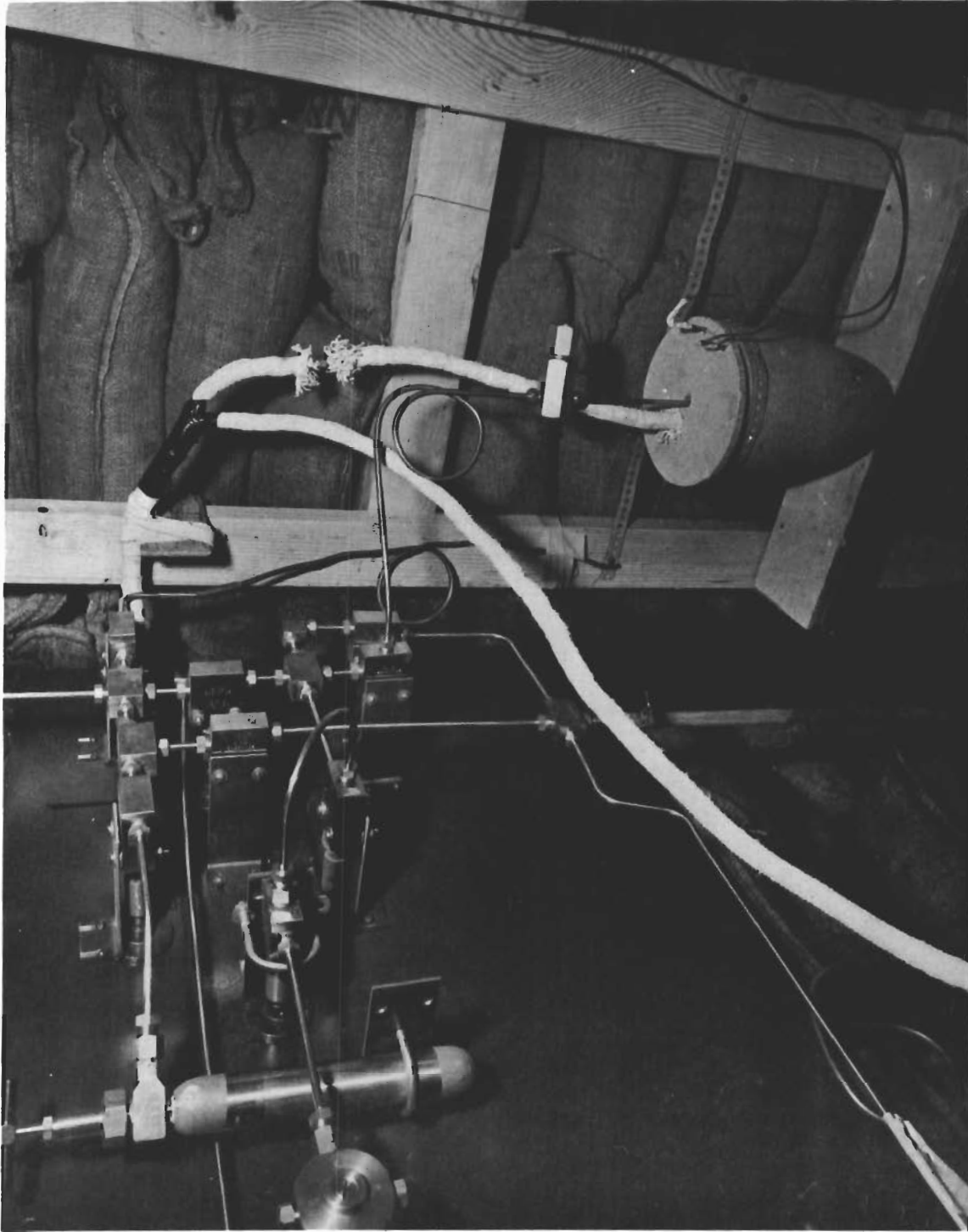
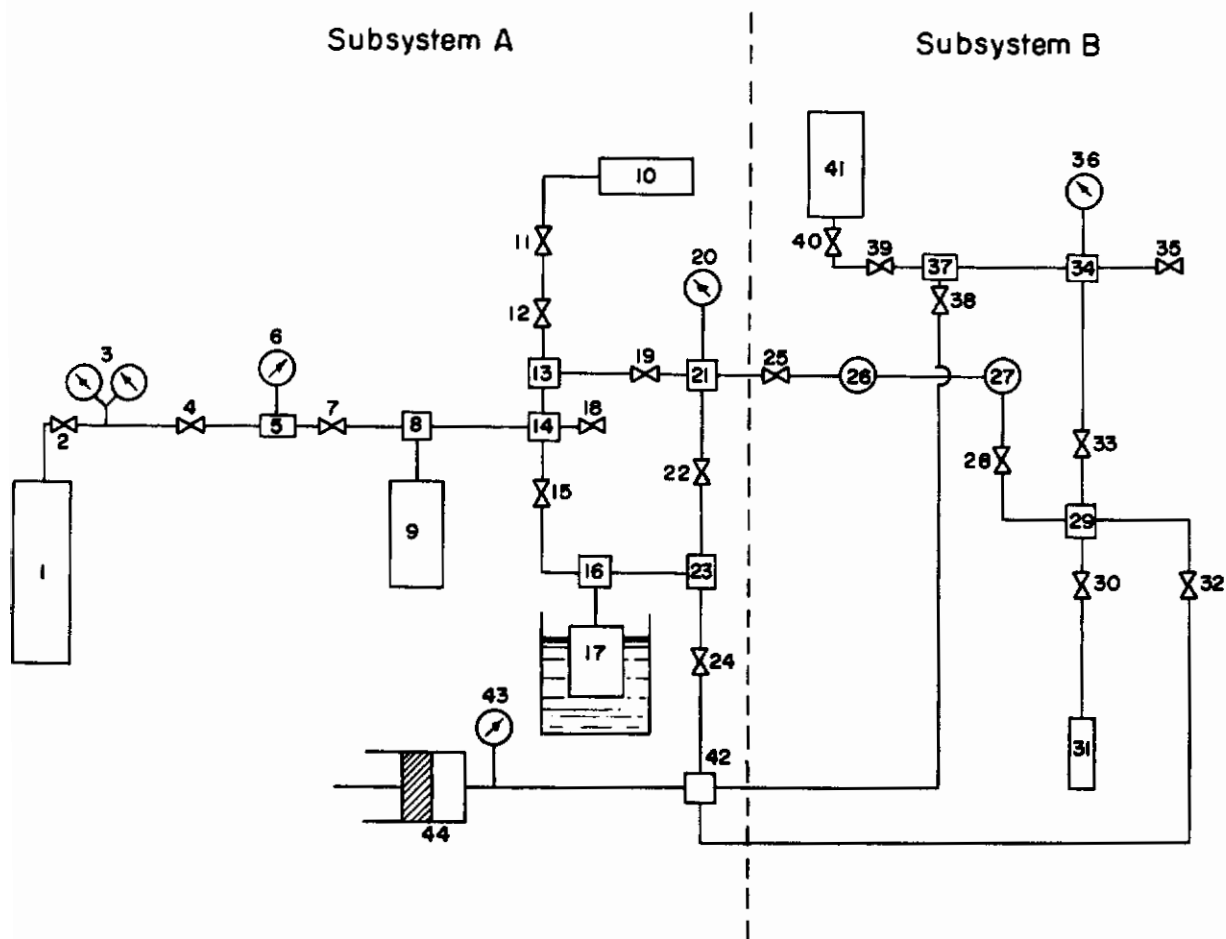


FIGURE 7. VIEW OF TEST AREA AND SET-UP FOR TEMPERATURE EXPERIMENTS



KEY

- | | | |
|------------------------------|------------------------------------|-----------------------|
| 1. Supply cylinder, 2000 psi | 16. Tee | 31. Test tube reactor |
| 2. Valve | 17. Conversion reactor | 32. Valve |
| 3. 0-1500 psi regulator | 18. Bleed valve | 33. Valve |
| 4. Valve | 19. Valve | 34. Cross |
| 5. Tee | 20. 0-20,000 psi gage | 35. Bleed valve |
| 6. 0-1000 psi gage | 21. Cross | 36. 0-20,000 psi gage |
| 7. Valve | 22. Valve | 37. Tee |
| 8. Tee | 23. Tee | 38. Valve |
| 9. Metering tank | 24. Valve | 39. Valve |
| 10. Sampling cylinder | 25. Valve | 40. Valve |
| 11. Valve | 26. Regulator, 10,000 psi delivery | 41. Sampling cylinder |
| 12. Valve | 27. Metering valve | 42. Cross |
| 13. Tee | 28. Valve | 43. Vacuum gage |
| 14. Cross | 29. Cross | 44. Vacuum pump |
| 15. Valve | 30. Valve | |

FIGURE 8. SCHEMATIC OF EXPERIMENTAL SYSTEM

experiments. Flow and surge experiments required modifications of Subsystem B. Storage tests were performed in specially fabricated steel boxes. Details of the experimental procedure for each experiment are given later in the report.

The high-pressure tubing and all valves and fittings were mounted on the steel instrument panel partially shown in Figure 7. Forty-inch extension handles connected to the valves passed through the front protective barrier to permit valve control from the protected work area.

Before assembly all parts were either cleaned for oxygen use by the manufacturer or cleaned in the Battelle laboratory. The parts were cleaned and rinsed in three successive baths of carbon tetrachloride and blown dry with gaseous nitrogen. Rubber gloves were used to handle parts but all equipment was assembled in the normal laboratory atmosphere.

At Kidde Aero-Space, all parts were degreased, rinsed, and then assembled in a dust-free room by men wearing sterilized gloves and special white suits. Such procedures could have been adopted at Battelle to insure minimum contamination but their adoption would not have permitted a reasonable evaluation of the hazards and difficulties normally encountered in field operations.

High-Pressure Oxygen Generation

To conduct experiments with oxygen gas at 7500 psi, it was necessary to generate higher pressures in Subsystem A (Figure 8) to compensate for expansion losses of the gas as it passed through the tubing and valves. The entire system was first purged of contaminants by several successive evacuations and pressurizations. The metering tank (9) was then charged with 450-psi gaseous oxygen and the conversion reactor (17) was completely immersed in a liquid-nitrogen bath. Gas from the metering tank was then allowed to pass into the reactor where the liquid oxygen was formed. As the gas condensed to a liquid, the pressure in the metering tank steadily dropped. It was assumed that the reactor was completely filled with liquid oxygen when no further drop in pressure was recorded on the gage (6) (about 200 psi).

Valve (15) was then closed and the nitrogen bath removed. Almost instantly, the liquid oxygen began to evolve into a gas. The high pressures were attained because of the differences in volume of the original gas and the regenerated gas.

Pressures in the conversion reactor were allowed to reach as high as 16,000 psi before the gas was expanded into Subsystem B. The test-tube reactor (31) was then charged to 7500 psi. The test-tube reactor had already been purged and contained the specimen to be evaluated. After the reactor was charged, the valve (28) was closed and the entire upstream system completely bled to atmospheric pressure.

The procedure outlined was followed in each experiment because fresh charges of oxygen were needed each time and the hazards of operation were reduced if a reserve of high-pressure gas was not stored during the course of the experiment.

Experiments Performed

Many of the experiments were planned to serve a dual purpose. For example, thermal, vibration, shock, and storage investigations provided information about the reactivity of the specimens and also information about the adequacy of the metal alloys from which the reactors were fabricated. Flow tests provided data on electrostatic charges, erosion effects, and again, material adequacy.

Appendix IV includes a complete tabulated summary of the experimental program. For each experiment, environmental conditions imposed such as temperature and pressure are given. Also shown for each experiment are the types of specimen or contaminant evaluated and the metal alloy from which the test reactor was fabricated.

Experimental Methods

For easier description of the details of each type of experiment, this section of the report will cover only experimental methods. Results, evaluations, and conclusions are described in the succeeding sections. The experiments are considered in the following six groups:

- Temperature
- Vibration
- Shock
- Storage
- Flow
- Surge.

Temperature

The effect of temperature variation was evaluated initially between the extremes of -65 and +260 F. However, after the first few experiments, evaluation at -65 F was discontinued because of the apparent low level of chemical reactivity evident even at the upper control temperature of +260 F. Thereafter, the lower control temperature was set at the existing room temperature which ranged from 50 to 75 F. The equipment used in performing these experiments is shown in Figure 9.

In performing the experiments, the temperature of the reactors and their contents was cycled between the low and high extremes as many as four times in a 6-hour period. Initial pressure at room temperature was 7500 psi. In most cases, as the temperature was raised to 260 F, sufficient gas was released from the reactor to compensate for expansion and to maintain the pressure at or near 7500 psi. In some experiments, the gas was not bled and the pressure was allowed to fluctuate with change in temperature. This meant that the pressure varied from as low as 2500 to as high as 12,200 psi. Also, as the temperature was varied during each cycle, changes and inconsistencies in

pressure readings from previous cycles of the same experiment were noted to detect evidence of possible reactions.

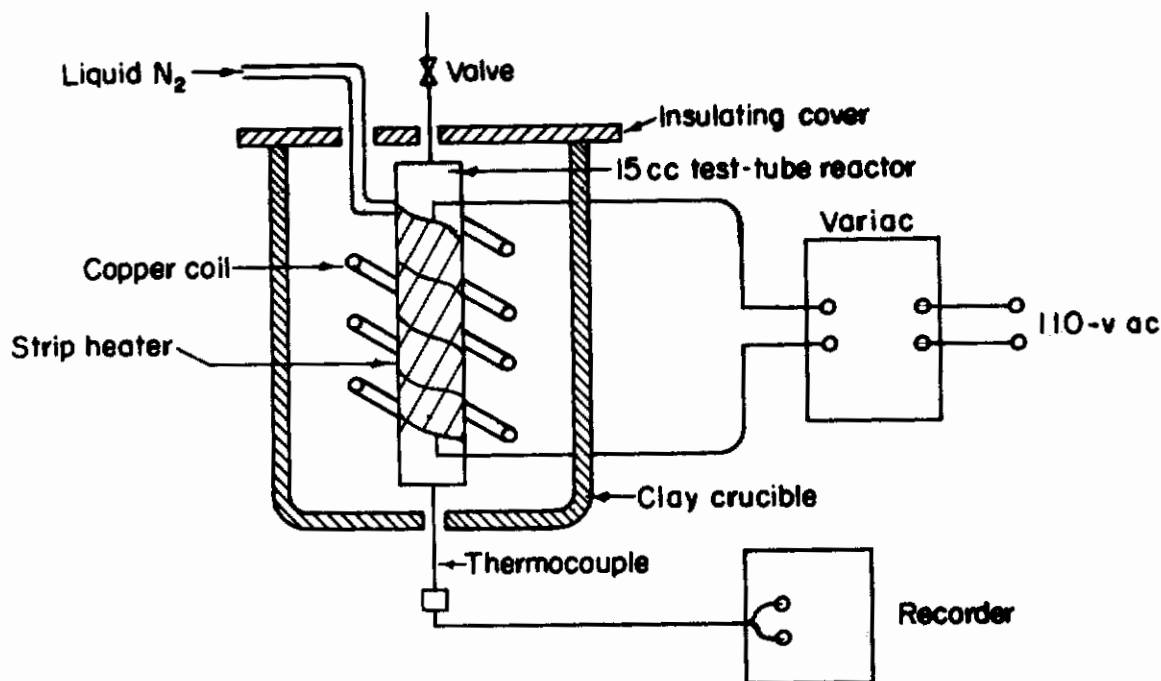


FIGURE 9. SYSTEM USED FOR TEMPERATURE-VARIATION EXPERIMENTS

Minor inconsistencies and small sudden changes did occur occasionally, but they always resulted in reduced rather than increased pressure readings. This can more likely be attributed to the presence of a small leak in one of the connections than to chemical reaction. A chemical reaction would be exothermic and, therefore, pressure would be expected to increase with increased temperature.

The -65 F control point was attained by passing liquid nitrogen through the copper coil. As the liquid escaped from the coil end it evaporated into a gas. The gas was trapped in the clay crucible and could escape only through the opening in the top. While escaping through the top, the cold nitrogen gas (-300 F) passed over and cooled the reactor. The upper temperature-control points between 70 and 260 F were attained by varying the voltage input to the strip heater. Two methods were used to cool the reactor and the oxygen gas to room temperature after 260 F had been reached. Liquid nitrogen was passed through the coil suddenly in one method. This sudden application was equivalent to a thermal shock. In the second method, the reactor was allowed to cool slowly by means of free convection.

Vibration

Vibration conditions were simulated by means of a pneumatically actuated vibrator clamped directly to the test reactor. The vibrator used was a standard UCV-6 model manufactured by Martin Engineering Company, Neponset, Illinois. Frequency of vibration was controlled by the pressure of the air delivered to the vibrator. Frequencies used in the experiments ranged from 35,800 to 50,250 cycles per minute. The effects of vibration were evaluated at room temperature and at 260 F at various frequencies and at pressures ranging from 5000 to 11,000 psi. Table 13 in Appendix IV includes a summary of the entire series of experiments performed. In general, the imposed vibrations were sustained at each frequency and temperature for 1/2 hour although for some experiments the period was extended to 2 hours.

Shock

Ten individual shock experiments were performed. In all cases the maximum imposed shock ranged between 22 and 28 g's. In general, the oxygen gas pressure inside the test-tube reactor ranged from 7500 to 8300 psi. Twenty-five shock loads were imposed at room temperature, whereas as many as 100 shocks were imposed at 260 F.

Figure 10 illustrates the manner in which the shock was transmitted to the charged reactor and the means by which the shock was measured and recorded. An accelerometer was clamped directly to the reactor and the imposed shock was calibrated and measured by the magnitude of the imposed acceleration recorded by a General Electric brush recorder, calibrated in "g" loads. The magnitude of the shock was controlled by the pressure of the air delivered to the small air cylinder which in turn was actuated by the solenoid valve.

Also shown in Figure 10 is a sample chart of the results of a typical experiment. The initial impact of the air cylinder piston was largely reduced because of the elasticity of the metal reactor, the compressibility of the air behind the piston, and the elastic spring of the connecting tubing. This resulted in an initial force of only 3 to 5 g's (the first pip). However, after this initial impact, the 25-g force was recorded (15 millivolts). Not all the energy was absorbed by the first impact and continued rebounds resulted in a series of diminishing shock loads.

Storage

Two separate storage experiments of 500 hours or more were performed. In the first, eight reactors, two each of copper, brass, Monel, and stainless steel were charged with 7500-psi oxygen at room temperature. Included in each reactor was either a hydrocarbon contaminant or a polymeric specimen.

The first storage experiment was a static one and room temperature was maintained for 616 hours except for an intermediate 24-hour period when each reactor was heated to 260 F. Figure 11 shows the system that was used to charge the reactors.

Cylinder (D) was first evacuated and then charged with the hydrocarbon gas at 1 atmosphere. The gas was transferred initially from the supply cylinder (A). After cylinder (D) was charged, the entire system beyond valve (C), including cylinder (J),

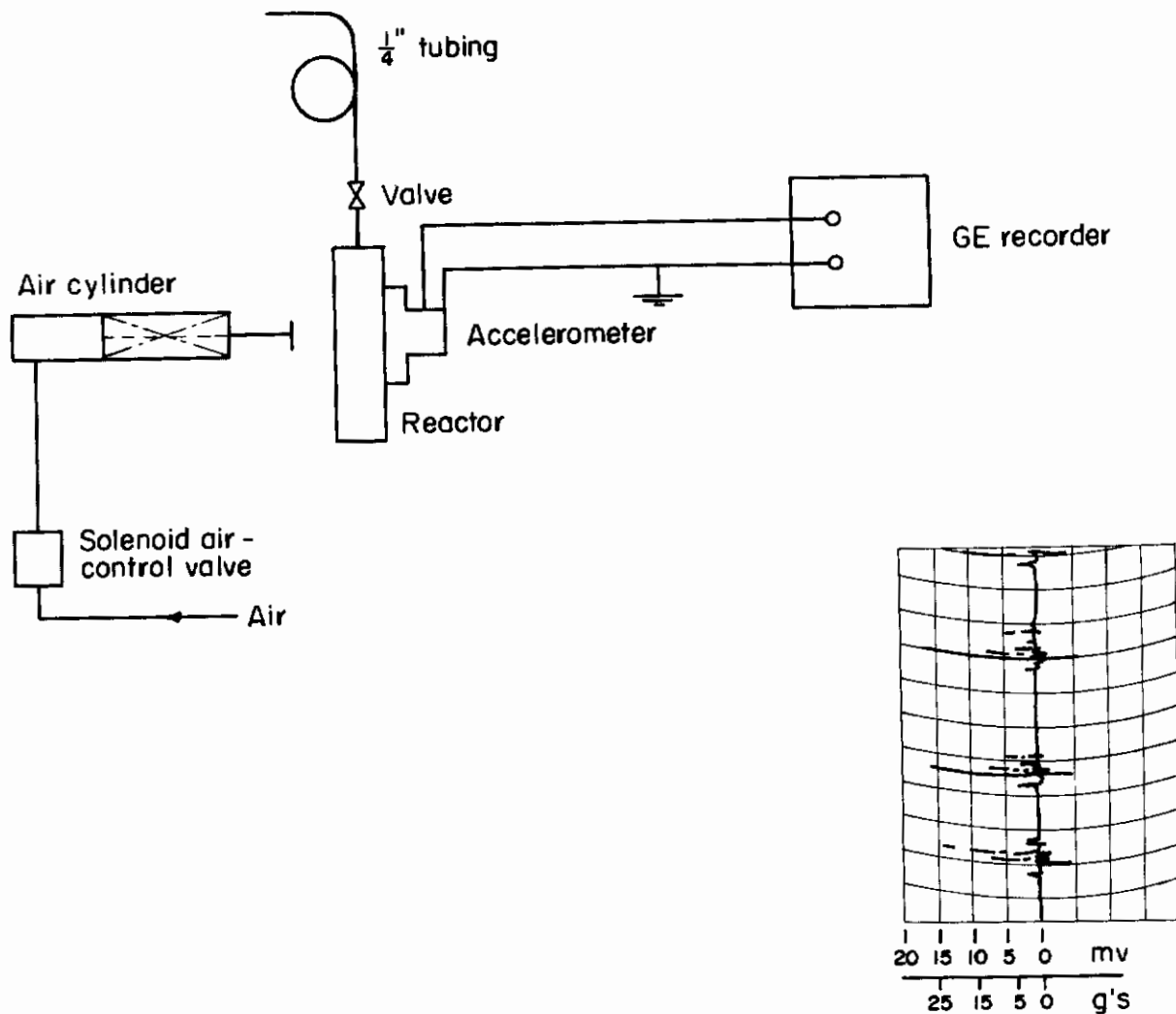


FIGURE 10. SYSTEM USED FOR SHOCK EXPERIMENTS AND TYPICAL CHART OF SHOCK LOADS IMPOSED

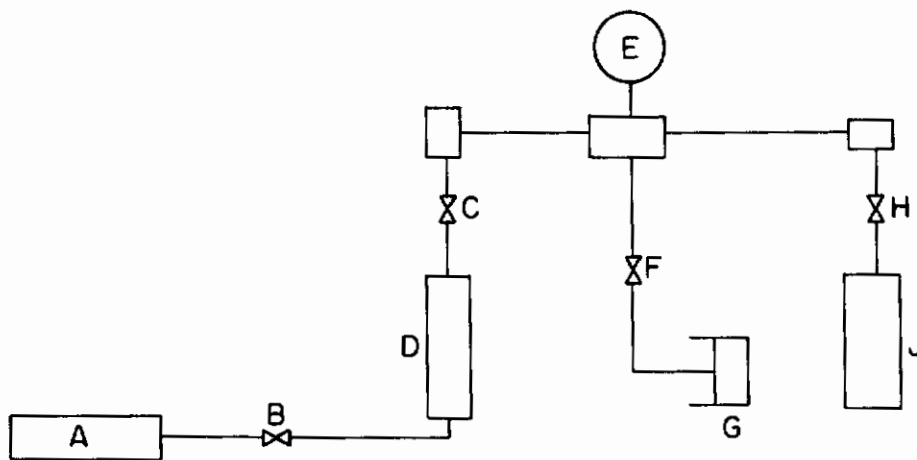


FIGURE 11. SYSTEM USED TO CHARGE REACTORS WITH GASEOUS HYDROCARBONS

was evacuated by vacuum pump (G) and the gas from (D) was allowed to expand into the evacuated system. Valve (C) was then closed and the system evacuated again. The gas remaining in (D) was allowed to expand again. This process was repeated until vacuum gage (E) indicated an absolute pressure reading in reactor (J) of from 1/2 to 3 inches of mercury, depending on the concentration required. Valve (H) was then closed and the test reactor (J) removed. Reactor (J) was then connected to the apparatus being used for the actual experiment and charged with 7500-psi oxygen. This technique was used for all experiments in which hydrocarbon gases were evaluated.

In the second storage experiment, five reactors of stainless steel were charged with 7500-psi oxygen at 260 F. This experiment lasted for 500 hours. The 260 F temperature was maintained throughout the experiment. The specimens tested in this second storage experiment were different from those used in the first experiment. Included in the second series of reactors were tensile specimens of Kel-F and Teflon, deposits of carbon dust, and strands of steel wool. Another condition of this experiment was the use of welded and brazed tubing connections.

Initially all of the reactors were constantly vibrated at 35,800 cycles per minute to simulate dynamic conditions. However, after only 94 hours, two valve connections began to loosen and the pressure in the respective reactors dropped below 2500 psi. For the remainder of the experiment, the reactors were not vibrated and only three of the original five reactors retained the 7500-psi pressure. Figure 12 shows the arrangement of the reactors and the special steel box constructed to house them.

Flow

One objective of the flow experiments was to determine erosion effects for different materials. A second objective was to measure the amount of electrostatic charge generated by the high-pressure high-velocity gas as it expanded through an orifice. The major difficulty encountered in these experiments was the shortness of the flow duration with each charge of high-pressure oxygen. Only a maximum of 45 milliliters of gas could be generated at one time and only 15 to 30 milliliters could be stored.

The arrangement used for the flow experiments is shown in Figure 13. Figure 14 includes details of the retainer assembly and the orifice.

The high-pressure gas was first generated in cylinder (A) where pressures as high as 12,000 psi were generated to permit longer blowdown periods. Valve (C) was then opened and high-pressure high-velocity gas flowed through the retainer-orifice assembly (E) and expanded to atmospheric pressure.

The blowdown period was measured from the time valve (C) was opened until pressure gage (B) indicated 1000 psi. Diameters of the orifices ranged from 0.005 to 0.013 inches. A 0.005-inch-diameter orifice allowed a total blowdown period of 1 minute for each charge. The blowdown period with the 0.013-inch-diameter orifice was only 20 seconds per charge. During a normal 8-hour day, a maximum of eight or nine charges were generated.

Electrostatic charges were measured as shown in Figure 13. Probes of different materials and geometries were inserted into the retainer assembly and placed about 1/8 inch behind the orifice exit. The static charge was picked up by the probe, measured by the Sweeney gage, and transcribed into a visual plot by the oscillograph recorder.

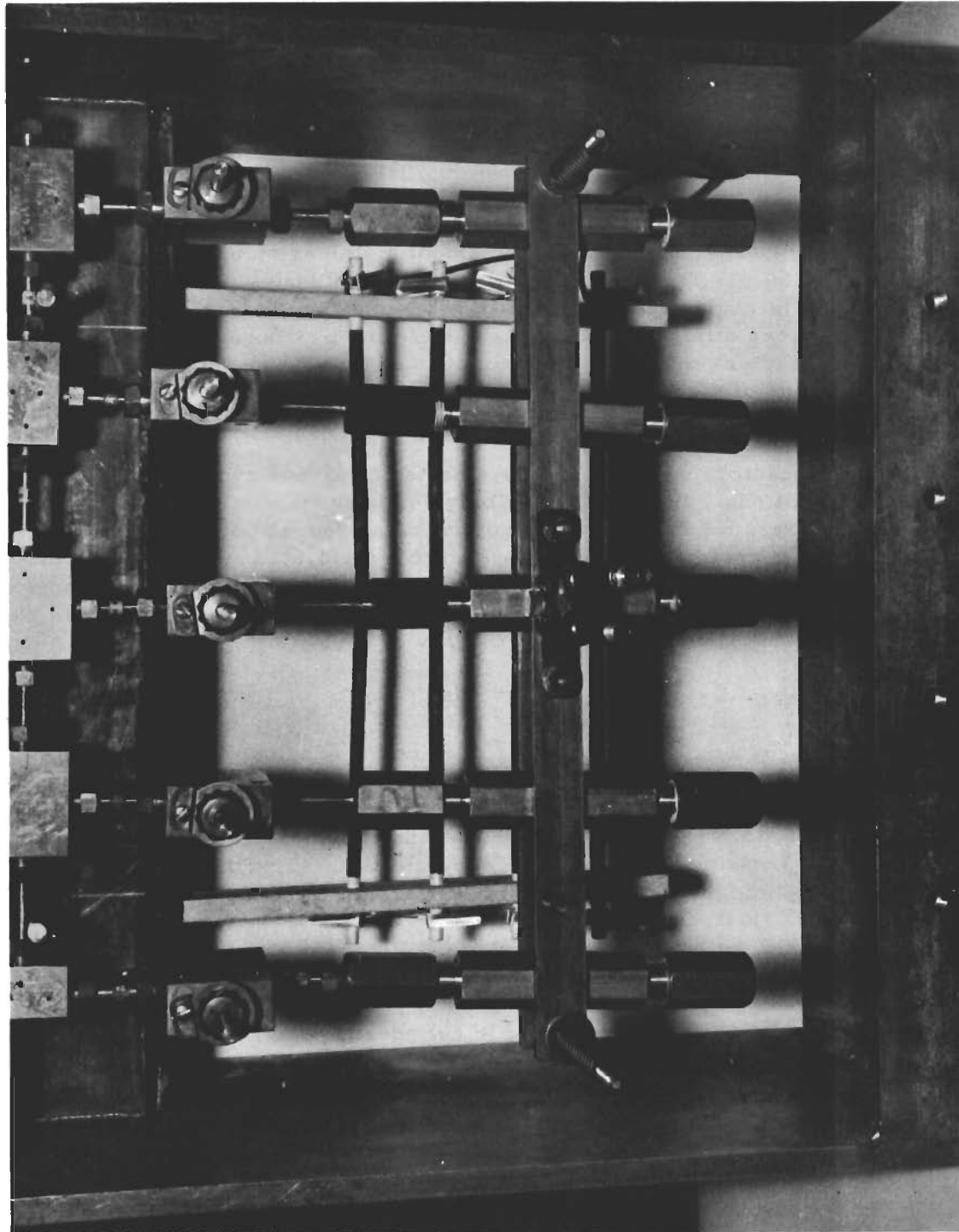


FIGURE 12. REACTORS ASSEMBLED FOR 500-HOUR DYNAMIC STORAGE.
EXPERIMENTS 126 THROUGH 130

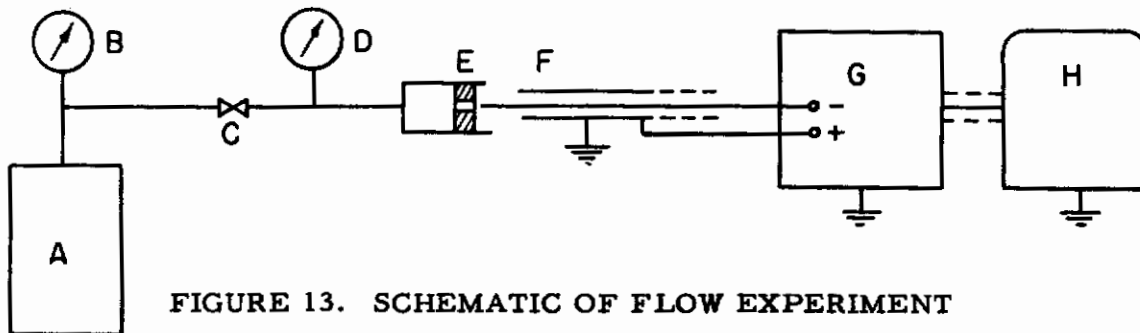


FIGURE 13. SCHEMATIC OF FLOW EXPERIMENT

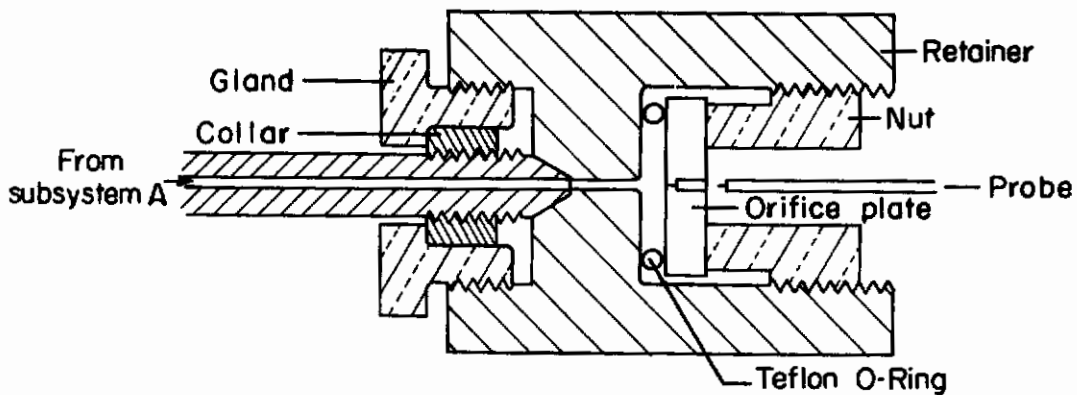


FIGURE 14. DETAILS OF ORIFICE AND RETAINER

Figure 15 shows the actual curve plotted during Experiment 93 when the static voltage was recorded as +0.20 volt. In Appendix IV, Table 16, specific details of experimental conditions, probes used, and voltages recorded are tabulated for all the flow experiments.

Surge

The primary aim in performing the surge experiments was to determine the temperature rise caused by rapid compression. A stainless steel receiver of 3.5-milliliter volume was used for these experiments. As shown in Figure 16, the receiver was immersed in an ice bath (E) to assure a constant reference temperature and to permit better measurement of the resulting rise in temperature.

The receiver (D) was charged to high pressure levels in one rapid charging cycle. Pressures ranging from 10,000 to 16,000 psi were generated in cylinder (A). Hand valve (C) was then opened rapidly and the gas was allowed to expand into the receiver. Depending upon the initial upstream pressure, the instantaneous pressures recorded in the receiver ranged from 5000 to 8300 psi. Simultaneously, the rise in temperature was measured by thermocouple (F) and was recorded on oscillograph (G).

An iron-constantin pencil thermocouple with a 1/8-inch stainless steel tubular sheath was used. The thermocouple wires were brought through the tube and welded at the tip, permitting direct measurement of the temperature fluctuation inside the receiver. The temperature rise measured was that of the gaseous contents of the receiver.

EVALUATION OF EXPERIMENTAL RESULTS

The discussion of experimental results is divided into seven sections. Presented in each section is a discussion of the materials investigated, the experiments performed, the results obtained, and the conclusions derived. The seven sections are:

- Materials Compatibility
- Hydrocarbon Contaminants
- Solid-Particle Contaminants
- Materials of Construction
- Electrostatic Charges
- Adiabatic Heating
- Experimental Equipment Evaluation.

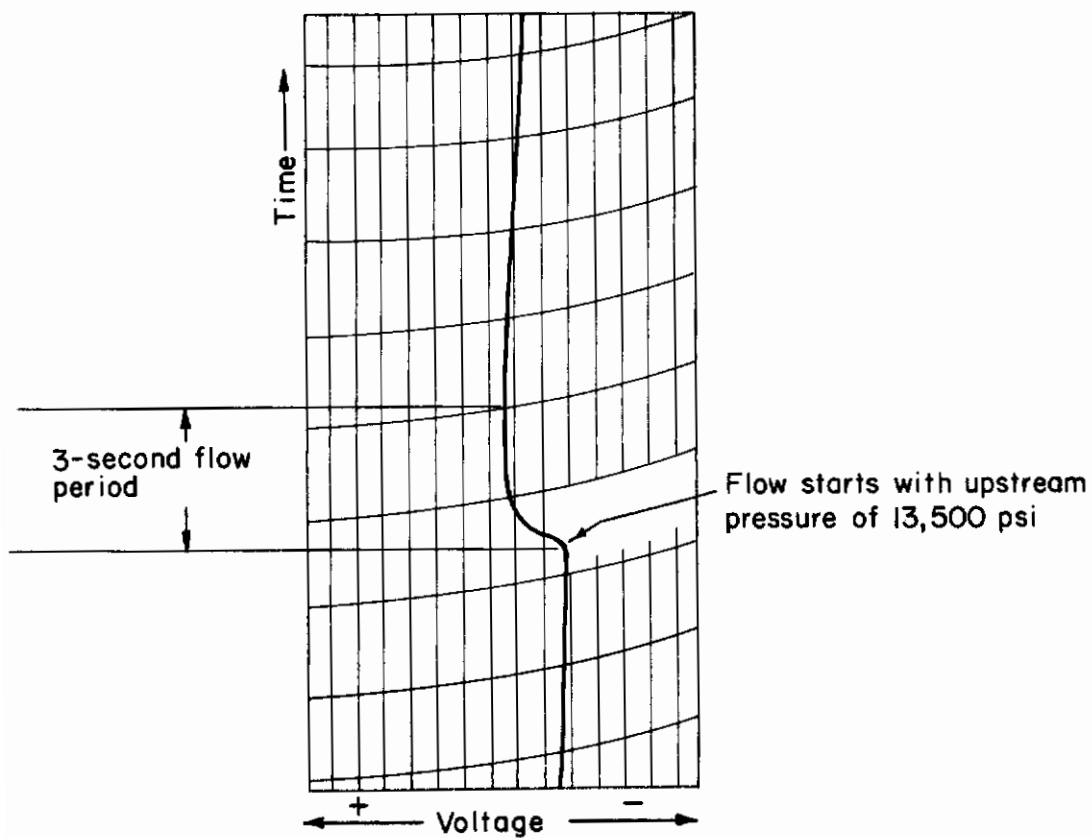


FIGURE 15. ELECTROSTATIC VOLTAGE RECORDED DURING EXPERIMENT 93

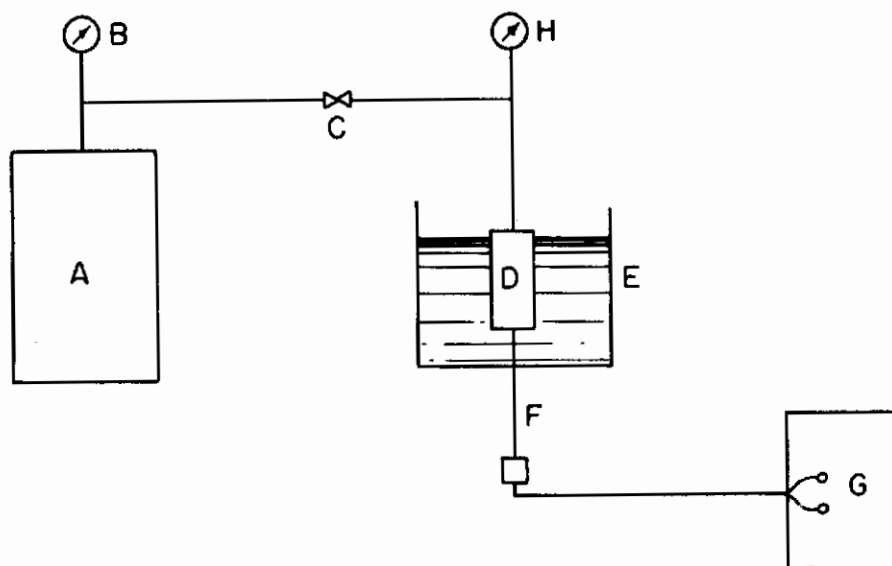


FIGURE 16. SYSTEM USED FOR SURGE EXPERIMENTS

Materials Compatibility

Materials Investigated

Investigations of materials compatibility were conducted for five polymers: Teflon, Kel-F, Viton, neoprene, and nylon. These were chosen because of their possible application as static or dynamic seals or bearings. The following experiments were performed:

- (1) Thermal and vibration tests were performed with Teflon, Kel-F, Viton, and neoprene O-rings when compressed as static seals and also when unconfined.
- (2) Thermal and storage tests were performed with Teflon, Kel-F, and nylon dumbbells to determine what changes in elastic properties result from different conditions and periods of exposure.
- (3) Flow experiments were performed with Teflon and Kel-F orifices to determine erosion resistance of these materials. The orifices were made from disks 3/16-inch thick and 3/4-inch diameter, with a 0.006-inch-diameter hole through the center.
- (4) Storage experiments were performed with shredded pieces of Kel-F, Teflon, and neoprene to determine whether frayed and ragged edges are more susceptible to chemical reaction than the smooth surface normally provided with gaskets and O-rings.

Evaluation of Results

During the experiments no spontaneous changes in pressure or temperature were recorded. This indicated that no gross chemical reaction such as combustion or detonation occurred. Mass spectroscopic analysis of the residual gases also indicated no combustion. However, tensile-test analysis and visual inspection of the specimens indicated that nylon, Viton, and neoprene suffered appreciable chemical change and deterioration of physical properties. Nylon especially deteriorated so badly that tensile tests were not possible.

The extent of the oxidation effect is shown in Table 1 by the changes in tensile strength and ductility as indicated by per cent elongation of standard O-rings. Teflon seems to be an exception in that both the strength and ductility of the O-rings increased slightly. Teflon O-rings increased 1.3 per cent in strength and 8 per cent in ductility. Kel-F decreased 5.5 per cent in strength, but ductility remained the same. Viton and neoprene showed decreases of 23.5 and 58 per cent in strength and decreases of 8.5 and 28.5 per cent in ductility. These results, of course, reflect only a small sampling and a more accurate and reliable comparison would be dependent upon a broader analysis.

In addition to loss of strength, neoprene and Viton O-rings exhibited a high degree of oxygen absorption. O-rings of both polymers when removed from the test reactor had swelled to almost twice their original size and surface blisters were observed. This effect was apparently caused by the absorption of high-pressure oxygen gas. After

remaining at ambient pressure for a short period, the O-rings returned to their original size. In some cases the blisters popped like over-inflated balloons. In all likelihood, seals made of these polymers would be inadequate for extended use because of oxygen embrittlement and high porosity of the polymer.

Teflon dumbbells exposed to high-pressure oxygen for 48 hours at 260 F showed an average change in tensile strength of -2 per cent and an average change in elongation of +10.7 per cent (Table 2). Kel-F dumbbells exposed for an equal period under identical conditions showed average changes of -10.2 per cent in strength and -30.0 per cent in elongation. The Teflon dumbbell exposed for 94 hours in Experiment 126 failed at a machining flaw when subjected to a tensile test. Therefore, the maximum elongation of 1.16 inches is not a true value.

The Teflon specimen exposed for 500 hours in Experiment 127 had exactly the same strength and ductility as the standard specimen. In the light of the demonstrated tendency of Teflon to increase in strength and ductility when exposed for short periods, the results of Experiment 127, if typical, can be interpreted to mean that the crossover point had been surpassed between 48 and 500 hours of exposure and further exposure may result in decreased strength and ductility.

The Kel-F specimen exposed in Experiment 128 demonstrated significant reduction of ductility (81.5 per cent). Corresponding loss in strength was 14.5 per cent. Furthermore, many compression shear failure cracks were visible below the surface of the Kel-F bar after exposure and probably one of these cracks caused the bar to fail prematurely.

Samples of these same materials were also exposed to 260 F for 48 hours in air at normal atmospheric pressure. The Teflon specimen exposed to air at atmospheric pressure increased in ductility appreciably more than the specimens that had been exposed to high-pressure oxygen. Even the strength of the Teflon bar increased by 6 per cent. Kel-F showed decreases of only 2.7 per cent in strength and 44.4 per cent in ductility. The appearance of the Kel-F specimen indicates that failure occurred prematurely because of a machining flaw. The sizable loss in ductility is attributed to this.

Flow experiments were performed to determine erosion resistance of Teflon and Kel-F. The area in the center of the Teflon orifice plate collapsed as shown in Figure 17 when first exposed to 10,000-psi oxygen. This plate was a 3/16-inch-thick disk with a 1/2-inch-diameter unsupported area in the center. It had a 0.006-inch-diameter hole. A second orifice with an unsupported area of 1/16-inch diameter and a 0.006-inch-diameter hole was then exposed to 10,000-psi oxygen. After only 2-1/2 minutes of oxygen flow, the hole was plugged. The oxygen gas, still under high pressure, was forced to escape around the periphery of the disk causing the Teflon to cold flow and to be extruded into the clearance space around the peripheral edge of the steel back-up disk.

The Kel-F disk, also with an unsupported area of 1/2-inch diameter, had sufficient strength to prevent the collapse encountered with Teflon. The Kel-F did not tend to cold flow; however, after 15 minutes of flow, the Kel-F disk showed appreciable concaving. Although the disk did not collapse, it appeared that collapse could have occurred momentarily.

TABLE 1. TENSILE-TEST RESULTS FOR TEFLON, KEL-F, VITON, AND NEOPRENE O-RINGS

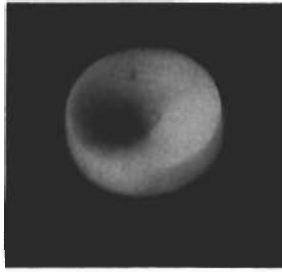
Experiment	Maximum Pull, pounds				Maximum Elongation, inches			
	Teflon	Kel-F	Viton	Neoprene	Teflon	Kel-F	Viton	Neoprene
Standard	19.5	65.7	15	17.5	1.12	0.147	1.29	1.39
11	18.5	--	6.5	--	1.12	--	0.92	--
13	20.0	--	12	--	1.26	--	1.28	--
14	--	58	--	8	--	0.13	--	1.24
15	--	53	--	5	--	0.18	--	1.18
18	19.5	59	13.5	{10.0 11.5}	1.16	0.16	1.30	{1.14 1.20}
19	21.0	--	14	--	1.30	--	1.22	--
20	--	78	--	1.5	--	0.13	--	0.40
21	--	62	--	8.5	--	0.14	--	0.80

TABLE 2. TEST CONDITIONS AND TENSILE-TEST RESULTS FOR TEFLON, KEL-F, AND NYLON DUMBBELLS

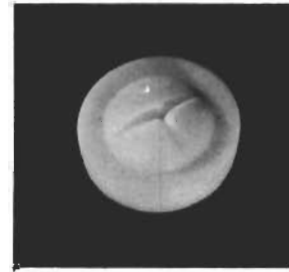
Experiment	Material	Pressure, psi	Temperature, F	Elapsed Time, hours	Results	
					Max Pull, pounds	Max Elongation, inches
--	Teflon (standard)	--	--	--	50	2.05
103	Teflon	15(a)	260	48	53	2.67
100	Teflon	7800/8000	260	48	50	2.34
100	Teflon	7800/8000	260	48	48	2.20
126	Teflon	7500	260	94	53	1.16(b)
127	Teflon	7500	260	500	50	2.00
--	Kel-F (standard)	--	--	--	187	0.54
102	Kel-F	15(a)	260	48	182	0.30(b)
101	Kel-F	7800	260	48	166	0.42
101	Kel-F	7800	260	48	170	0.34
128	Kel-F	7500	260	500	160	0.10
109	Nylon	5500/8500	260	47	Tensile test not possible because of embrittlement and specimen deterioration	
110	Nylon	5500/8500	70	46		

(a) Conducted in air.

(b) Early failure caused by machining flaw in sample.



a. Front View



b. Back View

FIGURE 17. TEFLON ORIFICE DISK AFTER EXPOSURE TO 10,000-PSI OXYGEN

Photomicrographs of the Kel-F disk (Figure 18) indicate that peripheral edge deterioration is appreciable. Deep gouges and scratches appear along the entire edge. The cross-sectional view shows how badly the leading edge has been rounded off. Also, it appears that the force exerted on the diametral surface has caused the Kel-F material to "melt" and flow in the same direction of the gas stream. This appears to be similar to the cold flow of the Teflon disk.

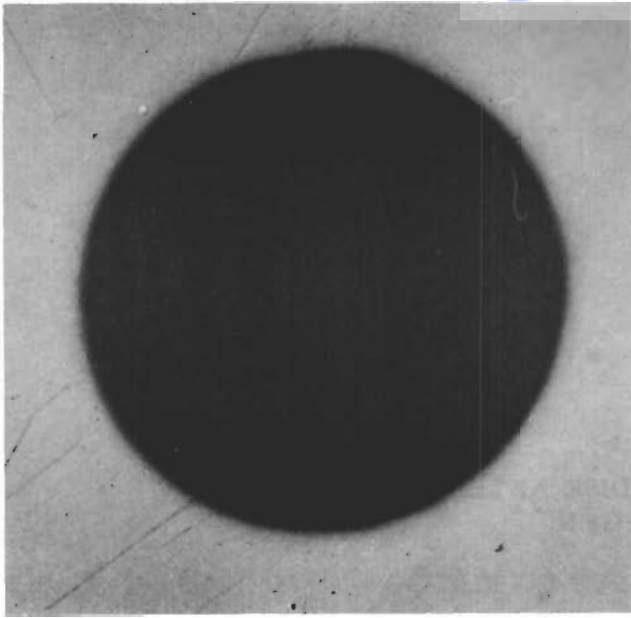
In the static 616-hour storage experiment, shredded specimens of Viton, Kel-F, and Teflon were subjected to continuous exposure to oxygen at 7500 psi. The mass spectroscopic analyses made of the residual gases showed no evidence of chemical reaction and there appeared to be no visual evidence of physical deterioration. Emission spectrographic analysis indicated no change in the Teflon.

Conclusions

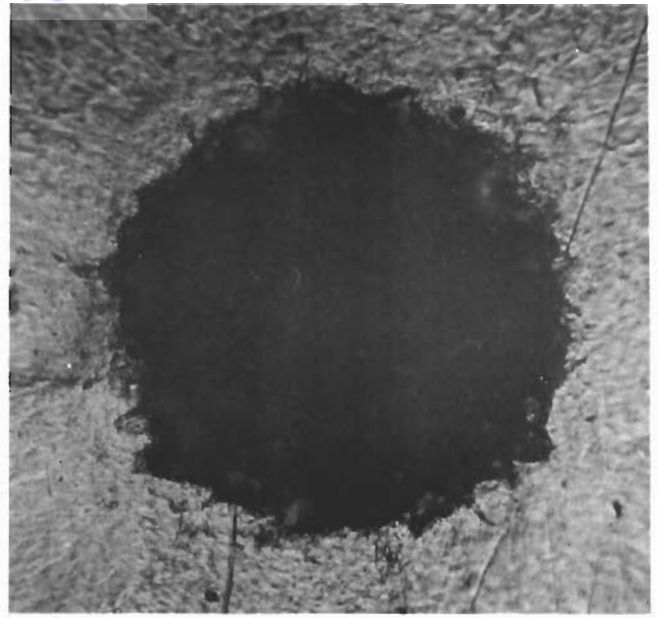
Teflon and Kel-F are both compatible with high-pressure oxygen systems with regard to chemical reactivity, and they manifest a high degree of stability. Viton, however, shows questionable compatibility although an insufficient number of samples were tested in this program to draw firm conclusions. AiResearch also reports some failures with Viton O-rings but nevertheless they are using them as seals in the Mercury control equipment. (10) In any case, neoprene seals were found to be incompatible with high-pressure oxygen.

Pure Teflon suffers from certain physical weaknesses. It tends to cold flow very easily, and because of its high ductility and lubricity, it is easily extruded out of shape when unconfined. Neither does a thin, unsupported Teflon disk have sufficient strength to prevent collapse when high-pressure forces are applied.

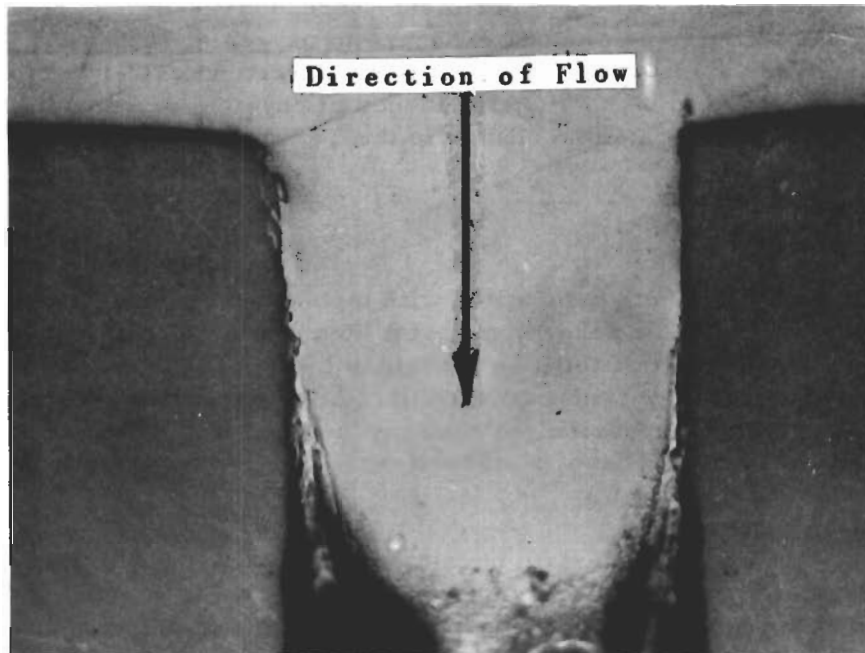
Kel-F has sufficient strength and rigidity to partially overcome the cold-flow problem for short periods and it can withstand instantaneous impacts from flow that would cause Teflon to collapse or extrude. However, Kel-F does not appear to be sufficiently ductile for seal use, nor does it provide the lubricity of Teflon. A possible solution, aside from the conventional compounding of Teflon with ceramic, glass fiber, and asbestos cloth, is use of a new compound of Teflon and Kel-F. This compound consists of 80 parts Kel-F and 20 parts Teflon. According to the developer, Minnesota Mining and Manufacturing Corporation, it is sufficiently strong to resist cold flow, is more



a. Face View Before Exposure



b. Face View After 15 Min of Flow



c. Cross-Sectional View After 15 Min of Flow

FIGURE 18. FACE AND CROSS-SECTIONAL VIEWS OF 0.006-INCH DIAMETER KEL-F ORIFICE

ductile than pure Kel-F, and retains the lubricity of Teflon. However, both Kel-F and Teflon should be employed as seals only when closely confined (like O-rings) to prevent possible collapse or cold flow.

Hydrocarbon Contaminants

Determination of the effects of various hydrocarbon contaminants was based on the acceptable limits imposed by Aeronautical Systems Division on aviators' breathing oxygen. These limits are given in Table 3.

TABLE 3. ACCEPTABLE LIMITS OF HYDROCARBON CONTAMINANTS

Contaminant	Symbol	PPM, vol
Methane	CH ₄	15.00
Acetylene	C ₂ H ₂	0.05
Ethylene	C ₂ H ₄	1.00
Propane	C ₃ H ₈	1.00
Butane	C ₄ H ₁₀	1.00
Pentane	C ₅ H ₁₂	0.20
Hexane	C ₆ H ₁₄	0.02
Decane	C ₁₀ H ₂₂	10.05

Experiments Performed

Four types of experiments were performed: (1) vibration, (2) shock, (3) storage for 616 hours at static conditions, and (4) exposure for short periods at temperatures as high as 400 F.

All of the hydrocarbons listed in Table 3 were investigated. Because of the rather minute concentrations required and the small volumes of gases involved, it was necessary to estimate the mixtures in each charge.* The method by which the reactors were charged with the gaseous hydrocarbon is described on page 17. Liquid hydrocarbon concentrations were determined by the amount of liquid released from a medicine dropper. After each experiment, a sample of the residual gas was analyzed by mass spectroscopy, and by this means the actual concentrations of various gases were determined. It also served to show by CO₂ and CO concentrations whether a chemical reaction had occurred. Table 4 lists the hydrocarbons investigated, the maximum temperature imposed, the original hydrocarbon charge used, and the amount of hydrocarbon found in the residual gas of each experiment.

*See Appendix V.

TABLE 4. CONCENTRATIONS, MAXIMUM TEMPERATURES, AND MASS SPECTROSCOPIC ANALYSES OF HYDROCARBON EXPERIMENTS

Experiment	Hydrocarbon	Maximum Temperature, F	Original Hydrocarbon Charge	Mass Spectroscopic Analysis of Residual Gas, ppm
23	Hexane	265	2 drops	50
25	"	275	6 drops	500
26	Decane	280	8 drops	<20
29	Pentane	264	2 drops	500
31	Methane	262	1 in. Hg	14
32	Propane	262	Ditto	70
33	"	280	13 in. Hg	450
34	Methane	262	6.5 in. Hg	170
35	Butane	265	4 in. Hg	90
36	Decane	Room	2 drops	<15
37	"	255	2 drops	<15
38	Acetylene	265	1 in. Hg	100
39	Pentane	66	2 drops	1040
40	Hexane	260	0.5 in. Hg	No trace
44	Methane	260	Ditto	Ditto
134	Ethylene	400	"	"
135	Propane	400	"	"
136	Acetylene	400	"	"
137	Methane	260	"	"
138	Ethylene	400	"	"
139	Acetylene	400	"	"
140	Methane	395	"	"
141	Propane	260	"	"
142	"	350	"	"
143	Methane	255	1.5 in. Hg	"
144	"	400	Ditto	30
145	Acetylene	260	"	60
146	"	395	"	80
147	Propane	260	"	No trace
148	"	405	"	No trace
149	Ethylene	265	"	30
150	"	400	"	100
151	Acetylene	265	3 in. Hg	250
152	Ethylene	265	Ditto	120
153	Methane	260	"	<50
154	Propane	270	"	430

Evaluation of Results

The most significant result of all the experiments performed with hydrocarbons is the apparent failure of the oxygen-hydrocarbon mixture to react violently or spontaneously even when a sudden charge of high-pressure gas was allowed to surge into a reactor which already contained such potentially explosive gases as acetylene.

In the first series of experiments performed (Experiments 23-26, 29, 31-39, 40, 44), the results obtained by mass spectroscopic analysis were too ambiguous and inconsistent to permit a definite conclusion as to whether or not there had been a chemical reaction. An early difficulty encountered was the impurity of the hexane used and the masking of the findings by carbon tetrachloride vapors. These difficulties were overcome by obtaining a new hexane sample and by a more careful cleaning and drying of the equipment. A more serious handicap that could not be completely alleviated was the tendency of the mass spectroscopic machine to produce CO and CO₂ from its own pump oil. These gases mixed with the sample gas and necessitated application of a correction to the results. However, because of the fluctuation in readings it could not be determined whether the analyzer produced different quantities of CO and CO₂ each time or whether increased quantities of these gases were present due to chemical reaction.

Probably the most important indications that chemical reaction did not occur considering the uncertainty of the CO and CO₂ readings were the steady temperature and pressure readings observed throughout the course of each experiment. Another indication that chemical reaction did not occur was the absence of water vapor in all of the samples analyzed by mass spectroscopy.

During the second series of experiments (Experiments 134-154), methane, acetylene, propane, and ethylene were investigated. The concentration of the hydrocarbon was determined by the pressure ratio of oxygen gas at 7500 psi to hydrocarbon gas at 1/2, 1-1/2, or 3 inches of mercury. Each hydrocarbon and each concentration was evaluated at 260 and 400 F. As in the previous series of experiments, analysis by mass spectroscopy failed to produce clear evidence of a chemical reaction. The failure to find a trace of the hydrocarbon in Experiments 134-143 is attributed to the probability that the concentration was below the sensitivity of the analyzer.

Conclusions

Apparently the hydrocarbon-oxygen mixture is a rather complex one in that merely mixing the two constituents does not appear to be the only thing necessary to initiate a chemical reaction. Case histories of storage vessels at 2000 psi or less suddenly exploding for no apparent reason seem to substantiate the suggestion that a third factor or sequence of events must be present. However, the triggering agent may not be the same in all cases. The only method whereby the explosive nature of hydrocarbon-oxygen mixtures may be properly and more fully understood is through an extensive series of carefully controlled deliberate explosions. Studies of this type have been conducted, but never at pressures of 500 atmospheres.

On the basis of the data available from the present experiments, the following can be concluded:

- (1) Below 400 F concentrations of 50 ppm or less are not highly reactive and do not constitute a major danger.
- (2) If a reaction did occur, it was either too rapid, too slow, or too slight to be detected by visual readings of the pressure gage or by temperature fluctuations recorded by the thermocouple.
- (3) If a reaction did occur, it did not go to completion. This conclusion is supported by the fact that traces of hydrocarbon were indicated in most gas analyses. The reaction may not have been sustained for two possible reasons: (1) because of the low concentration, the gas was too finely diffused and could not sustain a flame front and (2) the total heat of reaction was small and was too quickly dissipated to "set off" the remaining unburned gases.

Solid-Particle Contamination

Experiments Performed

Three types of experiments were performed:

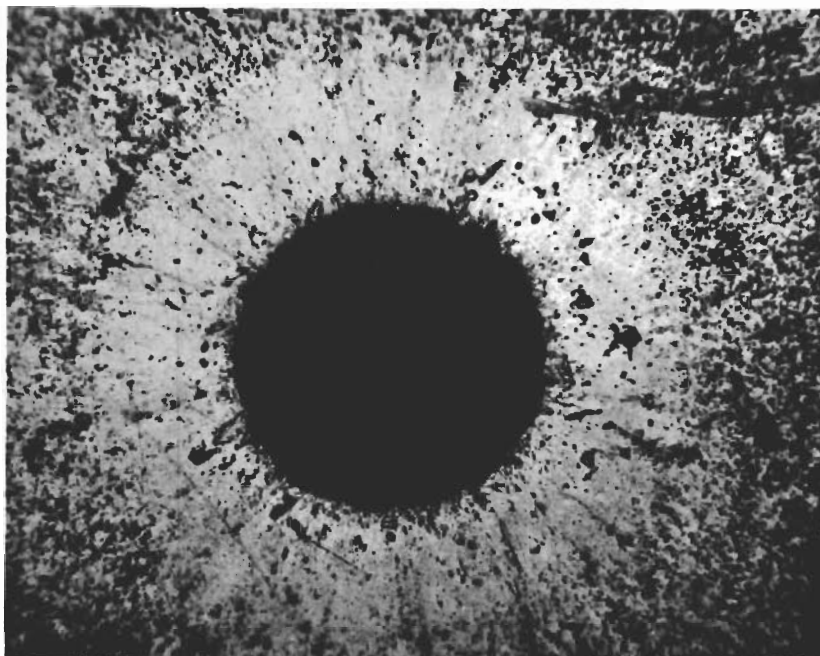
- (1) Unfiltered high-pressure gas was allowed to pass through brass, stainless steel, Teflon, and Kel-F small-diameter orifices.
- (2) Carbon steel and aluminum chips and filings were exposed for short periods (Experiments 27 and 28).
- (3) Carbon dust and carbon steel dust and filings were exposed for a 500-hour period (Experiments 129 and 130).

Evaluation of Results

Because the high-pressure oxygen gas was not filtered, small quantities of solid particles were always present in every experiment performed. This is apparent from the photomicrographs made during the flow experiments. Figure 19a shows the orifice immediately after removal but before any cleaning. In Figure 19b, the same orifice is shown after cleaning in denatured alcohol. Not only do these photomicrographs indicate presence of solid particles, they also indicate the nature of the flow streams entering the orifice. Note the comparatively clean area immediately surrounding the orifice. This indicates that the gas stream separated from the surface as the gas began to "bend" around the corner and into the orifice.

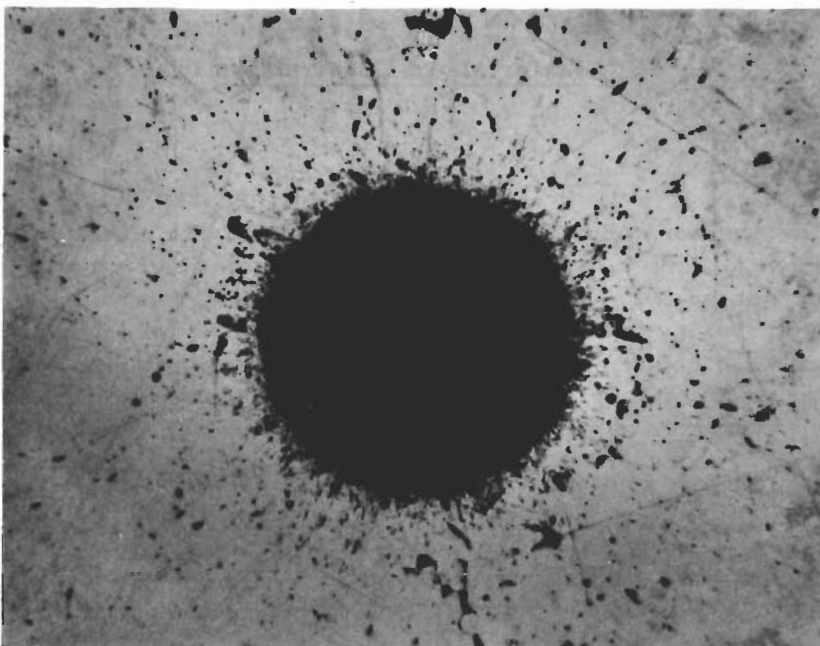
Although minute solid particles were always present, it appears that they had no deleterious effect and did not create any undue tendency for the oxygen gas to react with the particles or with any other contaminant which might have been present.

In Experiment 27, chips and filings of cold-rolled steel were exposed to 8000-psi oxygen at 262 F at 35,800 vibrations per minute for 220 minutes. In Experiment 28, aluminum chips and filings were similarly exposed. In neither case did the presence of the metallic particles have any apparent effect.



250X

a. Before Cleaning



250X

b. After Cleaning in Denatured Alcohol

FIGURE 19. 0.005-INCH-DIAMETER BRASS ORIFICE AFTER 13 MINUTES
47 SECONDS OF FLOW, BEFORE AND AFTER CLEANING

Contrails

In Experiment 129, graphite dust held in a glass vial was exposed to 7500-psi oxygen at 260 F for 94 hours at 35,800 cycles per minute and for another 406 hours under static conditions. Mass spectroscopic analysis of the residual gases showed a high concentration of CO₂ (5300 ppm). However, most of the carbon dust was found caked at the bottom of the vial after completion of the experiment. No evidence of actual combustion was noted.

Experiment 130 involved fine cold-rolled steel filings and dust. The specimen was contained in a glass vial. After exposure for 94 hours at 7500 psi, 260 F, and 35,800 cycles per minute, the valve connection was shaken loose and the oxygen gas escaped. The residual gases were contaminated with air and a mass spectroscopic analysis was not possible. Visual inspection showed that the steel particles became only slightly reddish and that the glass vial was likewise discolored. Again, no evidence of combustion was noted.

Conclusions

The experiments performed were too limited in scope to permit a proper evaluation of what effect the presence of solid particles has. On the basis of the literature, indications are that the presence of solid particles in a moving gas stream is the most critical consideration. This aspect of the problem is further discussed in later sections of the report.

Materials of Construction

Materials Investigated

Four materials were chosen for evaluation: Type 316 stainless steel, Monel, brass, and copper. Stainless steel and Monel are commonly accepted as good engineering alloys for oxygen service and most of the standard hardware and equipment available is fabricated from them. Brass and copper were selected because they have high ignition temperatures and copper especially will generally not sustain combustion if initiated by another source. Figure 20⁽⁹⁾ demonstrates how the spontaneous ignition temperature of brass and copper becomes almost constant after 1200 psi at about 1500 F, whereas the temperature of iron constantly drops. At 2000 psi the ignition temperatures of the three metals are:

Copper	1500 F
Brass	1427 F
Iron	1112 F.

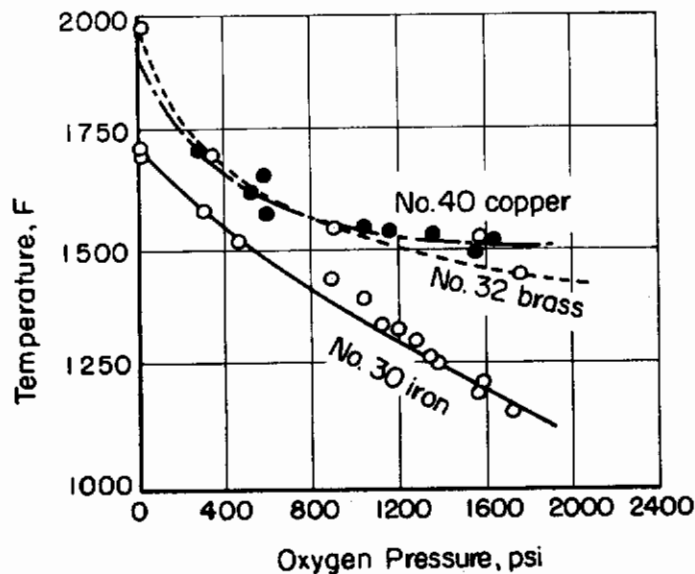


FIGURE 20. IGNITION TEMPERATURE OF METALS AS A FUNCTION OF OXYGEN PRESSURE

The observed ignition temperature of iron is much below the theoretical value of 1700 F that can be reached by instantaneous compression to 2000 psi, while that of copper is but slightly below. Another consideration in selecting these four materials is that they generally do not require surface plating or coatings for protection against oxidation as do carbon steels. Kidde Aero-Space and AiResearch used Type 4340 steel for spherical storage vessels. This alloy is excellent for pressure vessel fabrication but requires a nickel plating to protect the surface from excessive oxidation. Titanium alloys were not considered because of negative experimental results obtained at Battelle and Stanford during previous research programs.

Experiments Performed

Four types of experiments were performed. In the first series of experiments, one reactor fabricated of each metal was used for both static and dynamic experiments involving temperature variation, vibration, and shock (Experiments 11-39, Tables 12, 13, and 14 in Appendix IV). These reactors were each recharged with high-pressure oxygen as many as nine times. In a second series of experiments (Experiments 40-47), two reactors of each metal were used to statically store 7500-psi oxygen for 616 hours. In a third series of experiments, the effect of surface finish on oxidation rate for stainless steel, brass, and aluminum was evaluated. Specimens were exposed to both dry and moist high-pressure atmospheres at room temperature and 260 F (Experiments 115-121). The final series of experiments determined the amount of erosion caused by high-pressure high-velocity flow through a small orifice. In these experiments, brass and stainless steel orifice plates were used. The brass plate had a 0.005-inch-diameter orifice and the stainless steel plate a 0.013-inch-diameter orifice.

Evaluation of Results

Discussion of the evaluation of experimental data will be arranged as follows: (1) changes in physical properties, (2) changes in microstructure, (3) oxidation rate, (4) oxygen penetration, and (5) erosion.

Physical Properties. To determine the change in physical properties, tensile tests were performed with standard-type tensile-test bars prepared from the original metal and from the reactors used in Experiments 11-39. Figure 21 includes a dimensioned diagram of the reactors and dimensions of the tensile test bars and also shows how the test bars were cut from the reactor body. The properties determined were modulus of elasticity, yield strength, ultimate tensile strength, and per cent elongation. These values and other data are included in Table 5.

The two most important values that affect selection of a pressure-vessel material are tensile yield strength and per cent elongation. If the data in Table 5 are corrected to compensate for different periods of exposure and for the different number of pressure cycles, a significant comparison can be made as to the relative applicability of each metal investigated.

In absolute quantities, stainless steel has the greatest initial strength, having a tensile yield strength 14 per cent greater than Monel, 54 per cent greater than brass, and 68 per cent greater than copper. Also, the stainless steel alloy demonstrated the best percentage change in yield strength per pressure cycle, increasing at the rate of only 1.7 per cent per cycle. Brass and copper both showed decreases in tensile strength per pressure cycle whereas Monel increased almost three times more per cycle than stainless steel.

The advantage of having only a small positive change in tensile strength can be best understood through comparison of the coincident change in ductility (per cent elongation). Since loss in ductility is generally a negative value, it is a more important design factor than tensile strength in determining the useful life of a pressure vessel. The ductility of stainless steel decreased slightly less than 4 per cent per cycle whereas the ductility of Monel decreased almost 7 per cent per cycle. Although Monel increases in strength at a greater rate than stainless steel, its more rapid loss of ductility limits the useful life of a Monel pressure vessel more than would be the case with stainless steel. Brass shows the best performance in ductility but because of its tendency toward reduction of tensile strength per cycle and because of its initially low absolute tensile strength, it does not compare at all favorably with stainless steel or Monel for light-weight pressure-vessel application. Copper actually increases in ductility, which indicates work softening rather than work hardening. Continued plastic deformation of the copper reactor was evident each time the reactor was disassembled. Pure copper must be ruled out as a pressure-vessel material but alloys in which large quantities of copper are used, such as Monel, might be successfully utilized.

The over-all 35 per cent loss of ductility of stainless steel as a result of the reactors being charged only nine times seems to be dangerously high. Whether the embrittlement was accelerated by the high-pressure oxygen cannot be established unless a more nearly complete study is conducted in which a number of reactors, some pressurized with oxygen and some pressurized hydrostatically, are closely compared to determine exactly how much high-pressure oxygen embrittles the metal.

Microstructure. Part of each reactor used for the tensile tests to determine change in physical properties was reserved for microstructure analysis. Comparison of the microstructure of each of these specimens with corresponding standard specimens showed no difference in the microstructure except in the case of stainless steel. The two specimens of stainless steel, however, did not come from the same heat and apparently they had been finished differently. The specimen of unexposed metal showed an annealed microstructure whereas the stainless steel specimen from the reactor had a cold-worked microstructure.

The stainless steel reactor was fabricated from tubing whereas the copper, brass, and Monel reactors were machined from solid bars. The copper and brass specimens contained a cold-worked layer on the internal surface as a result of machining the hole. The depth of cold working in the brass was about 0.0015 inch and in the copper about 0.008 inch. In addition, the internal diameter of the copper specimen contained fine recrystallized grains to a depth of 0.003 inch. This was probably the result of first cold working the surface while machining the hole and subsequently heating the surface above its recrystallization temperature (lowered by cold working) by frictional heat (reaming the hole smooth). No evidence of change in microstructure due to the cycles of expansion caused by charging with high-pressure oxygen was evident. Neither was any change caused by possible oxygen diffusion evident.

Oxidation Rate. Five reactors used in the 616-hour storage experiment were sectioned and examined to determine how much the internal surfaces oxidized. These reactors are shown in Figures 22 and 23.

All of the internal surfaces had been reamed to a smooth lustrous finish prior to exposure. Monel (Experiment 46) was the only material that retained its original luster and it appeared to be totally unaffected by the long period of exposure. The surface of the brass reactor used in Experiment 45 also indicated a low oxidation rate although a slight hazing and yellowing was evident. The stainless steel reactor (Experiment 40), however, does show some effects of oxidation. The surface is dull and appears to have a powdery coating although no flaking or powdering actually occurred. The estimated depth of the oxide coating is of the order of 1 micron, and does not represent a significant amount of oxidation. Qualitatively, the degree of oxidation of all three metals can be considered inconsequential and under normal dry operating conditions will probably not have to be seriously considered.

Two different effects on copper resulted from the 616-hour exposure during Experiments 43 and 47. The reactor used in Experiment 47 shows the effects of appreciable oxidation. Only half the length of the reactor is shown in Figure 23. The upper half (not shown) had a blackish deposit of cupric oxide. The deposit was powdery and easily scraped from the base metal. The lower half of the reactor shown in Figure 23 has a heavy bluish deposit at a point equivalent to the mid-point of the reactor and a bluish-green deposit near the bottom. This deposit was flaky. The reddish coating at the very bottom is probably cuprous oxide.

In the other copper reactor, used in Experiment 43, the oxide coating was golden and had the appearance of a brass. The color is golden because of the diffraction of light caused by the very thin oxide layer, which is perhaps less than 1 micron thick. Because of leakage, this reactor did not maintain the 7500-psi pressure for the entire 616 hours. The difference in the amount of oxidation of the two reactors makes it apparent that the total period of exposure of the reactor used in Experiment 43 must have been only a few hours.

Contrails

TABLE 5. RESULTS OF TENSILE TESTS OF EXPOSED AND

Metal	Hours Under Pressure	Number of Pressure Cycles	Modulus of Elasticity, $E \times 10^6$		Ultimate Tensile Strength, 1000 psi		0.2 Per Cent Offset Yield Strength, 1000 psi		Per Cent Elongation, 1.25 inch	
			Actual	Average	Actual	Average	Actual	Average	Actual	Average
Stainless steel	38.4	9	24.8		150.0		132.0		10.4	
			25.9		152.5		136.5		10.4	
			25.4		151.2		130.0		10.4	
	None	None		25.2		151.2		132.8		10.4
	None	None	Not known			144.4 ^(a)		115.2 ^(a)		16.0 ^(a)
Monel	15.3	4	25.1		120.8		115.5		10.0	
			25.1		122.5		118.0		9.6	
			25.4		120.5		116.5		9.2	
				25.2		121.3		116.7		9.6
	None	None	25.4		113.5		96.7		13.6	
			25.9		114.2		101.2		12.8	
				25.7		113.8		98.9		13.2
Brass	103.4	14	15.6		64.0		52.8		21.6	
			16.0		64.8		55.3		20.0	
			16.2		64.4		54.4		19.2	
				15.9		64.4		54.2		20.3
	None	None	11.80		62.8		55.5		23.2	
			14.35		63.5		54.2		23.2	
				13.1		63.2		54.9		23.2
Copper	22.3	6	14.7		43.7		38.8		14.4	
			15.0		43.5		38.7		16.0	
			15.6		43.4		39.7		14.4	
				15.1		43.5		39.1		14.9
	None	None	15.0		47.6		46.1		10.4	
			15.9		46.7		45.7		11.2	
				15.45		47.2		45.9		10.8

(a) Values supplied by Superior Tube Co.

Contrails

UNEXPOSED STAINLESS STEEL, MONEL, BRASS AND COPPER

Per Cent Change in Properties Caused by Service Conditions			Per Cent Change Per Cycle in Properties Caused by Service Conditions		
Ultimate Tensile	Yield Strength	Elongation	Ultimate Tensile	Yield Strength	Elongation
+4.72	+15.3	-35.0	+ .524	+1.7	-3.9
+6.60	+18.0	-27.2	+1.65	+4.5	-6.8
+1.90	-1.28	-12.5	+ .136	-.092	-.89
-3.6	-14.8	+13.8	-.6	-2.48	+2.3

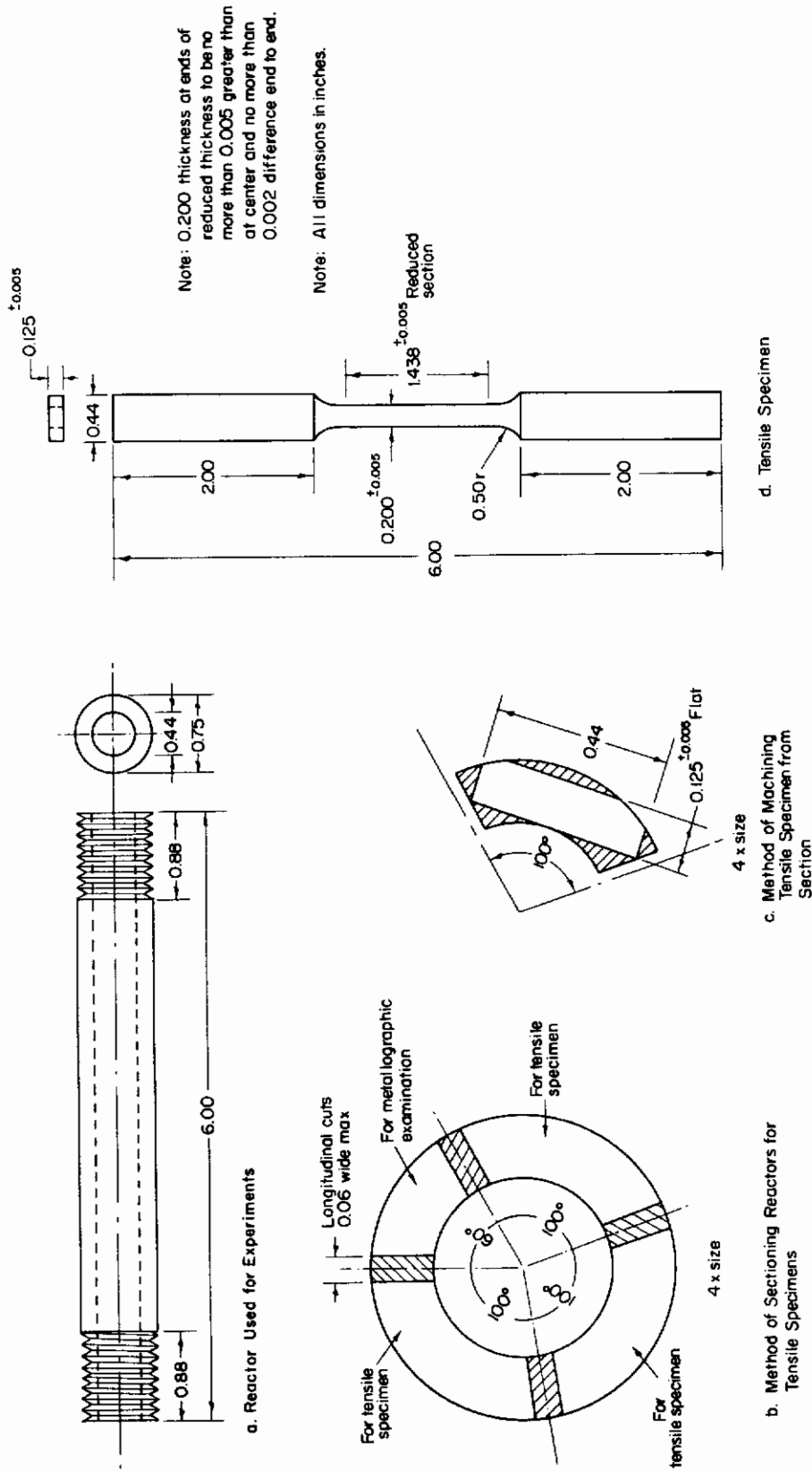
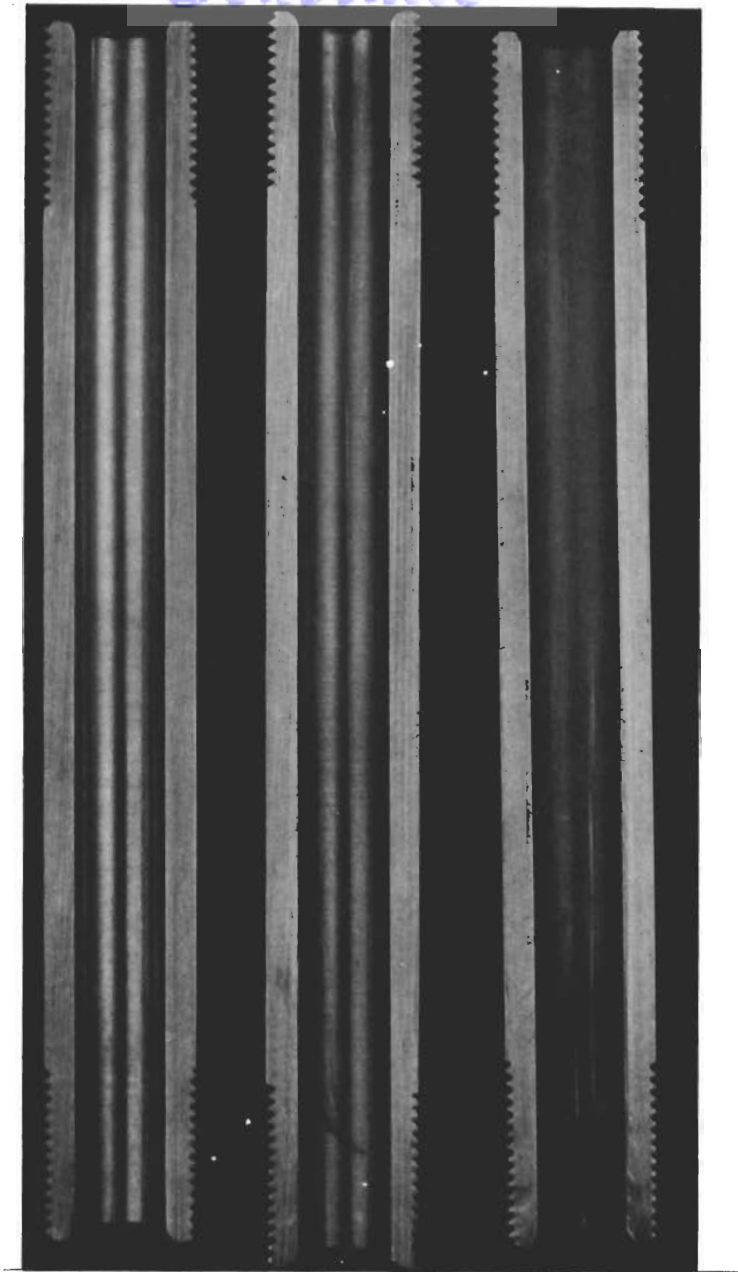


FIGURE 21. TEST-TUBE REACTOR AND TENSILE SPECIMENS

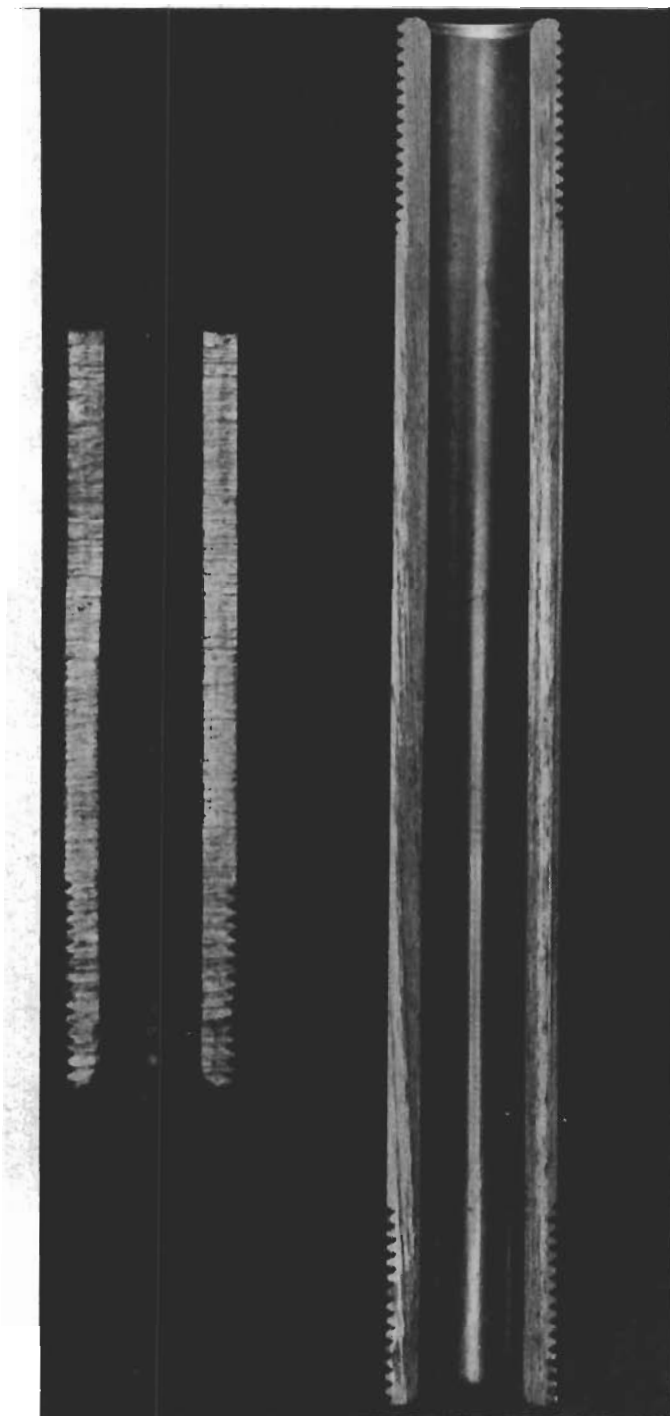


Monel
Experiment 46

Brass
Experiment 45

Stainless Steel
Experiment 40

FIGURE 22. SURFACE OXIDATION OF MONEL, BRASS, AND STAINLESS STEEL REACTORS EXPOSED FOR 616 HOURS TO 7500-PSI OXYGEN



Experiment 47

Experiment 43

FIGURE 23. SURFACE OXIDATION OF COPPER REACTORS EXPOSED FOR 616 HOURS TO HIGH-PRESSURE OXYGEN

In another series of experiments (Experiments 115-121), the effect of surface finish on oxidation rate was evaluated for three metals: stainless steel, brass, and aluminum. On the basis of visual inspection, it was concluded that discoloration due to oxidation was negligible in all cases for dry conditions. However, for moist conditions the oxidation of brass and aluminum was significant and brass especially was appreciably discolored. Stainless steel discolored very little even in moist atmospheres. Also, in all cases, the coarser finishes (100 microinches) showed the greatest discoloration (oxidation).

Oxygen Penetration. The vacuum-fusion method was used to determine the amount of oxygen gas present in the base metal. The method consists of melting a metal sample in a graphite crucible (in a vacuum) and collecting, measuring, and analyzing at low pressure the gases evolved. The oxygen-containing compounds and solutions are reduced and evolved as CO (at 1600 C and higher) and CO₂. Hydrides, nitrides, and their solutions yield free H₂ and N₂.

The first step in determining the concentrations of the various gases evolved is to freeze out the CO₂ and to determine the subsequent pressure drop. The remaining gas includes the CO, H₂, and N₂. These gases are oxidized by circulating them over hot CuO. The resulting water vapor is frozen out and the pressure drop caused by the removal of H₂ is determined. The CO oxidized to CO₂ in the previous step is frozen out at a lower temperature and by this last step the volume and weight of oxygen originally in the gas can be calculated.

The various metals analyzed by this method and the results derived by the analysis are tabulated in Table 6.

TABLE 6. VACUUM-FUSION ANALYSIS OF OXYGEN CONCENTRATIONS IN STAINLESS STEEL, MONEL, AND COPPER^(a)

Experiment	Metal	Oxygen, ppm ^(b)
Control	Monel	10
46	"	11
22, 26, 33, 34	"	10
Control	Copper	279, 332
43	"	375
47	"	336
14, 19, 23, 35, 36	"	205, 341, 337
40	Stainless steel ^(c)	40
12, 13, 17, 21,	"	46
25, 28, 32,		
37, 38		

(a) Brass is not amenable to vacuum-fusion analysis because of the gettering effect of zinc.

(b) Sensitivity of analysis is about ± 3 ppm.

(c) Control sample from original heat not available.

Conclusions

There appears to be no evidence of oxygen diffusion into or through the base metal. The amount of oxygen absorbed remained in the surface oxide film which probably never exceeded 1 micron in thickness, except for the copper reactor used in Experiment 43. Monel showed no oxygen pickup at all. However, analytical error due to sensitivity of the apparatus may be as great as 6 ppm (± 3 ppm may be possible). A control specimen of stainless steel was not available, but even without a means of comparison, it may be concluded on the basis of the low concentrations in the exposed specimens that the oxidation effect was negligible.

The values for copper seemed to indicate oxygen heterogeneity in the base metal and therefore comparative analysis was necessary. If the values of 341, 336, and 375 (see Table 6) are assumed to be typical of the individual specimens analyzed, then the increase in oxygen concentration can range from 4 ppm at best to 96 ppm at worst (using both values from the control specimen and the maximum and minimum values of the three exposed specimens). These values represent a maximum increase in oxygen concentration of 35.7 per cent. Such an apparently large increase may not be significant if one considers the relationship between film thickness and oxygen increase. For example, for the specific specimens used, an oxidation film of CuO only 1 micron thick would correspond to 20 ppm oxygen in the specimen. Therefore a concentration of 96 ppm would represent at most a film thickness of 4.8 microns, which is only moderate.

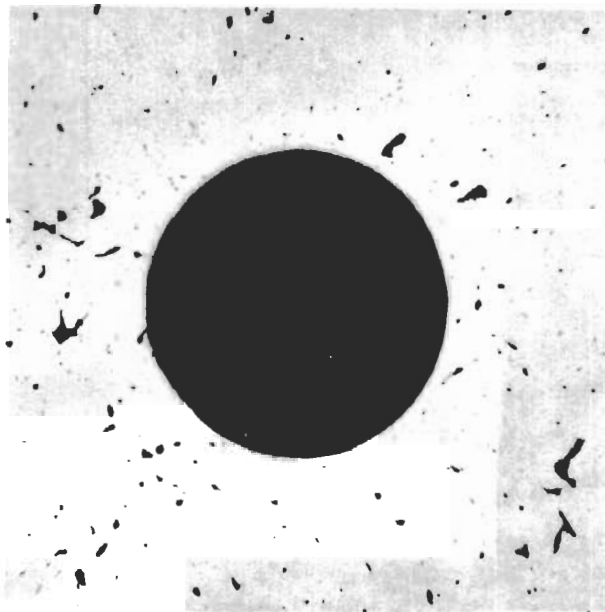
Erosion. A 0.005-inch-diameter brass orifice was exposed to 35.5 minutes of high-pressure high-velocity flow. Photomicrographs were taken after 3, 14, and 35.5-minute periods. These are shown in Figure 24. A gross peripheral edge deterioration after 35.5 minutes is quite evident. Some of the gouges and scratches are as deep as 0.0008 inch.

Figure 25 compares the cross section of the original orifice with the one exposed for 35.5 minutes. It can easily be seen that the sharp peripheral edge has been appreciably rounded by the gas flow. The radius of the rounded edge is about 0.0005 inch. Considering the relatively short flow period, the depth of the gouges, and the irregularity of the edge (Figure 24), it can be concluded that this amount of wear would seriously hamper proper sealing of a valve seat.

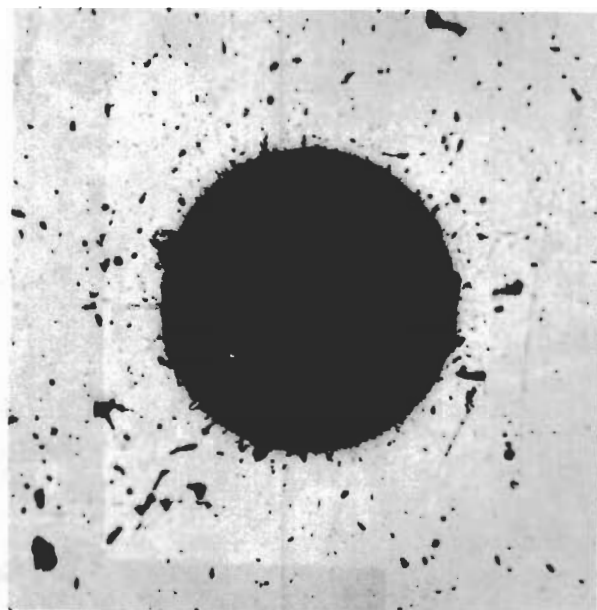
Figure 26 shows a 0.013-inch-diameter stainless steel orifice after 15 minutes of exposure. The amount of wear is appreciably less than that of the brass orifice after an equal period of exposure. Although stainless steel will probably wear less than brass, the lesser wear may be attributed in part to the fact that the diameter of the orifice was 2-1/2 times greater. Since the gas was not filtered and since minute particles were present in the gas, it is also possible that erosion was accelerated by particle impact. However great this factor may have been, it is unlikely that significant edge erosion can be attributed solely to this phenomenon. In addition, there appears to have been no significant diametral erosion in either metal, and considering the rapid erosion of the peripheral edge, diametral erosion is probably not a serious consideration.

Conclusions

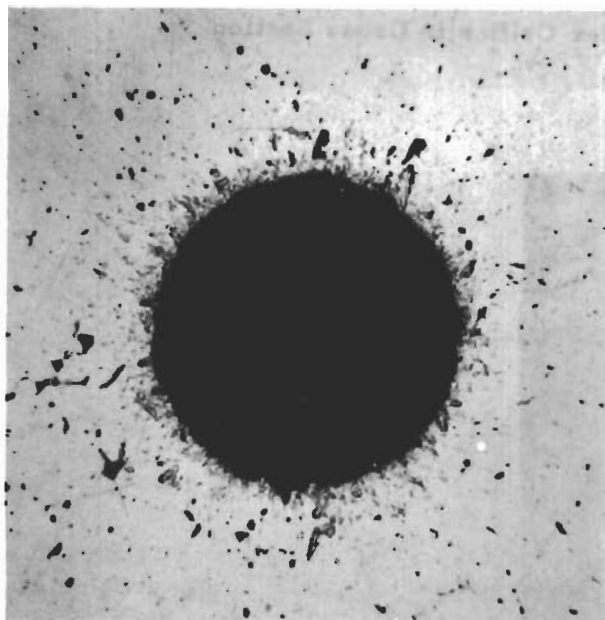
On the basis of the five evaluations just discussed, the four metals considered can be rated in the following order in terms of their possible application in high-pressure oxygen systems:



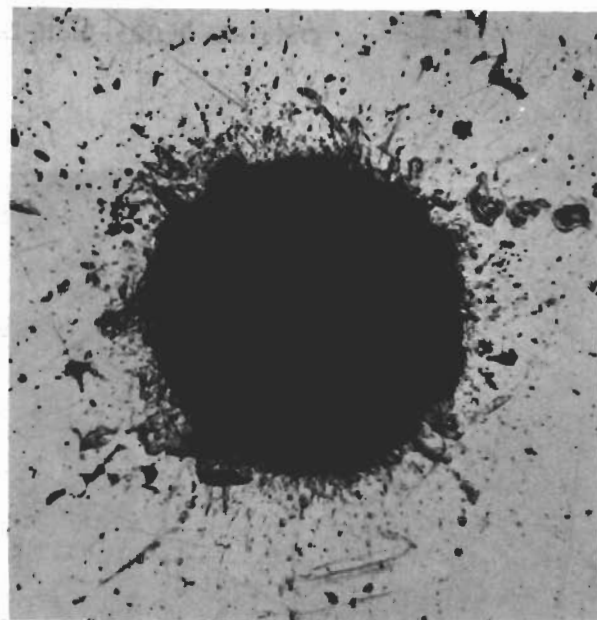
a. Original 0.005-Inch-Diameter Orifice



b. After 3 Min 7 Sec



c. After 13 Min 47 Sec



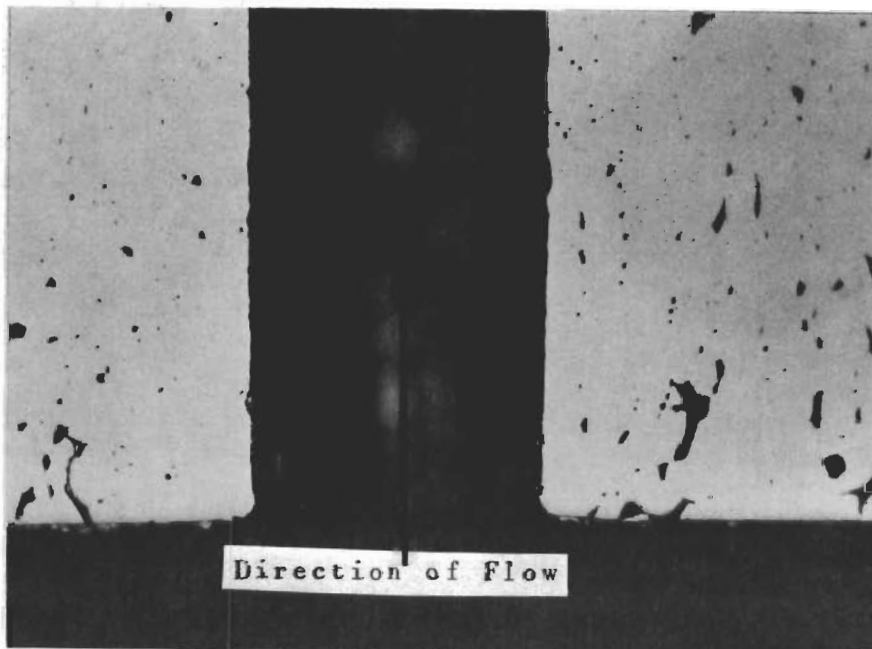
d. After 35 Min 29 Sec

FIGURE 24. PROGRESSIVE EROSION OF A 0.005-INCH-DIAMETER BRASS ORIFICE EXPOSED TO HIGH-PRESSURE HIGH-VELOCITY FLOW

Contrails



a. Original 0.005-Inch-Diameter Orifice in Cross Section



b. After 35 Min 29 Sec

FIGURE 25. CROSS SECTION THROUGH 0.005-INCH-DIAMETER BRASS ORIFICE

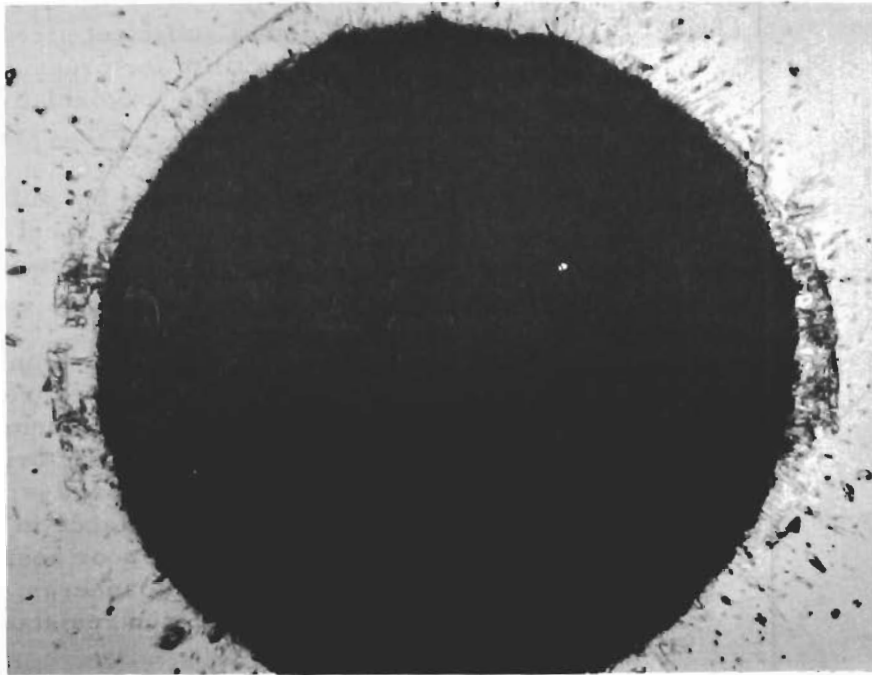


FIGURE 26. PHOTOMICROGRAPHS OF 0.013-INCH-DIAMETER STAINLESS STEEL ORIFICE AFTER 15 MINUTES OF FLOW

Contrails

Stainless steel (Type 316)	Good ⁺	Shows sufficient strength and ductility for pressure-vessel use; has low oxidation rate and good erosion resistance
Monel	Good ⁻	Is less strong but sufficient where weight is not a restricting factor; has lowest oxidation rate
Brass	Poor to fair	Has insufficient strength for lightweight pressure-vessel application, but demonstrates good retention of original physical properties; good oxidation resistance in dry atmospheres but poor resistance in moist atmospheres; has only fair erosion resistance
Pure copper	Very poor	Too weak to be used for pressure vessels; poor retention of physical properties; has high auto-ignition temperature but also has high oxidation rate when exposed for long periods

The above rating is based on the investigation and analysis of only a small sampling of each metal. More extensive and detailed investigations are required to determine quantitative results. Qualitatively, on the basis of the experiments performed, only stainless steel and Monel are acceptable alloys. Brass and pure copper, although possessing some desirable characteristics, should not be used because of other factors which cannot be sufficiently compensated.

Electrostatic Charges

Experiments Performed

The electrostatic charge generated by high-pressure high-velocity flow was determined during the flow experiments. Initially a thick brass orifice with a 0.040-inch-diameter hole was used. However, the flow period was too short to permit sufficient electrostatic charges to be generated or measured. A 0.013-inch-diameter orifice was tried also and during these experiments temperature of the flowing gas was recorded as well as electrostatic charge. At first, only one probe was used to measure both values but this proved unsatisfactory and so the temperature and electrostatic charge were then recorded in separate runs.

The majority of the experiments were performed with a 0.005-inch-diameter brass orifice plate. During these experiments, probes of different materials and geometries were used to determine whether the nature of the probe affected the voltage recorded.

Evaluation of Results

One phenomenon discovered was that the stainless steel probe would not record or pick up electrostatic charges unless it was cleaned after each exposure. The various probes used were made of stainless steel rod or tube, glass tube, graphite rod, polyethylene tube, and a cotton-covered probe. Pointed-, rounded-, and flat-end probes were investigated. Also grounded and ungrounded probes were tried. Electrostatic voltages were recorded in 31 of the 56 experiments performed. The magnitude of the charges recorded ranged from -0.19 to +0.80 volt. The maximum charge of +0.80 volt was always recorded when a 1/8-inch-diameter stainless steel tube with internal restrictions was used. The graphite probe yielded fairly consistent readings ranging from +0.21 to +0.32 volt. The glass probe picked up only minute charges of the order of +0.04 volt.

Conclusions

It is evident on the basis of the data gathered that electrostatic charges due to high-pressure oxygen flow are not significant in themselves. However, some factors which arise because of the flow of gas must be seriously considered. One possible problem is ozone formation caused by the cooling of the gas and the presence of electrostatic charges. The ozone molecule is much more active, chemically, than ordinary oxygen and therefore likely to lower the ignition temperature. A more important factor is the presence of dust or liquid moisture in the gas stream. It has been shown⁽⁹⁾ that gases passed through a pin-hole orifice under a pressure head of 1800 psi invariably show a strong electrostatic charge only when either dust or liquid moisture is present in the gas stream. These charges may be sufficiently large to cause ignition.

In the experiments performed at Battelle, some dust particles were present in the gas stream but probably they were not in sufficient quantity to increase the electrostatic charge greatly. Of course, the longest flow period was only 8 seconds and the pressure was not constant during the entire period.

Because the danger of detonation or chemical reaction being initiated by an electrostatic charge is potentially large, further investigations should be performed but with larger volumes which will permit longer flow periods. Also, attempts should be made to control and measure the amount of dust or moisture in the stream to compare the effect on the charges generated. In general, however, regardless of the negligible charge generated, equipment should be grounded wherever possible.

Adiabatic Heating

Experiments Performed

Details and results of the experiments performed are tabulated in Table 17, Appendix IV, and the experimental methods are described on page 22. Evaluation of the results and conclusions derived from the experiments is discussed below.

Evaluation of Results

The surge experiments comprised a series of nine separate tests. During these experiments a dead-end receiver of 3.5-milliliter volume was rapidly charged with oxygen gas. The instantaneous pressure ratio of final pressure to initial pressure ranged from 333:1 to 553:1. Initial temperature of the receiver and its content was 32 F. The rise in temperature of the gaseous contents was measured by means of an internal thermocouple probe. Maximum temperature rise above 32 F corresponding to the maximum pressure ratio was only 42 F. Minimum temperature rise was 21 F.

Figure 27 is a graphical representation of the time-dependent rise in pressure and temperature and the relationship between the two values.

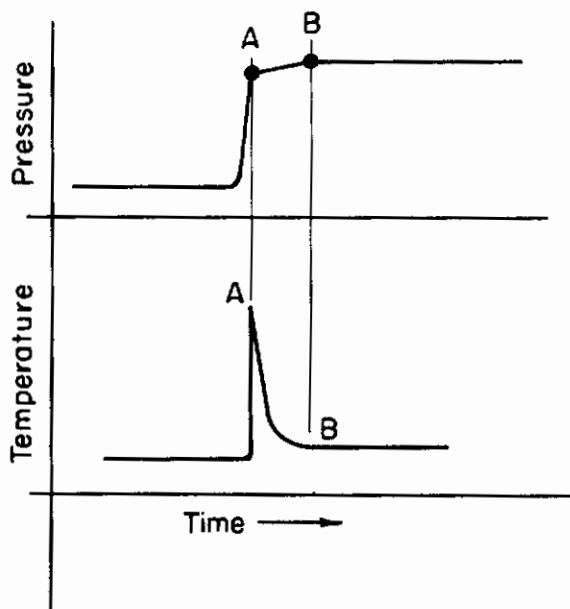


FIGURE 27. INSTANTANEOUS RISE IN PRESSURE AND TEMPERATURE CAUSED BY RAPID COMPRESSION

The pressure rise was determined at (A), although a slight, slow rise in pressure continued until (B), at which point the pressure leveled. Maximum temperature was also recorded at (A).

Several aspects of the experiment must be considered in evaluating the results. First, the initial temperature of the high-pressure gas ranged from -50 to -150 F. Second, the temperature of the high-pressure gas at the point at which it expanded into the receiver was not measured. Although the gas was heated as it passed through the small-diameter tubing connecting the high-pressure supply and the receiver, probably the gas was still 50 to 100 degrees below the 32 F reference point. The total temperature rise therefore could have been as much as 150 degrees and possibly more. In addition the temperature measured was probably lower than the actual gas temperature because of the heat losses through the boundary layer and the stainless steel shield.

Another important consideration, not evaluated, is the absolute volume of the receiver and the effect a different volume would have had on the final temperature. As a corollary to receiver volume, the questions of (1) minimum volume-maximum surface area ratio, (2) mass of the receiver, (3) heat-transfer coefficient of the material, and (4) number of paths available for heat dissipation must also be considered.

If the dead-end volume is very small in comparison to a large volume of high-pressure gas, such that the pressure of the source would be only slightly lowered during the surge period and, if the initial temperature of the high-pressure gas was elevated, it is possible that the resulting rise in temperature would be of a magnitude much greater than those recorded in the experiments.

The most critical consideration, of course, is the temperature rise of the receiver surface because, even if no contaminants are present, ignition can be initiated if the autoignition temperature of the metal is exceeded. Where other materials such as polymeric seals are exposed, the danger is even greater. Therefore in any design where gas may possibly surge into small spaces, careful consideration must be given to volume-surface area ratios and the mass of the surrounding material.

Conclusions

Rapid heating due to gas surging into confined spaces can produce a major hazard. During the experiments at Battelle, a pressure regulator failed and burned under surge conditions. Also AiResearch discovered that many materials including neoprene and Viton reacted chemically when impacted by a surging gas at 8000 psi.

However, there is also evidence that at lower pressures, or when the receiver volume is comparatively large, the effect of surge compression is minor. This conclusion is supported by the results of the surge experiments at Battelle and similar experiments performed at AiResearch.

On the basis of the experimental results and data available, it can be concluded that the rise in temperature due to adiabatic compression to 8000 psi is probably not sufficient to cause large masses of metal to ignite. However, the possibility of thin sectioned metal wire and of polymers such as neoprene igniting is great. Also the danger of organic or hydrocarbon contaminants chemically reacting is serious since many of these have ignition temperatures below 500 F, especially in high-pressure gaseous oxygen.

Experimental Equipment Evaluation

The evaluation of the experimental equipment covered three specific items: (1) the high-pressure regulator, (2) the high-pressure valves, and (3) the high-pressure tubing connections.

High-Pressure Regulator

The original experimental set-up (Figure 8) included a 10,000-psi delivery regulator. The regulator was irreparably damaged when 16,000-psi oxygen was inadvertently

allowed to surge into the regulator with the delivery pressure set below 1000 psi. The surge of gas caused ignition inside the regulator and the stainless steel body began to burn. Immediate use of a CO₂ extinguisher prevented damage to the other equipment.

The regulator body was dismantled and cross sectioned. Ignition was apparently in Area A as shown in Figures 28 and 29. Burning spread quickly through Area B and into Area C. Figure 29 is a photograph of the cross-sectioned regulator showing the extent of the damage. Photographs and a description of the experiment were forwarded to the manufacturer for his appraisal of the cause of the ignition. He suggested the following possible causes:

"Regarding the cause of the ignition and burning of the internal parts, from your photo of the cross-section it appears that the point of ignition was probably in the filter area ref. 24* and related parts. It is our feeling that friction and the heat of compression could very likely cause ignition on an edge or projection in this area. The velocity of particulates in the gas stream impinging on this area could also be a source of friction and ignition.....

From other cases of oxygen regulator burn-outs where the inlet pressure was in the 1500-2000 psi, evidence points to the high velocity of particulates impinging on internal parts as the probable source of ignition. In your case the rapid flow of 16,000 psi of oxygen was the major contributing factor causing the ignition..**

Items 14 and 15 in Area A probably aided the ignition. Item 14 is a neoprene O-ring and Item 15 is an 80- and 200-mesh lektromesh filter made of 303-C stainless steel. Substitution of Kel-F or Teflon compounds for the neoprene O-ring would probably diminish the tendency of the O-ring to ignite. Also, if the filter were relocated in an area where rapid compression could not occur and where heat could be more easily dissipated, the danger would be greatly reduced.

Final appraisal of the regulator by the Battelle research staff indicates that it can probably perform reliably when operated under rated conditions. High-pressure surge conditions should be prevented, and where possible, filters should be inserted into the system in front of the regulator.

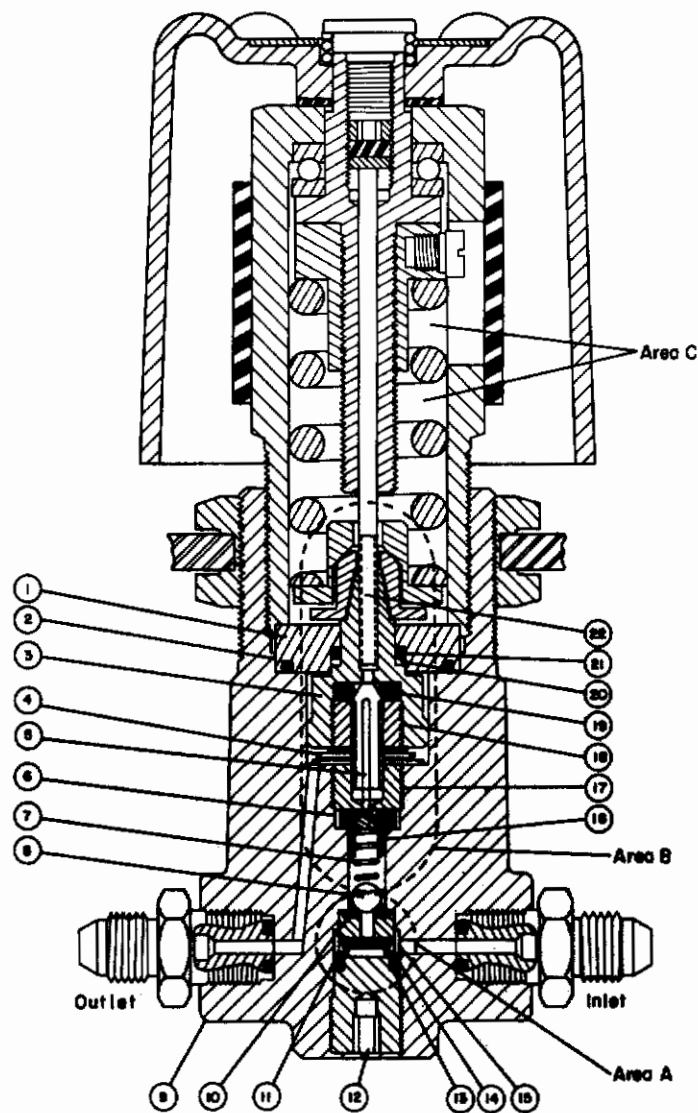
High-Pressure Valves

The high-pressure valves used throughout the experiments were standard items specially prepared for oxygen use. The three types of valves used were (1) two-way straight valves with solid stems, (2) two-way angle valves with solid stems, and (3) two-way straight valves with two-piece stems. The valve bodies are mass produced from Type 316 stainless steel bar stock. One-piece stems are machined from Type 420 stainless steel and the stem tip is hardened and polished to a fine finish. The lower part of the two-piece stem is Type 316 stainless steel.

Difficulties with the valves were experienced after only very few hours of operation. Thereupon, all the valves were disassembled, cleaned in carbon tetrachloride,

*No. 15 in Figure 28.

**Letter of December 11, 1961, from manufacturer.



KEY

- | | | |
|--------------------------|--------------------|--------------------------------|
| 1. Upper diaphragm plate | 9. Body | 16. Valve stem |
| 2. O-ring | 10. Molded seat | 17. Seat-retaining nut - lower |
| 3. Centralizer | 11. Seat retainer | 18. Seat-retaining nut - upper |
| 4. Spring | 12. Back plug | 19. Seat unit |
| 5. Valve stem | 13. Back-up washer | 20. O-ring |
| 6. Seat unit | 14. O-ring | 21. Back-up washer |
| 7. Valve spring | 15. Filter unit | 22. Bleed stem extension |
| 8. Ball check | | |

FIGURE 28. CROSS SECTION OF HIGH-PRESSURE REGULATOR

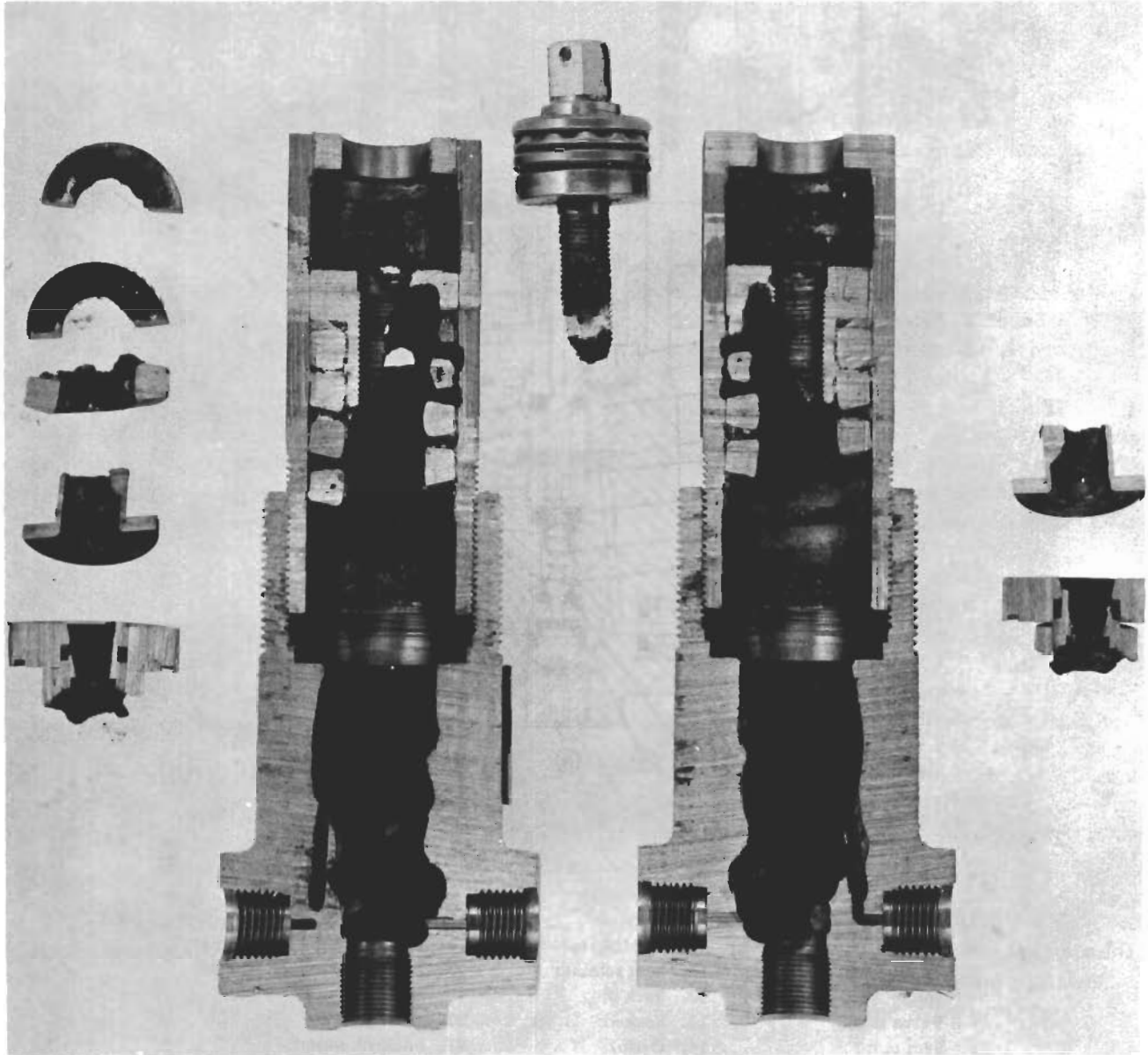


FIGURE 29. REGULATOR BODY AFTER INTERNAL COMBUSTION AND BURNOUT

and reassembled. The gland nut (Figure 30) of each valve was tightened sufficiently to seat the seal prior to use and then retightened after a short period of use. Leakage of gas through the seal was not evident throughout the remainder of the experiments; however, after the third month of operation significant leakage developed through the seat and stem interface.

Some of the valves were disassembled again and it was noted that the stem cone had been roughened appreciably. Only the stem cone was redressed and polished but this did not significantly reduce the leakage because the seat had also been roughened during previous use. It was also noted that stem runout was as much as 0.014 inch. The two-piece stem valve did not provide reliable performance either, and the two-piece cones were also roughened.

Although these valves are rated at 30,000-psi working pressure, in this program, many of them leaked. Furthermore, although the stem tips were heat treated by the manufacturer, they were roughened and damaged after only a few cycles of operation. However, it does not seem likely that increased hardness or the substitution of a Hastelloy or carbide-tipped stem would solve the problem of leakage caused by wear of the stem-seat interface.

The basic design of the valve might be adequate if the seat-wear problem were overcome and if the stem and seat alignment were more precise. The use of a ceramic-Teflon or similar composite material for the stem tip and/or replaceable seat would probably increase the usable life and the reliability of the valve appreciably. The use of Teflon compounds, however, would limit the working temperatures to 400-500 F.

High-Pressure Tubing Connections

Except for some connections in the two storage experiments which were welded or brazed, all other tubing connections used during the experimental program were of the mechanical type illustrated in Figure 31. This is a standard connection, originally developed by the U. S. Bureau of Mines.

In general, standard-length tubing connections were purchased and used. The conical end and the thread were machined at the factory. Other lengths of tubing were machined at Battelle. These were coned and threaded with special hand tools.

Ideally, the sealing between the tubing and the body is by a "line" contact rather than a "face" contact. The included cone angle of the tube is more acute than the corresponding cone angle of the body seat. However, unless there is perfect alignment of the tube and the body, some plastic deformation is necessary to facilitate a leakproof seal. Even when the two parts are perfectly aligned, it is difficult to ascertain whether they are sealed. This is due primarily to the fact that no minimum torque ratings have been specified for these connections and sealing is dependent upon the "feel" of the assembler.

When the experimental system (Figure 8) was first assembled, the fittings were tightened with standard hand tools. However, the fittings leaked. Conversations with engineers at Kidde Aero-Space revealed that they had encountered the same difficulties. Kidde Aero-Space was able to achieve seals only by retightening each connection with an oversize wrench.

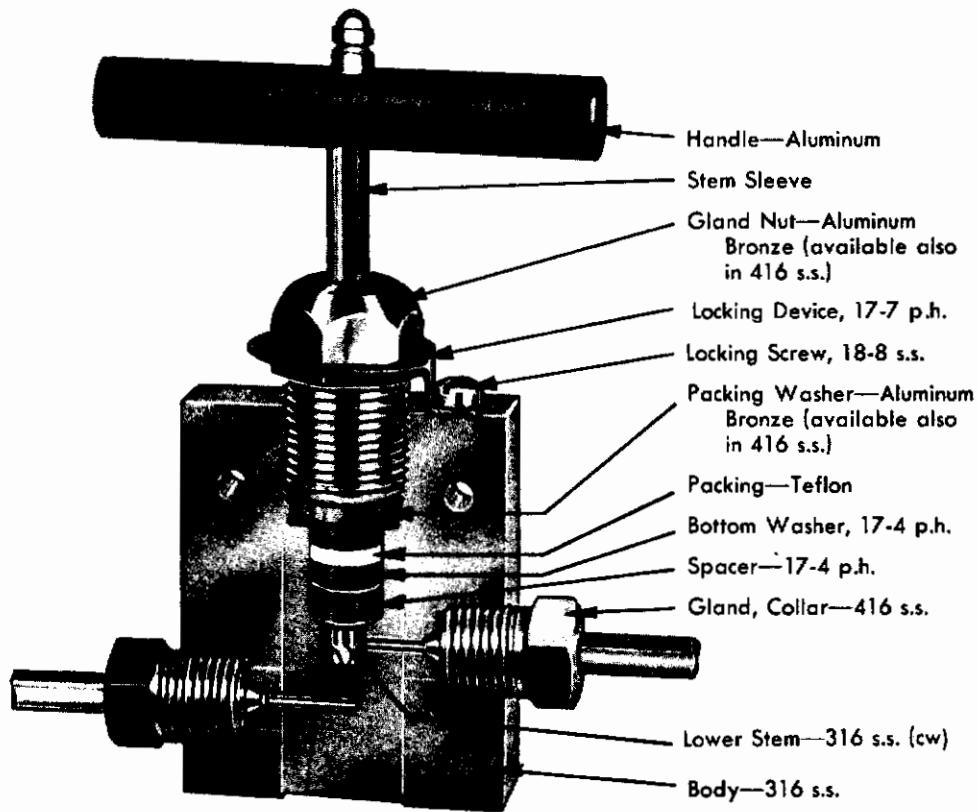


FIGURE 30. STANDARD VALVE RATED AT 30,000 PSI

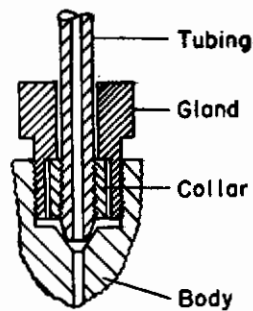


FIGURE 31. MECHANICAL TUBING CONNECTION

A similar procedure was followed at Battelle and most fittings were successfully sealed. However, disassembly and retightening of the fittings caused appreciable plastic deformation of the tubing cones. Obviously, the fittings had been over-torqued. The most difficult seals to maintain were those which were remade every time a new test reactor was inserted into the experimental system. These connections became so badly deformed that it was impossible to remove the collar from the tubing.

In general, although this connection is widely used in high-pressure work, it was found to be a continual source of trouble during this program. Unless exact torque loads can be specified so that proper seals are not dependent upon individual "feel" or manual dexterity, there is no positive way of assuring a proper seal. It may very well be impossible, however, to specify exact torque values because of friction losses in the threads.

CONCLUSIONS

Since the basic aims of the research were to evaluate the relative safety of 7500-psi gaseous oxygen systems and to identify the hazards which can be expected in their operation, the conclusions listed below concern these subjects specifically.

Although some of the research results indicate that relative safety can be maintained apart from absolutely ideal conditions, it cannot be assumed that high standards of cleanliness and handling technique are not desirable. Whenever ideal conditions and procedures are possible, they must be insisted upon. However, although danger increases with less ideal conditions, certain compromises can sometimes be tolerated. Only through continued research and through accumulated engineering experience can a more confident assessment of the extent of these allowable compromises be made. Until the time that further research and engineering provides additional information for formulation of recommendations, the conclusions given below can be used as general guides:

- (1) Contaminated oxygen gas at 7500 psi, as investigated in this program and under the environmental conditions imposed, when considered independently of the equipment or system employed, is relatively safe from spontaneous combustion or detonation.
- (2) Hazardous chemical reactions of 7500-psi oxygen gas with foreign elements seem to be dependent upon conditions other than simple mixing, proximity, or high-velocity flow. Temperature is believed to be the most critical variable and the minimum temperature at which a reaction will occur is in turn dependent upon the existing pressure.
- (3) Hazards and difficulties encountered in the operation of high-pressure gaseous oxygen systems seem to be attributable primarily to poor system design and to the use of poorly designed equipment.

In addition to the general conclusions above the following more technical and specific conclusions have been drawn:

- (1) Absolutely clean, dust-free atmospheres are not essential to safe operation.
- (2) Concentrations of hydrocarbons in the order of 50 ppm or less are not dangerously reactive.
- (3) Electrostatic charges caused by short flow periods through a small orifice appear to be negligible.
- (4) Stainless steel and Monel are acceptable materials of construction.
- (5) Uncoated or unplated copper appears to oxidize too readily to be used extensively.
- (6) Although cases of combustion involving Teflon and Kel-F have been reported, the experiments conducted show that these are acceptable nonmetallic sealing materials.

RECOMMENDATIONS

Two primary recommendations have been formulated on the basis of the conclusions presented above.

- (1) A broader, more detailed study of materials compatibility with 7500-psi oxygen gas should be pursued. This study should be an attempt to derive a more exact understanding of the conditions that initiate combustion. Extensive experimentation with stainless steel, Monel, anodized aluminum, Teflon compounds, Kel-F compounds, and various thread lubricants and sealants should be conducted to permit a proper statistical analysis. These experiments should have two objectives:
 - (a) Determination of the spontaneous ignition temperature under static conditions and after various periods of exposure.
 - (b) Determination of the spontaneous ignition temperature during surge conditions and evaluation of the influence of the volume to surface-area ratio.
- (2) Because of the inadequacy of available equipment to provide reliable, long-time performance for absolutely leakproof operation, a development program should be initiated. This program should be planned to investigate critical design criteria. The components that require further study, in estimated order of priority, are:
 - Fittings
 - Valves, manual and remote

- Lightweight pressure vessels
- Regulators.

REFERENCES

- (1) Keating, D. A. , "Design Study of High-Pressure-Oxygen Vessels", WADC Technical Report 59-767 (February, 1960).
- (2) Jackson, et al. , "A Study of the Titanium Liquid-Oxygen Pyrophoric Reaction", WADD Technical Report 60-258 (June, 1960).
- (3) Jackson, et al. , "A Study of the Mechanisms of Titanium-Oxygen Explosive Reaction", ASD Technical Report No. 61-479 (September, 1961).
- (4) Littman, et al. , "Reactions of Titanium with Water and Aqueous Solutions", Stanford Research Institute (June, 1958).
- (5) Greenspan, L. , National Bureau of Standards, "Ignition of Kel-F and Teflon", Rev. Sci. Instr. , 29, 172-3 (February, 1958).
- (6) Reynales, C. H. , "Compatibility of Materials with Oxygen", Douglas Aircraft Company Report D81-444 (October, 1958).
- (7) Luccubue, J. R. , "Fluorlube-Aluminum Detonation Point", Convair Astronautics Report No. 780-1500 (June 12, 1958).
- (8) Hersey, M. D. , "Oxygen-Oil Explosions", Department of Interior, Bureau of Mines, Preliminary Reports, 1, 2, and 3 (July, 1923).
- (9) Hersey, M. D. , "Study of Oxygen-Oil Explosion Hazards", Am. Soc. Naval Engineers, 36, 231 (1924).
- (10) Gillerman, J. B. , "Telescoped Testing of Environmental System Speeded Mercury Design", Space/Aeronautics, 76-79 (May, 1961).

Contrails

APPENDIX I

BIBLIOGRAPHY

- (1) Beecraft, R. I., and Severson, C. A., "Behavior of Polytetrafluoroethylene (Teflon) Under High Pressure", J. Appl. Phys., 30 (11), 1793-98 (November 1959).
- (2) Bureau of Aeronautics, Dept. of Navy, Report TED AE-5131.
- (3) Clark, E. L., et al., "Bench Scale Equipment and Techniques - High Pressure Reactions", Ind. Eng. Chem., 39 (12), 1555-64 (December 1947).
- (4) Comings, E. W., High Pressure Technology, McGraw Hill Book Co., Inc. (1956).
- (5) Cook, G. A., et al., "Explosion Limits of Ozone-Oxygen Mixtures", Ind. Eng. Chem., 48 (4), 736-38 (April 1956).
- (6) Frederick, D. D., "Designing for Safety", Autoclave Engrs. Tech. Bull. No. 101.
- (7) Gillerman, J. B., "Telescoped Testing of Environmental System Speeded Mercury Design", Space/Aeronautics, 76-79 (May 1961).
- (8) Glasebrook, A. L., Hercules Powder Co., "Safety in Study of Chemical Reactions at High Pressure", Autoclave Engrs. Tech. Bulletin No. 100.
- (9) Glasebrook, A. L., and Montgomery, J. B., "High Pressure Laboratory", Ind. Eng. Chem., 41 (10), 2368-73 (October 1949).
- (10) Grosse, A. V., and Conway, J. B., "Combustion of Metals in Oxygen", Ind. Eng. Chem., 50 (4), 663-672 (April 1958).
- (11) Hersey, M. D., "Oxygen-Oil Explosions", Dept. of Int., Bur. of Mines, Preliminary Rpts. 1, 2, and 3 (July 1923).
- (12) Hersey, M. D., "Study of Oxygen-Oil Explosion Hazards", Am. Soc. Naval Engrs., 36, 231 (1924).
- (13) Jackson, et al., "A Study of the Titanium-Oxygen Pyrophoric Reaction", WADD Tech Rpt. 60-258 (June 1960).
- (14) Jackson, et al., "A Study of the Mechanics of Titanium-Oxygen Explosive Reaction", ASD Tech Rpt. 61-479 (September 1961).
- (15) Keating, D. A., "Design Study of High-Pressure Oxygen Vessels", WADC Tech. Rpt. 59-767 (February 1960).
- (16) Kiefer, R. W., "Safety at High Pressure", Ind. Eng. Chem., 49 (12), 2017-18 (December 1957).
- (17) Littman, et al., "Reactions of Titanium With Water and Aqueous Solutions", Stanford Research Institute (June 1958).

Contrails

- (18) Loving, F. A. , "Barricading Hazardous Reactions", Ind. Eng. Chem. , 49 (10), 1744-46 (October 1957).
- (19) Porter, et al. , "Design and Construction of Barricades", Ind. Eng. Chem. , 48 (5), 841-45 (May 1956).
- (20) Poulter, T. C. , "Effects of Pressure Cycling on Physical Properties of Materials", Product Engineering, 81-85 (August 1947).
- (21) Reynales, C. H. , "Compatibility of Materials With Oxygen", Douglas Aircraft Co. , Rpt. D81-444 (October 1958).
- (22) Reynales, C. H. , "Safety Aspects in the Design and Operation of Oxygen Systems", Douglas Aircraft Co. , Inc. , Eng. Paper 741.
- (23) Stephens, H. R. , and Walker, K. E. , "Safety in Small-Scale High Pressure Experiments", Ind. Eng. Chem. , 49 (12), 2022-25 (December 1957).

APPENDIX II

ENERGY OF CHEMICAL REACTION

The method of calculation is described on page 5. Initial conditions assumed for all calculations are:

Volume of pressure vessel	0.056 l (3.42 in. ³)*
Pressure	510 atm (7500 psi)
Temperature	298.2 K (79 F)

Volume at High Pressure

The parameters of pressure, volume, and temperature for a real gas can be represented by the expression $PV = ZRT$ where Z is defined as the compressibility factor. Figure 32 shows values of Z for oxygen as determined by means of Van der Waals equation:

$$\left(P + \frac{a}{V^2}\right) (V - b) = RT \quad (\text{II-1})$$

where

- a and b = constants
- P = pressure, atmospheres
- V = volume, liters/mole
- T = temperature, K
- R = gas constant (0.082 $\frac{\text{liter atm}}{\text{deg mole}}$).

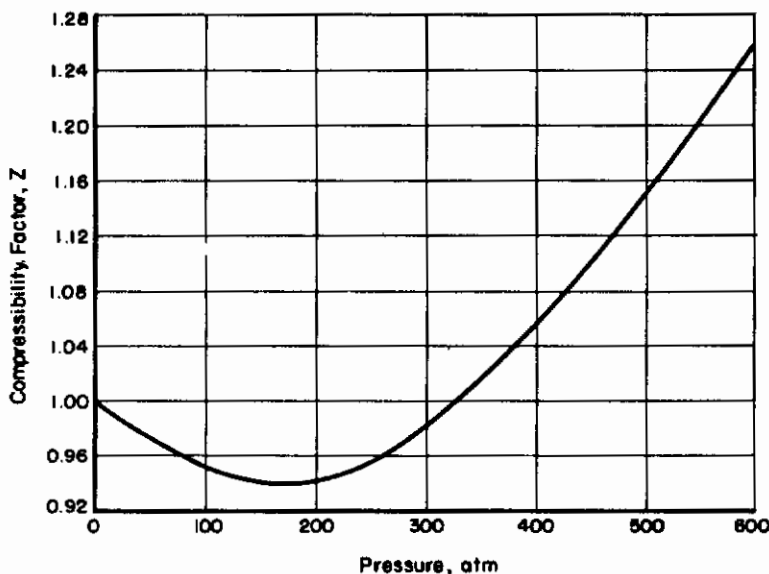


FIGURE 32. COMPRESSIBILITY FACTOR FOR OXYGEN AT 298.2 K

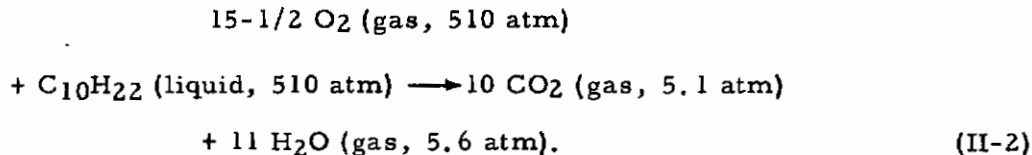
*Equals 1 gram-mole (0.0352 lb) of oxygen for initial PVT relationship.

Lewis and Randall^{(1)*} recommended Van der Waals constants, $a = 1.009$ and $b = 0.0264$. The values of the compressibility factor, Z , as calculated using these constants compare favorably with the values given in a National Bureau of Standards circular⁽²⁾ and with those found by Amagat⁽³⁾.

Decane

As an example of a combustible contaminant we can consider n-decane at a concentration of one part per thousand. The value for the heat of combustion at constant volume, ΔE , is needed. It might be satisfactory simply to use the heat of combustion at constant pressure and to ignore all corrections; however, the more rigorous analysis is presented below. Many of the correction terms are taken from calculations used in oxygen-bomb calorimetry⁽⁴⁾.

The concentration of the resulting CO_2 gas is one part per hundred and its pressure is 1/100 of the oxygen pressure, or 5.1 atm based on the reaction:



Although gaseous water cannot actually exist at 5.6 atm and 25 C, the heat effect for such a hypothetical product can be determined. This procedure will make a later step easier.

In order to find the total ΔE for Reaction (II-2), the ΔE 's for the following steps are found and their sum taken.

- (a) $15\text{-}1/2 \text{ O}_2 \text{ (gas, 510 atm)} \longrightarrow 15\text{-}1/2 \text{ O}_2 \text{ (gas, 1 atm)}$
- (b) $\text{C}_{10}\text{H}_{22} \text{ (liquid, 510 atm)} \longrightarrow \text{C}_{10}\text{H}_{22} \text{ (liquid, 1 atm)}$
- (c) $\text{C}_{10}\text{H}_{22} \text{ (liquid, 1 atm)} + 15\text{-}1/2 \text{ O}_2 \text{ (gas, 1 atm)} \longrightarrow 10 \text{ CO}_2 \text{ (gas, 1 atm)}$
 $\qquad \qquad \qquad + 11 \text{ H}_2\text{O} \text{ (gas, 1 atm)}$
- (d) $11 \text{ H}_2\text{O} \text{ (gas, 1 atm)} \longrightarrow 11 \text{ H}_2\text{O} \text{ (gas, 5.6 atm)}$
- (e) $10 \text{ CO}_2 \text{ (gas, 1 atm)} \longrightarrow 10 \text{ CO}_2 \text{ (gas, 5.1 atm)}$.

Step (a). The energy of expansion of oxygen is determined from thermodynamics by the relation:

$$\left(\frac{\partial E}{\partial P} \right)_T = -T \left(\frac{\partial V}{\partial T} \right)_P - P \left(\frac{\partial V}{\partial P} \right)_T .$$

By substitution of the equation $\left(z = \frac{PV}{RT} \right)$ and by integration, ΔE is expressed as

*References for Appendix II are listed on page 69.

Contrails

$$\Delta E = -RT \left[\Delta Z + \int_{P_1}^{P_2} \frac{T}{P} \left(\frac{\partial Z}{\partial P} \right) dp \right].$$

Evaluation by graphical integration gives for ΔE , 500 cal/mole, or, for Step (a), a total of 7.75 kcal. The positive sign indicates that energy is absorbed in the expansion.

Step (b). The energy change due to compression of a liquid is small. Decompression of 142 grams of $C_{10}H_{22}$ from 510 atm, therefore provides only 0.50 kcal based on the datum:

$$\left(\frac{\partial E}{\partial P} \right)_T = -0.007 \text{ cal/g atm.}$$

Step (c). The heat of combustion of n-decane at constant pressure under standard conditions is -1504.35 kcal. (5) The energy of combustion is expressed as

$$\Delta E = \Delta H - \Delta nRT,$$

where Δn is the increase in the number of moles of gas. ΔE is therefore -1507.65 kcal.

Step (d). For moderate pressures the energy of compression can be expressed by the equation

$$\left(\frac{\partial E}{\partial P} \right)_T = -\frac{a}{RT},$$

where a is Van der Waals constant. ΔE for Step (d) is -0.27 kcal.

Step (e). The calorimetrically determined value of $\left(\frac{\partial E}{\partial P} \right)_T$ for CO_2 results in a ΔE value of -0.28 kcal.

The sum of these five effects for Reaction (II-2) is -1499.95 kcal. Therefore, when 1 mole of O_2 reacts with 0.001 mole of decane, it may be assumed that -1500 kcal of energy is available.

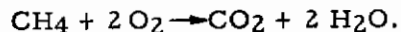
The heat capacities of the products and the unburned O_2 at constant volume must be determined to find the temperature rise resulting from the heat of combustion. Values for $\frac{C_p}{C_v}$ for oxygen up to 100 atm are given in Reference (2) Appendix II. By extrapolation an approximate value for C_v at 510 atm is 5.8 cal/mole degree or for 0.9845 mole, about 5.7 cal/degree. The heat capacity of CO_2 and H_2O is about 0.065 cal/degree for each. The total heat capacity for the entire mixture is therefore 5.83 cal/degree and accordingly the temperature rise is the total energy (1500 kcal) divided by the heat capacity or 260 C. The final temperature therefore would be 285 C (545 F).

Contrails

Correcting the estimate of C_v (taken originally at 25 C) for temperature and recalculating, the estimated final temperature would be 525 F. Substitution in Van der Waals equation results in a pressure of 1190 atm (17,500 psi).

Methane

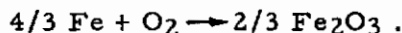
A similar process of calculation, however, with a concentration of only 15 ppm indicates that ΔE is only 2.86 cal based on the reaction



The temperature rise is only 0.9 F and the pressure rise is about 11 psi.

Iron

Iron wire will burn in oxygen at 1 atmosphere. At high pressures, if combustion is initiated, it may even be that an iron or stainless steel container itself may burn. To determine the magnitude of such a heat effect the following reaction was investigated:



It is supposed that the iron is present in the form of wire or rod and that it burns "candle fashion", the heat produced being contained in the iron oxide and in the unburned oxygen. In a manner similar to that previously used, ΔE for the reaction was calculated to be -129.9 kcal. Since high temperatures and pressures will be reached, a fairly complete table of C_v values for the products is needed. The C_v values averaged over a temperature range are expressed as

$$\overline{C_v} = \frac{1}{T-300} \int_{300}^T C_v dt$$

where T is degrees K. The heat content of the material at temperature T will be $C_v(T-300)$. For solids the heat capacity at constant volume is approximately equal to the heat capacity at constant pressure. Values of C_p were taken from Kelley's compilation⁽⁶⁾.

Fortunately, C_v for gases does not vary greatly with pressure, especially at high temperatures. Values for high temperature were, therefore, calculated with the aid of Kelley's tables. At lower temperatures, values for C_v of the gases were estimated from Reference (2) Appendix II. The results of these calculations are given in Table 7.

When the temperature reaches about 3000 K, Fe_2O_3 will no longer be formed and the reaction will produce $\text{Fe}_{.95}\text{O}$ instead. In the calculation it was assumed that the first 0.25 mole of oxygen would burn to Fe_2O_3 and the rest would form $\text{Fe}_{.95}\text{O}$. The results are shown in Table 8.

TABLE 7. MEAN HEAT CAPACITY AT CONSTANT VOLUME FROM 300 TO 5000 K

Temperature, K	\bar{C}_v , cal/deg mole				
	Fe ₂ O ₃	CuO	O ₂	CO ₂	H ₂ O
400	27.50	10.9	5.3		
500	28.85	11.2	5.40	8.70	
700	31.15	11.72			
1000	34.31	12.37	5.80	9.50	12
1500	34.22	13.57	6.10	10.29	7.5
2000	35.0	14.6	6.33	10.87	8.21
2500			6.52	11.22	8.76
3000			6.70	11.52	9.17
3500			6.85	11.74	9.52
4000			6.96	11.92	9.84
4500			7.11	12.09	10.09
5000			7.22	12.21	10.29

TABLE 8. ADIABATIC TEMPERATURES AND CALCULATED PRESSURES FOR COMBUSTION OF IRON TO FORM Fe₂O₃ AND Fe₉₅O

Fraction of Oxygen Consumed	Weight of Iron Burned, g	Temperature		Pressure	
		K	F	Atm	PSI
0.01	0.74	533	450	1140	16,800
0.02	1.49	740	820	1670	24,500
0.05	3.72	1250	1740	2900	42,600
0.10	7.45	1930	2960	4420	65,000
0.25	18.62	3230	5300	5860	86,100
0.40	34.52	3670	6090	4900	72,000
0.70	66.3	4090	6850	2440	35,600
1.00	98.1	4330	7280	0	0

In actual fact, such high internal temperatures can not be reached since the metal container would absorb some of the heat of reaction. The total energy available from the reaction when distributed throughout an iron bomb weighing 8-1/2 pounds and its contents would raise the temperature from 300 to 565 K, that is, to 510 F. The calculation is based on the heat capacity of iron.

Copper

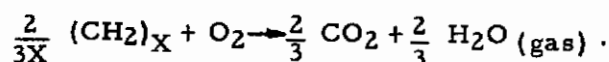
The combustion of copper in oxygen at 510 atmospheres is treated in the same way as iron. The reaction is $2 \text{Cu} + \text{O}_2 \rightarrow 2 \text{CuO}$ for which $\Delta E = -73.1$ kcal. At some temperature above 2000 K, CuO will no longer be the stable product, and further reaction will proceed according to the reaction $4 \text{Cu} + \text{O}_2 \rightarrow 2 \text{Cu}_2\text{O}$ for which $\Delta E = -78.59$ kcal. In these calculations it was assumed that the first 0.4 mole of oxygen forms CuO while further reaction forms Cu₂O. The results are tabulated in Table 9. The complete reaction would provide sufficient energy to raise the temperature of an 8-1/2-pound iron container to 370 F.

TABLE 9. ADIABATIC TEMPERATURES AND CALCULATED PRESSURES FOR COMBUSTION OF COPPER TO FORM CuO AND Cu₂O

Fraction of Oxygen Consumed	Weight of Copper Burned, g	Temperature		Pressure	
		K	F	Atm	PSI
0.01	1.27	425	257	840	12,400
0.02	2.54	548	478	1150	16,900
0.04	5.08	758	856	1660	24,400
0.10	12.71	1206	1663	2570	37,800
0.20	25.42	1670	2500	3100	45,500
0.30	38.13	1950	3000	3060	45,000
0.40	50.84	2145	3350	2790	41,000
0.60	101.68	2220	3490	1930	28,400
0.80	152.52	2250	3540	950	13,900
1.00	203.36	2270	3580	0	0

Plastic

As an example of a polymeric material the following reaction was considered:



The combustion energy is arbitrarily taken as 10.3 kcal/gram which is close to the correct value for paraffins, polyethylene, polystyrene, etc. It would be too high for polymers containing oxygen, sulfur, or nitrogen.

For this reaction, ΔE equals -96 kcal. The products in this case are gaseous and there is a continuous pressure rise. The results are shown in Table 10. The total heat produced is sufficient to raise the temperature of 8-1/2 pounds of iron to 450 F.

TABLE 10. ADIABATIC TEMPERATURE AND CALCULATED PRESSURES
FOR COMBUSTION OF (CH₂) IN OXYGEN

Fraction of Oxygen Consumed	Weight of Fuel, g	Temperature		Pressure	
		K	F	Atm	PSI
0.01	0.09	475	345	980	14,400
0.02	0.19	635	645	1,390	20,400
0.04	0.37	940	1,180	2,310	34,000
0.10	0.93	1,720	2,590	3,890	57,200
0.20	1.87	2,700	4,350	5,690	83,500
0.40	3.73	4,140	6,950	7,980	117,500
0.60	5.60	5,150	8,770	10,150	147,500
0.80	7.46	5,900	10,100	13,000	191,000
1.00	9.33	6,500	11,200	16,600	244,000

REFERENCES

- (1) Lewis, G. N., and Randall, M., Thermodynamics and the Free Energy of Chemical Substance, McGraw-Hill Book Company, New York (1923), p 196.
- (2) "Tables of Thermal Properties of Gases", National Bureau of Standards Circular 564 (1955).
- (3) Amagat, E. H., Ann. chim. et phys., 29 (6), 68 (1893).
- (4) Hubbard, W. N., Scott, D. W., and Waddington, G., J. Phys. Chem., 58, 152-62 (1954).
- (5) "Selected Values of Properties of Hydrocarbons", National Bureau of Standards Circular C461 (1947).
- (6) Kelly, K. K., "High-Temperature Heat Content, Heat Capacity, and Data for the Elements and Inorganic Compounds", Bureau of Mines, Bulletin 584 (1960).

Contrails

APPENDIX III

PRESSURE-TEMPERATURE RELATIONSHIPS

Three methods were used to calculate the final pressure evolved by letting a vessel completely filled with liquid oxygen warm to selected temperatures. In the calculations the following values were used:

$$\rho = 1.20 \frac{\text{grams}}{\text{cc}} \text{ at } 77.35 \text{ K}$$

$$P_c = 50.14 \text{ atm}$$

$$T_c = 154.78 \text{ K}$$

$$M = 32 \text{ grams/mole}$$

$$R = 82.06 \text{ cm}^3 \text{ atm/g mole K.}$$

Perfect Gas Laws

The perfect gas law is an expression which describes the pressure-volume-temperature relationship for ideal gases. However, it is only approximately representative of the characteristics of real gases at low pressures. At elevated pressures a compressibility factor is applied to account for the nonconformance of the perfect gas law. The compressibility factor will be reviewed in the next section and some values for oxygen will be tabulated in a summary of results.

$$P = \frac{\rho RT}{M}$$

$$\frac{\rho R}{M} = 3.077 \frac{\text{atm}}{\text{K}}$$

$$\therefore P = 3.077 T \text{ atm,}$$

where $T = K$.

Theorem of Corresponding States

There are available generalized compressibility charts^{(1)*} for reduced pressures (P_R) of "0" to a maximum of "40". At approximately room temperature the estimated reduced pressure is of the order of 110 and, therefore, to calculate the actual pressure-temperature relationship at room temperature, the chart was extended (Figure 33) and the values extrapolated. Unquestionably, inaccuracies occurring from such a technique cannot be completely overcome.

*References for Appendix III are listed on page 75.

Contrails

The method consisted of finding values of \bar{Z} (assumed compressibility factor) that correspond with Z (compressibility factor gotten from the Nelson-Obert Chart) at an identical value for P_R for different reduced temperatures (T_R).

A sample calculation is shown below.

- (1) Assume $T = 170.3 \text{ K}$ (306.5 R)
 $T_R = 1.1$.

- (2) The equation for pressure as a function of compressibility factor is

$$P = Z \frac{\rho RT}{M}$$

$$P = 3.077 (TZ), \quad T = \text{K};$$

$$\therefore P_R = 10.45 Z, \quad T = 170.3 \text{ K}.$$

- (3) Assume $\bar{Z} = 3.6$, $\therefore P_R = 37.62$.

- (4) On Figure 33 the intersection of $P_R = 37.62$ and $T_R = 1.1$ yields a values of $Z = 3.12$.

- (5) Assume $\bar{Z} = 3.85$, $\therefore P_R = 40.19$.

- (6) The intersection of $P_R = 40.19$ and $T_R = 1.1$ yields $Z = 3.89$.

- (7) Finally assume $\bar{Z} = 3.9$, $\therefore P_R = 40.70$.

- (8) The intersection of $P_R = 40.70$ and $T_R = 1.1$ yields $Z = 3.9$.

It can then be concluded that at $T = 170.3 \text{ K}$, the compressibility factor would be 3.9, and the gas pressure would be 30,040 psi.

Conclusion

In Table 11 the results of the two methods are tabulated.

TABLE 11. THEORETICAL PRESSURES GENERATED BY EVOLVING LIQUID OXYGEN INTO A GAS AT EQUAL DENSITY

Temperature, K	Perfect Gas Law, P(Ideal), psi	Theorem of Corr. States	
		Z _(cs)	Pressure _(cs) , psi
170.25	7,700	3.90	30,040
201.2	9,100	4.80	43,690
247.7	11,200	5.42	60,710
278.6	12,600	5.80	73,100
309.6	14,000	6.03	84,450

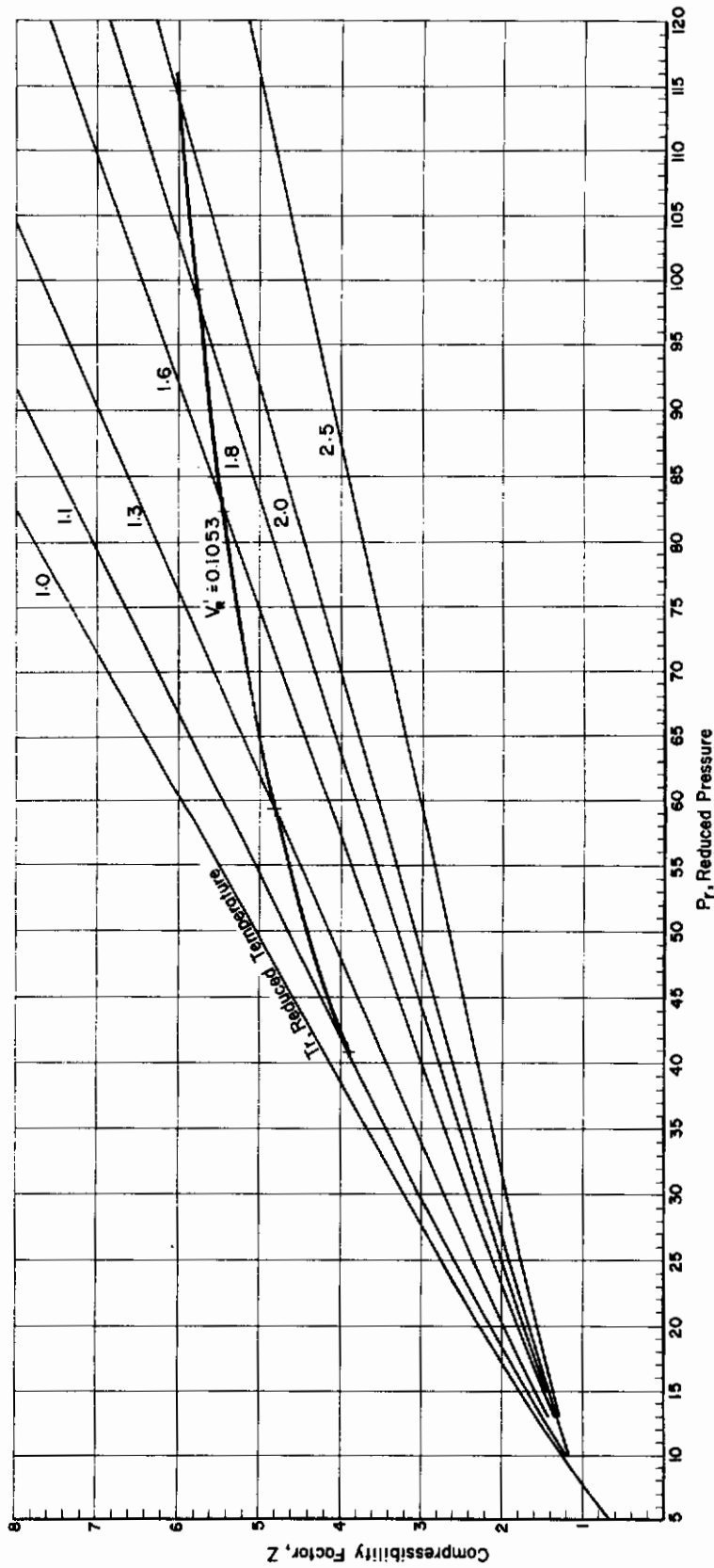


FIGURE 33. GENERALIZED COMPRESSIBILITY CHART FOR HIGH-PRESSURE RANGE

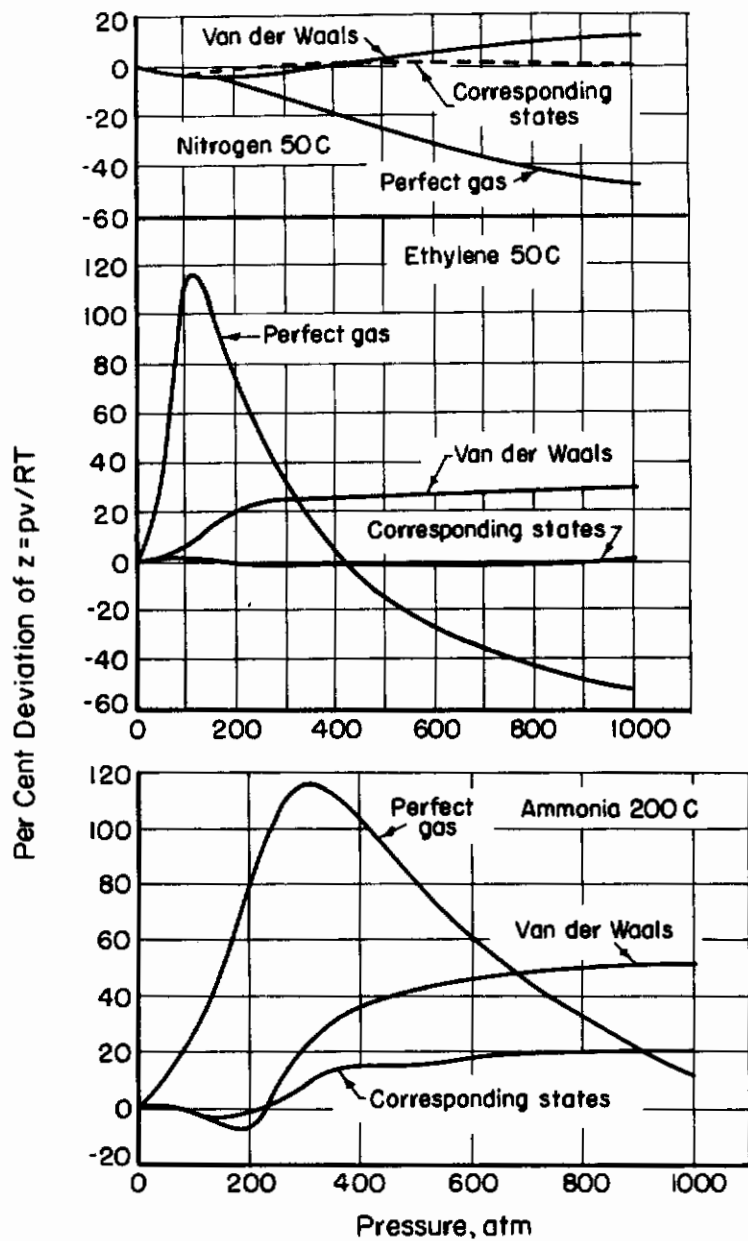


FIGURE 34. PER CENT DEVIATION OF THE COMPRESSIBILITY FACTOR FOR ETHYLENE, NITROGEN, AND AMMONIA FROM OBSERVED MEASUREMENTS

As shown in Figure 34⁽²⁾ the perfect gas law gives increasingly lower values as the pressure increases beyond 300 atmospheres for nitrogen, ammonia, and ethylene. There is no reason to believe that in the case of oxygen its use should result in more or less accurate results. Also, it can be seen in Figure 34 that the percentage deviation resulting from the theorem of corresponding states is fairly constant and would appear to remain so if the curves were extended. Therefore, of the values calculated the ones which must be considered accurate are those calculated by the theorem of corresponding states.

REFERENCES

- (1) Obert, E. F. , Concepts of Thermodynamics, McGraw-Hill Book Company (1960), Figure B-10.
- (2) Comings, E. W. , High Pressure Technology, McGraw-Hill Book Company (1956), Figure 8.

Contrails

APPENDIX IV

TABLES OF EXPERIMENTS PERFORMED

TABLE 12. TEMPERATURE-VARIATION EXPERIMENTS

Experiment	Reactor Metal	Specimen or Contaminant	Pressure, psi		Temperature, F		Duration	Comments
			Minimum	Maximum	Minimum	Maximum		
11	Monel	Teflon } Viton } O-ring	800	8,400	Room		1 hr 25 min	
12	Stainless steel	Ditto	3,000	7,100	-58	255	1 hr 40 min	
13	Ditto	"	3,100	9,900	+18	275	5 hr	
14	Copper	Kel-F } Neoprene } O-ring	2,500	8,600	-72	268	4 hr 30 min	
15	Brass	Ditto	3,000	8,800	-68	285	4 hr 40 min	
16	Monel	Phthalocyanine	3,000	9,200	-70	275	4 hr 55 min	
17	Stainless steel	Phthalocyanine	2,700	9,800	Not recorded		5 hr 10 min	
18	Brass	Teflon, Viton Kel-F, Neoprene	3,000	12,200	-55	300	70 hr	
105	Stainless steel	None	4,000	6,800	+60	353	19 hr 10 min	
106	Ditto	None	6,050	7,000	+64	332	4 hr 40 min	Leak
107	"	None	8,250	10,850	+70	350	4 hr 40 min	Leak
108	"	None	3,400	9,600	+70	150	4 hr 50 min	Leak
109	"	None	7,300	14,800	+28	367	5 hr 40 min	
110	"	None	6,200	12,200	+55	367	19 hr	Leak
111	"	None	10,000	16,000	+53	290	4 hr 10 min	
113	"	Teflon dumbbell	4,400	8,200	--	260	48 hr	
114	"	Kel-F dumbbell	3,400	8,350	--	260	Ditto	
115a	"	Ditto		15	--	260	"	
115b	"	Aluminum	4,000	8,300	Room	"	"	Dry
116a	"	Teflon dumbbell		15	--	260	"	
116b	"	Stainless steel	4,400	8,200	Room	"	"	Dry
117	"	Ditto	5,200	8,250	--	260	"	Saturated with H ₂ O
118	"	"	5,600	8,400	--	260	"	Dry
119	"	Aluminum	6,200	8,800	--	260	"	Saturated with H ₂ O
120	"	Brass	6,200	8,800	--	260	"	Dry
121	"	Brass	6,200	8,800	--	260	"	Saturated with H ₂ O
122	"	Nylon	6,400	8,500	--	260	"	
123	"	Nylon	5,500	9,900	Room	"	"	Pressure rose spontaneously
134	"	Ethylene	--	7,500	Room	400	3 hr	Leak
135	"	Propane	7,300	8,300	130	400	4 hr 25 min	
136	"	Acetylene	6,200	8,200	65	400	5 hr	
137	"	Methane	2,400	8,200	175	400	19 hr	Slow leak
138	"	Ethylene	5,500	8,600	80	400	4 hr 30 min	
139	"	Acetylene	6,800	8,400	70	400	6 hr	
140	"	Methane	6,000	8,300	65	400	5 hr 30 min	
141	"	Propane	7,200	8,200	75	260	1 hr	
142	"	Propane	7,400	8,400	80	350	1 hr	
143	"	Methane	7,800	8,600	70	255	1 hr	
144	"	Methane	6,500	8,300	75	400	1 hr 45 min	
145	"	Acetylene	7,300	8,300	70	260	50 min	
146	"	Acetylene	7,000	8,400	70	400	1 hr 10 min	
147	"	Propane	7,600	8,500	80	260	1 hr	
148	"	Propane	6,500	8,200	80	400	1 hr 25 min	
149	"	Ethylene	7,000	8,200	75	260	40 min	
150	"	Ethylene	7,400	8,500	80	400	45 min	
151	"	Acetylene	7,000	8,500	70	260	50 min	
152	"	Ethylene	7,000	8,400	75	260	50 min	
153	"	Methane	7,600	8,600	80	260	50 min	
154	"	Propane	7,000	8,400	75	260	45 min	

Contrails

TABLE 13. VIBRATION EXPERIMENTS

Experiment	Reactor Metal	Contaminant or Specimen	Pressure, psi		Temperature, F		Vibrations, cps	Duration, minutes
			Minimum	Maximum	Minimum	Maximum		
19	Copper	Teflon } Viton } O-ring	3100	7,800	+68	275	35,800	340
				7,800	+68			
				5,000	+68			
				5,500	+68			
				6,200				
				6,200	275			
				6,200	275			
				6,200	275			
				6,200	275			
				6,200	275			
20	Brass	Kel-F } Neoprene } O-ring	3000	10,600	65	270	35,800	360
				8,300	78			
				8,200	78			
				8,200	78			
				10,600				
				10,600	270			
				10,600	270			
				10,600	270			
				10,600	270			
				10,600	270			
21	Stainless steel	Ditto	3000	11,000	78	270	35,800	300
				8,600	78			
				8,600	78			
				8,600	78			
				11,000				
				11,000	270			
				11,000	270			
				11,000	270			
				11,000	270			
				11,000	270			
22	Monel	Teflon } Viton } O-ring	3200	8,200	78	262	35,800	205
				7,500	78			
				7,800				
23	Copper	2 drops hexane	3000	8,000	71	265	35,800	300
				8,000	82			
				8,000				
24	Brass	4 drops pentane	2000	8,200	74	262	35,800	320
				8,200	85			
				7,800				
25	Stainless steel	6 drops hexane	3400	8,200	74	275	35,800	300
				8,000	85			
				8,200				
26	Monel	8 drops decane	2700	8,200	78	280	35,800	340
				8,000	88			
				8,000				
27	Brass	Cold-rolled steel chips	3450	8,000	85	262	35,800	200
				8,000	95			
				7,900				
28	Stainless steel	Aluminum chips	3000	8,000	67	262	35,800	220
				8,000	78			
				8,000				
29	Brass	2 drops pentane	2800	8,200	74	264	35,800	300
				8,000	78			
				8,100				

TABLE 14. SHOCK EXPERIMENTS

Experiment	Reactor Metal	Contaminant or Specimen	Pressure, psi		Temperature, F		Number of Shocks at 25 G's	Duration, minutes
			Minimum	Maximum	Minimum	Maximum		
30	Brass	None	2800	8300	74	81	26	60
31	Brass	Methane	3000	8000	88	262	110	280
32	Stainless steel	Propane	3400	8300	95	262	200	290
33	Monel	Propane	3400	8200	88	280	125	135
34	Monel	Methane	3200	8000	95	262	125	240
35	Copper	Butane	3300	8300	92	265	125	260
36	Copper	2 drops decane	3700	5500	Room		25	170
37	Stainless steel	2 drops decane	4000	8000	76	255	125	95
38	Stainless steel	Acetylene	4000	8600	76	265	125	330
39	Brass	2 drops pentane	4200	5000	52	66	50	165

TABLE 15. STORAGE EXPERIMENTS

Experiment	Reactor Metal	Contaminant or Specimen	Test Sequence, hours				Visual Results
			8000 PSI, Room Temperature	13,000 PSI, 260 F	8000 PSI, Room Temperature	7500 PSI, 260 F, 35,800 Vib./Min Static	
40	Stainless steel	1 drop of hexane in ball of cotton	186	24	406		Surface oxidation visible; reddish discoloration in area of reaction
41	Brass	Methane	336	24	264		Clean
42	Monel	Butane	360	24	240		Clean
43	Copper	Propane	162	24	430		Surface color changed to golden yellow
44	Stainless steel	Methane	472	24	120		Surface oxidation
45	Brass	Shredded Viton	496	24	86		Clean
46	Monel	Shredded Kel-F	520	24	62		Clean
47	Copper	Shredded Teflon	544	24	2		Heavy bluish-black surface oxidation
126	Stainless steel	Teflon bar, steel wool		60		94 --(a)	Teflon bar unchanged; steel wool slightly rust colored
127	Stainless steel	Teflon bar, Teflon- asbestos packing				94 406	No visible effect
128	Stainless steel	Kel-F bar, steel wool				94 406	Kel-F bar became milk white and brittle; compression shear stress failures below surface; steel wool more deeply rust colored but still not appreciable
129	Stainless steel	Carbon dust				94 406	Carbon dust caked; liquid present in glass container
130	Stainless steel	Steel filings and dust				94 --(a)	Steel filings reddish in color; glass container discolored

(a) Leaks developed because of vibration. Gas escaped and pressure dropped to atmosphere.

Contrails

TABLE 16. FLOW EXPERIMENTS

Experiment	Orifice Material	Orifice Diameter, mils	Initial Upstream Pressure, psi	Elapsed Time, seconds	Voltage, volts	Gas Temperature, F	Probe	Comments
48	Brass	40	8,000	5	-0.1	--	A	
49	"	40	3,500	--	0	--	A	
50	"	40	12,000	--	0	--	A	
51	"	40	14,000	15	0	--	A	
52	"	40	14,200	--	0	--	B	
53	"	40	8,000	--	0	--	B	
54	"	40	15,200	--	0	>100	A	
55	"	40	8,800	--	0	139	A	
56	"	13	12,000	3	0	154	A	
57	"	13	12,500	--	-0.02 to 0.08	--	A	
58	"	13	15,200	4	-0.02 to 0.08	92	A	
59	"	13	13,500	5	+0.02 to 0.10	98	A	
60	"	13	15,200	--	0	>32	C	
61	"	13	12,000	--	0	--(a)	C	
62	"	5	14,000	3	0	--	C	
63	"	5	9,000	5	0	--	A	
64	"	5	15,200	4	+0.02	--	A	
65	"	5	12,200	6	+0.04	--	D	
66	"	5	12,200	3	0	--	D	
67	"	5	12,200	5	0	--	D	
68	"	5	13,400	3	0	--	D	
69	"	5	12,200	5	+0.02	--	D	
70	"	5	12,400	3	+0.13	--	D	
71	"	5	12,200	5	0	--	D	
72	"	5	12,400	3	0	--	D	
73	"	5	12,400	6	+0.28 to 0.76	--	E	
74	"	5	12,200	3	0	--	E	
75	"	5	14,000	7	+0.16	--	D	
76	"	5	16,000	5	+0.80	--	E	
77	"	5	12,000	3	+0.21	--	F	
78	"	5	13,000	5	+0.25	--	F	
79	"	5	14,000	3	0	--	G	
80	"	5	13,500	6	+0.32	--	F	
81	"	5	8,100	2	-0.04	--	H	
82	"	5	14,500	4	-0.04	--	H	
83	"	5	16,400	4	-0.04	--	J	
84	"	5	7,500	4	-0.02	--	J	
85	"	5	14,000	4	0	--	J	
86	"	5	12,000	5	-0.04	--	J	
87	"	5	11,400	3	0	--	K	
88	"	5	12,500	4	+0.06 to >0.6	--	E	
89	"	5	12,500	3	0	--	E	
90	"	5	12,500	4	0.79	--	E	
91	"	5	13,000	3	0.18	--	E	
92	"	5	12,500	4	0.66	--	E	
93	"	5	13,500	3	+0.20	--	F, D	
94	"	5	12,500	5	+0.04	--	F, D	
95	"	5	10,400	3	+0.23	--	L	
96	"	5	14,000	7	0	--	L	
97	"	5	12,500	3	0	--	M	

TABLE 16. (Continued)

Experiment	Orifice Material	Orifice Diameter, mils	Initial Upstream Pressure, psi	Elapsed Time, seconds	Voltage, volts	Gas Temperature, F	Probe	Comments
98	Brass	5	13,000	6	0	--	M	
99	"	5	12,500	4	-0.18	--	N	
100	"	5	12,500	6	+0.2 to -0.6	--	N	
101	"	5	15,000	4	-0.12	--	N	
102	"	5	11,000	7	-0.19	--	N	
103	"	5	12,500	4	+0.04	--	N	
104	"	5	12,200	8	-0.14	--	N	
124	"	5	11,000 average	32 min, 22 sec	--	--	--	
125	Stainless steel	13	11,000 average	15 min, 02 sec	--	--	--	
131	Teflon	6	10,000	--	--	--	--	Orifice disk collapsed
132	Teflon	6	10,000	5 min, 35 sec	--	--	--	Back-up used; orifice hole blocked
133	Kel-F	6	8,000	15 min	--	--	--	

Note: A = 1/16-diam pointed stainless steel rod
 B = 1/16-diam rounded stainless steel rod (GRD)
 C = 1/8-diam flat end stainless steel rod (GRD)
 D = 1/8-diam stainless steel tube
 E = 1/8-diam stainless steel tube with restrictions
 F = No. 3H pointed graphite lead
 G = No. 3H flat end lead

H = glass tube
 J = glass tube wrapped in aluminum foil
 K = 1/4-diam polyethylene tube
 L = 1/16-diam coil aluminum foil
 M = cotton-tipped swab
 N = stainless steel tube with Duco cement

(a) Temperature readings discontinued for the remainder of the experiments.

TABLE 17. SURGE EXPERIMENTS

Experiment	Initial Pressure, psi	Final Pressure, psi	Pressure Ratio	Initial Temperature, F	Final Temperature, F
112A	15	5000	333	32	53
112B	15	7000	467	32	64
112C	15	8300	553	32	74
112D	15	7000	467	32	67
112E	15	8200	547	32	73
112F	15	6000	400	32	65
112G	15	6000	400	32	65
112H	15	8100	540	32	73
112J	15	5000	333	32	59

Contrails

APPENDIX V

PARTIAL PRESSURE OF HYDROCARBON GAS FOR CONCENTRATION OF 10 PARTS PER MILLION

For a mixture of two gases the volumetric concentrations can be approximately determined from a knowledge of the partial pressures. Application of the compressibility factor permits calculations to estimate the concentration of hydrocarbon gas contaminants in high-pressure gaseous oxygen.

The general expression for a nonideal gas is:

$$PV = n Z R T.$$

The equation can be rewritten in terms of the molar quantity. The molar quantity for the hydrocarbon gas can then be divided by a similar quantity for the oxygen gas.

$$\frac{n_{\text{HC}}}{n_{\text{O}_2}} = \frac{(PV)_{\text{HC}} (Z R T)_{\text{O}_2}}{(PV)_{\text{O}_2} (Z R T)_{\text{HC}}}$$

If we assume that R, T, and V are equal for both gases and that Z_{HC} equals one, the expression is simplified as follows:

$$\frac{n_{\text{HC}}}{n_{\text{O}_2}} = \frac{P_{\text{HC}} Z_{\text{O}_2}}{P_{\text{O}_2}}.$$

The ratio of $\frac{n_{\text{HC}}}{n_{\text{O}_2}}$ is assumed to be 10^{-5} (10 parts per million). Therefore, the pressure of the hydrocarbon is

$$P_{\text{HC}} = \frac{P_{\text{O}_2} \times 10^{-5}}{Z_{\text{O}_2}}.$$

The pressure of the oxygen gas is 500 atmospheres and its compressibility factor is approximately 1.2 at room temperature.

Therefore

$$P_{\text{HC}} = 500 \text{ atm} \times 30 \frac{\text{inches mercury}}{\text{atm}} \times \frac{10^{-5}}{1.2}$$

$$P_{\text{HC}} = 0.125 \text{ inches mercury.}$$

Therefore, a hydrocarbon gas at an absolute pressure of 1/8-inch mercury when mixed with gaseous oxygen at 7500 psi and approximately room temperature provides a contamination concentration approximately equivalent to 10 parts per million.

Contrails